Separation of homogeneous catalysts using Organic Solvent Nanofiltration

TC Masinda

16912748

Dissertation submitted in partial fulfilment of the requirements for the degree
Magister Scientiae in Chemistry
at the Potchefstroom Campus of the North-West University

Supervisor:	Prof. H.C.M. Vosloo
Co-supervisor:	Dr. P. van der Gryp
Assistant Supervisor:	Prof. S.F. Mapolie

November 2016

Summary

Keywords: 1-octene metathesis; Grubbs-type precatalyst; Organic Solvent Nanofiltration; PuraMem™

One technology that has shown in literature to have great potential for separating homogeneous catalysts from their reaction mixture is organic solvent nanofiltration (OSN), which is a pressure-driven, membrane-based separation technique. It is used in this study, for the effective separation of new Grubbs-type precatalysts from their reaction mixtures in the metathesis of 1-octene using membranes not studied before to add to the list of membranes that are already reported in literature. Both the metathesis activity and catalyst lifetime of each precatalyst were also investigated.

The study was divided into three parts:

i) The synthesis of new Grubbs-type precatalysts containing pyridinyl-alcoholato ligands, i.e. benzylidene-chloro[1,3-bis-(2,4,6-trimethylphenyl)-2-imidazolidinylidene]-[1-(2'-pyridinyl)-1-alkyl-1-phenyl-methanolato]ruthenium with alkyl = isopropyl (**1**), 4'-methylphenyl (**2**) or 3'-methylphenyl (**3**).
ii) Activity and lifetime studies of these precatalysts for the metathesis of 1-octene.
ii) OSN-separation performance.

The pyridinyl-alcoholato ligands and their corresponding Grubbs-type precatalysts were succesfully synthesized and characterized using FTIR, NMR and mass spectrometric techniques.

The precatalysts were studied for the metathesis reaction of 1-octene at 80 °C with a catalyst load of 1:7000 (Ru/1-octene molar ratio). Selectivity and turnover numbers (TON) were used to describe the effectiveness of these precatalysts during the metathesis reaction of 1-octene to ethene and 7-tetradecene (primary metathesis products, i.e. PMPs). All the precatalysts showed conversions of the 1-octene to the PMPs of greater than 60% at 80 °C. Precatalyst **1** showed a selectivity of 99,90% and a TON of 5268, while precatalyst **2** and **3** gave a selectivity of 99,83% with a TON of 5983 and a selectivity of 99.85% with a TON of 6401 respectively.

In terms of lifetime, the precatalysts showed a decrease in activity after the second addition of 1-octene. Precatalysts **2** and **3** showed a slight decrease to 56% and 66% PMPs

respectively while **1** showed no activity at all after the second addition of 1-octene. Upon the third addition of 1-octene no activity was observed.

The PuraMem™ 280 and PuraMem™ S380 membranes were used for the OSN technique. The permeation performance (flux) and catalyst rejection were determined. Permeation performances with fluxes ranging from 9 to 35 $L.m^{-2}.h^{-1}$ were obtained for the PuraMem™ series of membranes. The PuraMem™ 280 membrane successfully separated the Grubbs-type precatalysts from their post-reaction mixtures at 50 bar, with catalyst rejections >97%. Very poor rejections of the precatalysts were observed with the PuraMem™ S380 membrane.

Opsomming

Skeiding van homogene katalisatore deur van Organiese Oplosmiddel Nanofiltrasie gebruik te maak

Sleutelwoorde: 1-okteen; Grubbs-tipe prekatalisatore; Organiese Oplosmiddel Nanofiltrasie; PuraMem™

Een tegnologie wat in die literatuur groot potensiaal getoon het om homogene katalisatore van hul reaksiemengsels te skei, is organiese oplosmiddel nanofiltrasie (OSN) wat 'n drukgedrewe, membraangebaseerde skeidingstegniek is. In hierdie studie is dit gebruik vir die effektiewe skeiding van nuwe Grubbs-tipe prekatalisatore van hul reaksiemengsels in die metatese van 1-okteen deur van membrane gebruik te maak wat nie voorheen vir hierdie doel bestudeer is nie; om sodoende die membraanlys wat reeds in die literatuur gerapporteer is, uit te brei. Beide die metatese-aktiwiteit en katalisatorleeftyd van elke prekatalisator is ook ondersoek.

Die studie is in drie dele verdeel:

i) Die sintese van nuwe Grubbs-tipe prekatalisatore wat 'n piridiniel-alkoholato ligand bevat, nl. bensilideen-chloor[1,3-bis-(2,4,6-trimetielfeniel)-2-imidasolidinilideen]-[1-(2'-piridiniel)-1-alkiel-1-feniel-metanolato]rutenium met die alkiel = isopropiel (**1**), 4'-metielfeniel (**2**) of 3'-metielfeniel (**3**).
ii) Aktiwiteits- en leeftydstudies van hierdie prekatalisatore vir die metatese van 1-okteen.
ii) OSN-skeidingsverrigting.

Die piridiniel-alkohlato ligande en hul ooreenstemmende Grubbs-tipe prekatalisatore is suksesvol gesintetiseer en met behulp van FTIR-, KMR- en massaspektrometriese tegnieke gekarakteriseer.

Die prekatalisatore is vir die metatesereaksie van 1-okteen by 80 °C met 'n katalisatorlading van 1:7000 (Ru/1-okteenmolverhouding). Selektiwiteitswaardes en omsettingsgetalle (TON) is gebruik om die effektiwiteit van die prekatalisatore tydens die metatesereaksie van 1-okteen na eteen en 7-tetradeseen (primêre metateseprodukte, nl. PMPs) te beskryf. Al die katalisatore het omsettings van 1-okteen na die PMPs van groter as 60% by 80 °C getoon. Prekatalisator **1** het 'n selektiwiteit van 99,90% met 'n TON van 5268 getoon, terwyl

prekatalisatore **2** en **3** ’n selektiwiteit van 99,83% met ’n TON van 5983 en prekatalisator **3** ’n selektiwiteit van 99.85% met ’n TON van 6401 respektiewelik gelewer het.

Wat katalisatorleeftyd betref, het die prekatalisatore ’n afname in aktiwiteit na die tweede byvoeging van 1-okteen getoon. Prekatalisatore **2** en **3** het ’n effense afname tot 56% en 66% PMPs respektiewelik getoon terwyl **1** geen aktiwiteit na die tweede byvoeging getoon het nie. Met 'n derde byvoeging van 1-okteen is geen aktiwiteit waargeneem nie.

Die PuraMem^{TM} 280 en PuraMem^{TM} S380 membrane is vir die OSN-tegniek gebruik. Die skeidingsverrigting (vloed) en katalisatorverwerping is bepaal. Permeasieverrigtings met vloede wat wissel van 9 tot 35 $L.m^{-2}.h^{-1}$ is met die PuraMem^{TM} membraanreeks verkry. Die PuraMem^{TM} 280 membraan het die Grubbs-tipe prekatalisatore met katalisatorverwerpings >97% suksesvol van hul nareaksiemengsels by 50 bar geskei. Baie swak verwerpings van die prekatalisatore is met die PuraMem^{TM} S380 membraan waargeneem.

Dedicated to my late Uncle with love

Acknowledgements

Special thanks to the Heavenly Father who created me for making this project possible and blessing me with courage and wisdom so that I could persevere throughout my study.

My sincere appreciation and gratitude to the following people, you were all unique in your own ways:

- Prof. Manie Vosloo, for granting me the opportunity to do my masters with his research group. Thank you for the endless contributions towards my study.
- Dr. Percy Van Der Gryp for all his knowledge of membranes.
- Dr Tegene Tole, your Input in this dissertation was phenomenal, May God Continue to bless you!!!
- Dr. Johan Jordaan for all the analytical input. You always made time to assist me.
- Oom Jan Kroeze and Adrian Brock for always helping me with the whole nanofiltration setup.
- Mr. Andre Joubert for the NMR spectra.
- Dr. Charles Williams, Mr. John Bogopane, Mr. Andrew Fouche and Mrs. Lynette Van Der Walt for the chemicals.
- Miss Mirriam Ntaote (Nana) for the clean office and laboratory environment.
- The entire catalysis and synthesis research group and the CRB staff.
- Prof. Jan Smit and Mrs. Zelda Friesling, colleagues at the science centre for the encouragement while working as a volunteer at the science centre.
- DST-NRF Centre of Excellence in Catalysis (c*change) and the North-West University for the financial support.
- Miss Aobakwe Hilary Jood for her soul-stirring support and other non-scientific support.
- All my friends who encouraged me through hard times.
- To my entire family, Mrs. Phindiwe Gloria Gouws (Mom), Mr. Thabo R Holele and the late Mr. Msindisi Robertson Masinda (Uncle). You were all an inspiration throughout my study.

Table of Contents

Summary i
Opsomming iii
Acknowledgements vi
Table of Contents vii
List of Figures ix
List of Tables xi
List of Appendices xii
List of Abbreviations xiii
List of Complexes xv
List of Equations xvii

Chapter 1 Introduction and aims of study 1
1.1 Background 1
1.2 Aim and Objectives 3
1.3 Scope of investigation 4
1.4 Layout of dissertation 4
1.5 References 5

Chapter 2 Literature review 7
2.1 Organic Solvent Nanofiltration (OSN) 7
2.2 Alkene Metathesis 14
2.3 References 24

Chapter 3 Experimental 28
3.1 Materials 28
3.2 Analytical techniques and calculation methods 29
3.3 OSN experimental procedures and set-up 33
3.4 Preparation of complexes 35
3.5 Metathesis experiments 39
3.6 Ruthenium extraction methodology and ICP-OES analysis 40
3.7 References 41

Chapter 4 Results and Discussions 42
4.1 Membrane characterization and selection 42
4.2 Metathesis 49
4.3 Lifetime of complexes **1**-**3** 52
4.4 Organic Solvent Nanofiltration (OSN) Rejection Results and Discussion. 54
4.5 Concluding remarks 58
4.6 References 59

Chapter 5 Conclusions and Recommendations 60
5.1 Conclusions 60
5.2 Recommendations 61
5.3 References 61

Appendix – FTIR spectra 62
Appendix – Mass spectra 64
Appendix - ^{1}H-NMR spectra 65
Appendix - ^{13}C-NMR spectra 68
Appendix - ^{31}P-NMR spectra 71

List of Figures

Figure 1.1: General alkene metathesis reaction....1
Figure 1.2: Grubbs-type precatalysts synthesized for this study....2
Figure 1.3: Description of ligands in Grubbs-type precatalysts....2
Figure 1.4: Grubbs first generation (**7**) and Grubbs second (**8**) generation catalysts....3
Figure 2.1: Schematic representation of a two-phase system separated by a membrane....7
Figure 2.2: Typical structures of membranes....9
Figure 2.3: Well-defined metal alkylidene complexes....18
Figure 2.4: Dissociative mechanism with Grubbs-type complexes....19
Figure 2.5: Catalytic cycle in the productive mechanism of C_8 metathesis....20
Figure 2.6: Design concepts for thermally switchable initiators....21
Figure 2.7: Simplified mechanism with a Hoveyda-Grubbs-type (**D2**-type) precatalyst....21
Figure 2.8: "Dissociation" step for a Hoyveda-Grubbs-type precatalyst....22
Figure 2.9: Representation of the hemilability concept....22
Figure 2.10: Simplified mechanism with **D3**-type precatalysts....23
Figure 2.11: The PUK-Grubbs-2 type precatalyst (**9**)....23
Figure 3.1: A calibration curve for the determination of the GC response factor for 1-octene....31
Figure 3.2: Photo of the experimental set-up used....33
Figure 3.3: Solid-Works diagram showing different parts of the pressure cell....33
Figure 3.4: A schematic representation of the experimental set-up....34
Figure 3.5: Synthesis of ligands **L1**-**L3**....35
Figure 3.6: Lithiation of ligands **L1**-**L3**....37
Figure 3.7: Synthesis of complexes **1**-**3**....37
Figure 3.8: A schematic diagram for performing metathesis reactions....40
Figure 4.1: Pure 1-octene flux vs time at different pressures with PuraMem™280 membrane....43
Figure 4.2: Pure 1-octene flux vs time at different pressures with PuraMem™S380 membrane....43
Figure 4.3: Pure 1-tetradecene flux vs time at different pressures with PuraMem™280 membrane....44
Figure 4.4: Pure 1-tetradecene flux vs time at different pressures with PuraMem™S380 membrane....44
Figure 4.5: Plot of pure C_8, C_{14} and binary mixture compositions vs Total Flux of Binary mixture (1-octene & 1-tetradecene) for PuraMem™ 280 membrane....46
Figure 4.6: Plot of pure C_8, C_{14} and binary mixture compositions vs Total Flux of binary mixture (1-octene and 1-tetradecene) for PuraMem™ S380....46

Figure 4.7: A plot of feed composition vs permeate composition of binary mixtures (1-octene & 1-tetradecene) for PuraMem™280 membrane 48

Figure 4.8: A plot of feed composition vs permeate composition of binary mixtures (1-octene & 1-tetradecene) for PuraMem™ S380.....48

Figure 4.9: The conversion of 1-octene and the formation of PMPs, IPs and SMPs with complex **1** at 80°C and a Ru:1-octene molar ratio of 1:7000 50

Figure 4.10: The conversion of 1-octene and the formation of PMPs, IPs and SMPs with complex **2** at 80°C and a Ru:1-octene molar ratio of 1:7000 50

Figure 4.11: The conversion of 1-octene and the formation of PMPs, IPs and SMPs with complex **3** at 80°C and a Ru:1-octene molar ratio of 1:7000 51

Figure 4.12: PMPs formation upon succesive additions of 1-octene during metathesis in the presence of **1** at 80 °C and a Ru:1-octene molar ratio of 1:7000.....52

Figure 4.13: PMPs formation upon succesive additions of 1-octene during metathesis in the presence of **2** at 80 °C and a Ru:1-octene molar ratio of 1:7000.....53

Figure 4.14: PMPs formation upon succesive additions of 1-octene during metathesis in the presence of **3** at 80 °C and a Ru:1-octene molar ratio of 1:7000.....53

Figure 4.15: PMPs formation of successive metathesis reactions at 80 °C and a Ru:1-octene molar ratio of 1:7000 after OSN recycling of **1** with PuraMem™ 280.....55

Figure 4.16: PMPs formation of successive metathesis reactions at 80 °C and a Ru:1-octene molar ratio of 1:7000 after OSN recycling of **2** with PuraMem™ 280.....55

Figure 4.17: PMPs formation of successive metathesis reactions at 80 °C and a Ru:1-octene molar ratio of 1:7000 after OSN recycling of **3** with PuraMem™ 280.....56

Figure 4.18: PMPs formation of successive metathesis reactions at 80 °C and a Ru:1-octene molar ratio of 1:7000 after OSN recycling of **1** with PuraMem™ S380 57

Figure 4.19: PMPs formation of successive metathesis reactions at 80 °C and a Ru:1-octene molar ratio of 1:7000 after OSN recycling of **2** with PuraMem™ S380 57

Figure 4.20: PMPs formation of successive metathesis reactions at 80 °C and a Ru:1-octene molar ratio of 1:7000 after OSN recycling of **3** with PuraMem™ S380 58

List of Tables

Table 2.1: OSN membranes used previously with different top layer material and MWCO 10

Table 2.2: Summary of the previous work done on the separation of different homogeneous catalysts via OSN 11

Table 2.3: Comparison between heterogeneous and homogeneous catalysts.....17

Table 3.1: Summary of the manufacturer specification sheet for the PuraMem™ series of membranes 29

Table 4.1: Flux results of pure 1-octene with PuraMem™ at different pressures.....47

Table 4.2: Flux results of pure 1-tetradecene with PuraMem™ at different pressures.....47

Table 4.3: Summary of metathesis reaction results of 1-octene at 80 °C and a Ru/1-octene molar ratio of 1:7000 at 2100 min compared to that of **9**.....51

Table 4.4: Rejection results for PuraMem™ 280 with complexes **1**, **2** and **3**.....56

Table 4.5: Rejection results for PuraMem™ S380 with complexes **1**, **2** and **3** 58

List of Appendices

Appendix 1: FTIR spectra 62
Appendix 2: Mass spectra 64
Appendix 3: ^{1}H-NMR spectra 65
Appendix 4: ^{13}C-NMR spectra 68
Appendix 5: ^{31}P-NMR spectra 71

List of Abbreviations

^{1}H NMR	:	Proton nuclear magnetic resonance
^{13}C NMR	:	Carbon-13 nuclear magnetic resonance
^{31}P-NMR	:	Phosphorus-31 nuclear magnetic resonance
ADMET	:	Acyclic diene metathesis
bp	:	boiling point
C	:	Concerntration
C_8	:	1-Octene
C_{14}	:	Tetradecene
CM	:	Cross metathesis
DMF	:	Dimethylformamide
E	:	Electric potential
EYM	:	Enyne metathesis
FID	:	Flame ionization detector
GC	:	Gas chromatography
GC-MS	:	Gas chromatography – mass spectrometry
ICP–OES	:	Inductively coupled plasma-optical emission spectrometry
iPr	:	Isopropyl
is	:	Internal standard
IR	:	Infrared
IPs	:	Isomerization products
MF	:	Microfiltration
MW	:	Molecular weight
MWCO	:	Molecular weight cut-off
n.a.	:	Not available
n.d.	:	Not determined
NF	:	Nanofiltration
NHC	:	N-heterocyclic carbene
OSN	:	Organic solvent nanofiltration
P	:	Pressure
PA	:	Polyamide
PDMS	:	Polydimethylsiloxane
PES	:	Polyethersulfone
Ph	:	Phenol
PI	:	Polyimide

PMPs	:	Primary metathesis products
Gr2Ph	:	PUK-Grubbs 2-type precatalyst
RCM	:	Ring-closing metathesis
RF	:	Response factor
RO	:	Reverse osmosis
ROCM	:	Ring-opening cross metathesis
ROM	:	Ring-opening metathesis
ROMP	:	Ring-opening metathesis polymerization
RRM	:	Ring-reaarrangement metathesis
S	:	Selectivity
SHOP	:	Shell higher olefin process
SHP	:	Steric hindrance pore
SM	:	Self-metathesis
SMPs	:	Secondary metathesis products
SRNF	:	Solvent resistant nanofiltration
T	:	Temperature
THF	:	Tetrahydrofuran
TLC	:	Thin layer chromatography
TOF	:	Turnover frequency
TON	:	Turnover number
UF	:	Ultrafiltration

List of Complexes

1

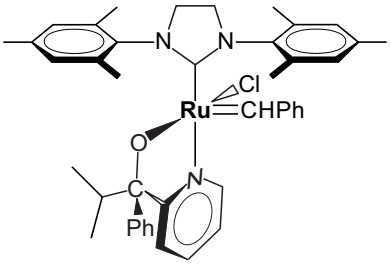

Benzylidene-chloro[1,3-bis-(2,4,6-trimethylphenyl)-2-imidazolidinylidene]-[1-(2'-pyridinyl)-1-isopropyl-1-phenyl-methanolato]ruthenium

2

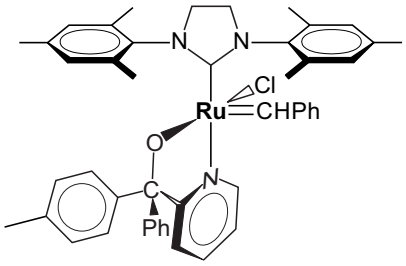

Benzylidene-chloro[1,3-bis-(2,4,6-trimethylphenyl)-2-imidazolidinylidene]-[1-(2'-pyridinyl)-1-(4'-methylphenyl)-1-phenyl-methanolato]ruthenium

3

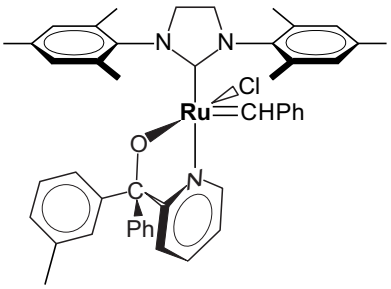

Benzylidene-chloro[1,3-bis-(2,4,6-trimethylphenyl)-2-imidazolidinylidene]-[1-(2'-pyridinyl)-1-(3'-methylphenyl)-1-phenyl-methanolato]ruthenium

4

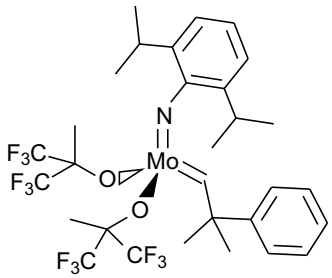

2,6-Diisopropylphenylimidoneophylidene molybdenum(VI) bis(hexafluoro-t-butoxide) (Schrock)

5

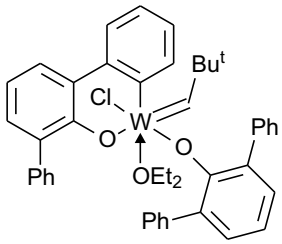

Cyclometalated aryloxy(chloro)neopentylidene tungsten

6	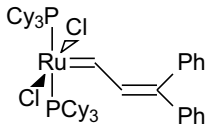	3,3-diphenylcyclopropene-dichloro(tris-tricyclohexylphosphine)ruthenium
7	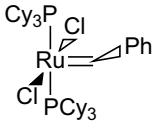	Benzylidene-dichloro[bis(tricyclohexylphosphine)]ruthenium (Grubbs 1)
8	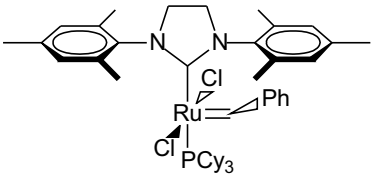	Benzylidene-dichloro(tricyclohexylphosphine)[1,3-bis(2,4,6-trimethylphenyl)-2-imidazolidinylidene] ruthenium (Grubbs 2)
9	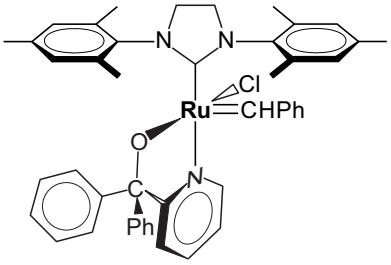	Benzylidene-chloro[1,3-bis-(2,4,6-trimethylphenyl)-2-imidazolidinylidene]-[1-(2'-pyridinyl)-1,1-diphenyl-methanolato]ruthenium (PUK-Grubbs 2)

List of Equations

Flux (*J*):

$$J = \frac{V_P}{A.\Delta t}$$

Rejection Percentage (R):

$$R = \left(1 - \frac{C_P}{C_R}\right) \times 100$$

Volume of internal standard nonane (V_{is}):

$$V_{is} = \left(\frac{V_{nonane}}{V_{1\text{-}octene}}\right) \times V_{sample}$$

For Volumes of C_8, PMPs, SMPs or IPs (V_X):

$$\mathrm{V_X} = \mathrm{V_{is}} \times (\mathrm{A_x} \times \mathrm{A_{is}}) \times \left(\frac{1}{\mathrm{RF}}\right)$$

For moles of C_8, IPs, PMPs or SMPs (n_X):

$$\mathrm{n_x} = \frac{\mathrm{V_x} \times \rho_\mathrm{x}}{\mathrm{MW_x}}$$

For mole percentage of C_8, IPs, PMPs or SMPs:

$$\%\mathrm{n_x} = \left(\frac{n_x}{n_{tot}}\right) \times 100$$

Selectivity (S):

$$\mathrm{S} = \left\{\frac{\%\mathrm{PMPs}}{\%(\mathrm{PMPs} + \mathrm{SMPs})}\right\} \times 100$$

Turnover number (TON):

$$\mathrm{TON} = \left\{\frac{\%\mathrm{PMPs} \times (\text{1-octene/Ru})}{100\%}\right\}$$

Chapter 1
Introduction and aims of study

1.1 Background

Homogeneous catalysts are used for the production of a broad range of organic compounds.[1,2] In the past, homogeneous catalysts were difficult to remove from their post-reaction mixtures, which resulted in the usage of heavy energy processes like extraction and distillation.[3,4]

One technology in literature[5,6] that has shown good potential to separate the catalyst from the reaction mixture is membrane technology. Although membrane technology is well established as a means of purifying water, its application to separate organic mixtures has increased over the past number of years in areas such as the pharmaceutical, fine chemical and petrochemical industries.[7] Some advantages of membrane technology is that there are commercially available membranes which are stable in organic solvents and that the process is energy-saving.[8]

In the past, there had been several investigations to recycle different homogeneous catalysts from their reaction mixtures using organic solvent nanofiltration (OSN) membrane or alternatively known as solvent resistant nanofiltration (SRNF) membranes.[6,9] The groups of Vankelecom,[10,11] Livingston[12,13] and others[14,15] successfully applied the OSN technique as an optional technique for separating and recycling homogeneous catalysts.

Some research has been done on recycling alkene metathesis catalysts, especially Grubbs-type precatalysts[6,16] from their reaction mixtures. Grubbs-type precatalysts are a series of transition metal carbene complexes for olefin metathesis, they accelerate the rate of formation of new alkene (olefin) molecules.[17] Alkene metathesis, **Figure 1.1**, is a catalyst-driven organic reaction where an alkene goes through a transalkylidenation process and new alkene molecules are formed.[18-19]

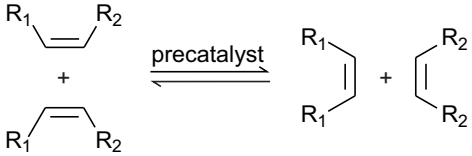

Figure 1.1: General alkene metathesis reaction.

For this study, new Grubbs-type precatalysts **1, 2** and **3** (**Figure 1.2**) were synthesized and investigated for the metathesis reaction of 1-octene.

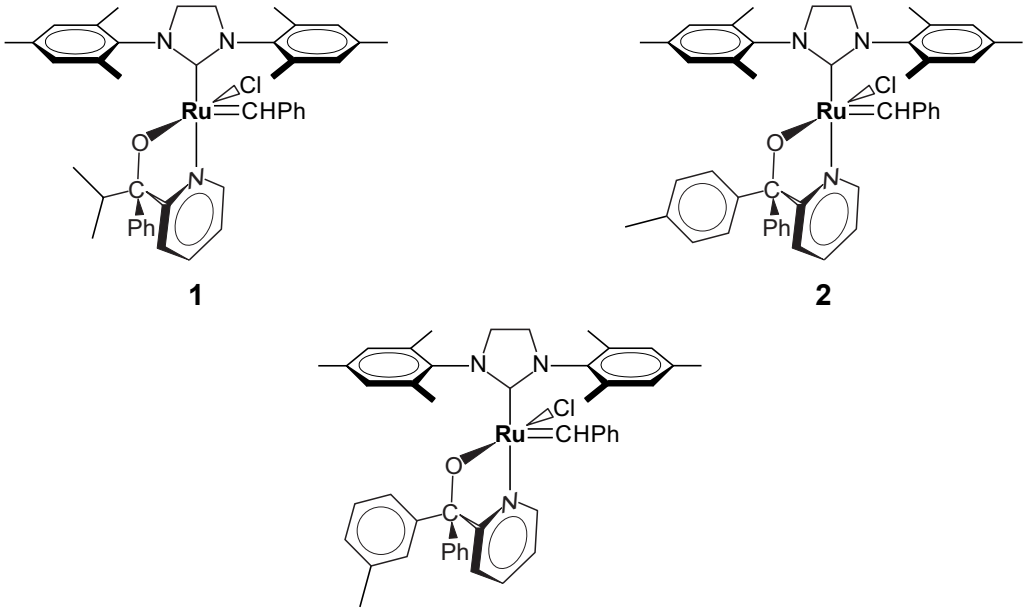

Figure 1.2: Grubbs-type precatalysts synthesized for this study.

The Grubbs 2-type precatalysts have shown in literature to have longer lifetimes, which allows them to be used industrially.[6] Past studies have been focusing on increasing the catalyst's initiation rate via electronic and steric adjustment of the different ligands, see **Figure 1.3**:

i. Anionic ligands (X's bound to the Ru metal)[20-21]

ii. Alkylidene moiety (carbene unit, =CHR)[22-23]

iii. Ancillary ligands (L_1 and L_2 ligands)[24-26]

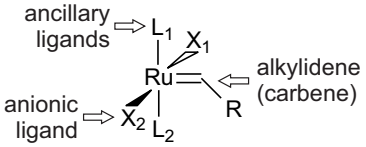

Figure 1.3: Description of ligands in Grubbs-type precatalysts.[6]

Lifetime, selectivity and stability are seen as the most important properties for the development of a catalyst for industrial application.[27] Verpoort[28-29] applied various catalyst synthesis ideas of adjusting and binding of the dissociating ligand, L_2, and the anionic ligand,

X_2, with bidentate O,N-chelated Schiff-base ligands that were introduced to the Grubbs first (**7**) and second generation (**8**) complexes in order to increase the catalyst lifetime which Grubbs[30] also attempted.

7 **8**

Figure 1.4: Grubbs first generation (**7**) and Grubbs second generation (**8**) precatalysts.

Jordaan,[31] Huijsmans[32] and Loock[33] conducted studies to improve the activity, selectivity and lifetime of similar precatalysts. Jordaan[31] found that the aromatic R groups of the N^O hemilabile ligand had a great influence on the activity and lifetime of the Grubbs-type precatalyst. A number of hemilabile ligands with various R groups on the N^O hemilabile ligand, their Grubbs derivatives and the metathesis behaviour of these precatalysts were investigated by computational and experimental means.[31-33]

It will be shown in this study that OSN can be used to separate **1**,**2**, and **3** (**Figure 1.2**) from their reaction mixtures. Their activity and ability to be recycled will also be tested.

1.2 Aim and Objectives

The study focuses on the research fields of OSN and alkene metathesis. According to literature,[6] commercially available Grubbs-type precatalysts have been separated from their post-reaction mixtures using OSN with different organic stable membranes.[34]

There are new Grubbs precatalysts and OSN membranes that are continously being developed and improved for, *inter alia*, industrial use. It is therefore, the aim of this study to use new precatalysts and OSN membranes to add to what is already in literature regarding the efficiency of the recovery of the metal precatalysts by selected nanofiltration membranes.

To achieve the aim of the project, the following objectives are stated:

- To extend the selection of commercially available nanofiltration membranes already available in literature that are both solvent resistant and stable for the recovery of Grubbs-type precatalysts from their reaction mixtures.

- To use precatalysts **1**, **2** and **3** for the metathesis reaction of 1-octene and perform lifetime studies.
- To recover these Grubbs-type precatalysts from their post-reaction mixtures using OSN and re-use them.
- To use ICP-OES to determine/investigate the rejection (%) concentrations of the precatalysts.

1.3 Scope of investigation

Organic Solvent Nanofiltration (OSN)

i. OSN characterization

To add to what is already there in literature a list of OSN membranes capable of separating grubbs precatalysts were obtained. To achieve the separation of precatalysts from reaction mixtures, a good understanding of the permeation performances of pure 1-octene, 7-tetradecene components and binary mixtures (1-octene and 7-tetradecene) through the PuraMem™ series of membranes by determining the flux, *J*.

Metathesis

i. To show the metathesis reactions of 1-octene with complexes **1**, **2** and **3**, and determine their activity at 80 °C.

ii. To understand the catalytic lifetime of complexes **1**, **2** and **3** at 80 °C.

iii. To understand the rejection and recovery of complexes **1**, **2** and **3** with PuraMem™ series of membranes at 50 bar.

1.4 Layout of dissertation

The dissertation is divided into the following five chapters:

Chapter 1 gives a broad overview of the contents of the study.

In **Chapter 2** the literature survey on the two research fields of nanofiltration and metathesis are presented.

In **Chapter 3** all experimental apparatus and methods that were used in this study are described in detail.

Chapter 4 emphasizes the metathesis reaction of 1-octene metathesis with different precatalysts at 80 °C with molar ratio 1:7000 (Ru/1-octene). Their lifetime studies at 80 °C,

at a Ru/1octene molar ratio of 1:7000 and the separation process of the 1-octene metathesis system with OSN at 50 bar.

Chapter 5 summarizes the main conclusions of the work described in this dissertation and recommends possible future work.

1.5 References

1. Parshall, G.W., Ittel, S.D., *Homogeneous Catalysis*, Wiley (New York), 1992
2. Parshall, G.W., Nugent, W.A., *Chemtech*, 1998, **184**, 314, 376
3. Anastas, P.H., Williamson, T.C., Green Chemistry. Frontiers in Benign Chemical Synthesis and Processes, Oxford University Press, Oxford, 1998
4. Jodicke, G., Zenklusen, O., Weidenhaupt, A., Hungerbuhler, K., *J. Clean Prod*., 1999, **7**, 159
5. Wong, H.T., Pink, C.J., Ferreira, F.C., Livingston, A.G., *Green Chem*., 2006, **8**, 373
6. Van der Gryp, P., Barnard, A., Cronje, J.P., De Vlieger, D., Marx, S., Vosloo, H.C.M., *J. Membr. Sci*., 2010, **353**, 70
7. Brumaghim, J.L., Girolami, G.S., *Organometallics*, 1999, **18**, 192
8. See-Toh, Y.H., Silva, M., Livinsgton, A., *J. Membr Sci*, 2008, **324**, 220
9. Priske, M., Wiese, K.-D., Drews. A., Kraume, M., Baumgarten, *J. Membr. Sci*., 2010, **360**, 77
10. Aerts, S., Weyten, H., Beukenhoudt, A., Gevers, L.E.M., Vankelecom, I.F.J., Jacobs, P.A., *Chem. Commun*., 2004, 710
11. Vankelecom, I.F.J., De Smet, K., Gevers, L.E.M., Livingston, A., Nair, D., Aerts, S., Kuypers, S., Jacobs, P.A., *J. Membr. Sci*., 2004, **231**, 99–108
12. Luthra, S.S., Yang, X., Freitas dos Santos, L.M., White, L.S., Livingston, A.G., *J. Membr. Sci*., 2002, **201**, 65
13. Scarpello, J.T., Nair, D., Freitas dos Santos, L.M., Livingston, A.G., *J. Membr. Sci*., 2002, **203**, 71
14. Dijkstra, H. P., Van Klink, G.P.M., Van Koten, G., *Acc. Chem. Res*, 2002, **35**, 798-810
15. Gallego, I., Mallada, R., Urriolabeitia, E.P., Navarro, R., Menedez, M., *Inorg. Chim. Acta*, 2004, **357**, 4577-4581
16. Wijkens, P., Jastrezebski, J.T.B.H., Van der Schaaf, P.A., Kolly, R., Hafner, A., Van Koten, G., *Org. Lett.,* 2000, **2**, 1621
17. Wagner, P.H., *Chem. Ind*., 1992, 330
18. Parshall, C.W., *Homogeneous Catalysis*, Wiley (New York), 1980
19. Calderon, N., Chen, H.Y., Scott, K.W., *Tetrahedron Lett*., 1967, **34**, 3327
20. Yang, L.R., Mayr, M., Wurst, K., Buchmeiser, M., *Chem. Eur. J*., 2004, **10**, 5761
21. Conrad, J.C., Snelgrove, J.L., Eeelman, M.D., Hall, S., Fogg, D.E., *J. Mol. Catal., A: Chem*. 2006, **254**, 105
22. Michrowska, A., Bujok, R., Harutyunyan, S., Sashuk, V., Dolgonos, G., Grela, K., *J. Am. Chem. Soc*., 2004, **126**, 9318
23. Love, J.A., Morgan, J.P., Trnka, T.M., Grubbs, R.H., *Angew. Chem. Int. Ed*., 2002, **41**, 4035

24. Dinger, M.B., Mol, J.C., *Adv. Synth. Catal*., 2002, **344**, 671
25. Yun, J., Marinez, E.R., Grubbs, R.H., *Organometallics*, 2004, **23**, 4172
26. Rittler, T., Day, M.W., Grubbs, R. H., *J. Am. Chem. Soc*., 2006, **128**, 11768
27. Deckers, P.J.W., Non Flory-Schulz Ethene Oligomerization with Titanium-based Catalysts, PhD-thesis (University of Groningen), 2002
28. De Clerq, B and Verpoort, F., *Tetrahedron Lett*., 2002, **43**, 9101
29. De Clerq, B and Verpoort, F., *Adv. Synth. Catal*., 2002, **344**, 639
30. Chang, S., Jones, I.I.L., Wang, C., Henling, L.M., Grubbs, R.H., *Organometallics*, 1998, **17**, 3460
31. Jordaan, M., Experimental and Theoretical Investigation of New Grubbs-Type Catalysts for the Metathesis of Alkenes, PhD-thesis (North-West University), 2007
32. Huijsmans, C.A.A., Modelling and Synthesis of Grubbs-Type complexes with Hemilabile Ligands, MSc-dissertation (North-West University), 2009
33. Loock, M.M., The Alkene Metathesis Reactivity of the PUK-Grubbs 2-precatalyst, MSc-dissertation (North-West University), 2009
34. Van der Gryp, P., Separation of Grubbs-Based catalysts with nanofiltration, PhD-thesis (North-West University), 2008

Chapter 2
Literature review

2.1 Organic Solvent Nanofiltration (OSN)

2.1.1 Introduction

An interesting field, particularly in catalyst separation, is organic solvent nanofiltration (OSN). OSN is a pressure-driven, membrane-based technique for product/catalyst isolation which has demonstrated its proficiency in many studies.[1,2] Laboratory scale and commercial scale applications of OSN membranes have been reported.[1,2] In the development and application of membrane processes, the characterization of membranes and modelling are essential steps.[3]

2.1.2 Membranes

A membrane is a barrier which separates two phases and restricts the transport of various chemical species in a rather specific manner[4] when a driving force is applied. The membrane is at the heart of every membrane process and can be considered an interface between two phases.[5] A schematic representation of a typical membrane separation is given in **Figure 2.1**.

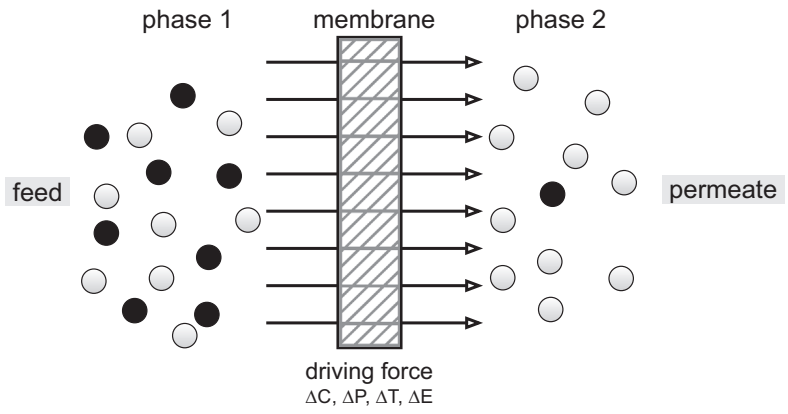

Figure 2.1: Schematic representation of a two-phase system separated by a membrane.[4]

Phase 1 is usually considered the feed or upstream side phase, while phase 2 is considered the permeate or downstream side. Separation can be achieved by different driving forces through the membrane; these include a pressure difference (ΔP), a temperature difference (ΔT), a concentration difference (ΔC) and a difference in electric potential (ΔE) across the membrane.[6]

The performance of a membrane is usually determined by two separation parameters, namely the flux of the different solvents through the membrane and the rejection of the different solutes by the membrane.[7]

Solvent flux, *J*, is the volume, mass or mol of a given solvent that passes through the membrane per unit area and time ($L.m^{-2}.h^{-1}$):

$$J = \frac{V_P}{A.\Delta t} \qquad 2.1$$

where V_p = volume solvent permeated through membrane

A = active membrane area

Δt = the difference in the time taken to permeate amount (volume) of solvent

Rejection (R) performance can be defined as the percentage of solute not permeating through the membrane:

$$R = \left(1 - \frac{C_P}{C_R}\right) \times 100 \qquad 2.2$$

where C_P =final concentration of the catalyst in the permeate

C_R = final concentration of the catalyst in the retentate

A membrane can be homogeneous or heterogeneous, symmetric or asymmetric in structure. Its thickness may vary between less than 100 nm to more than a centimeter.[4] Membranes are normally supplied in different formats, namely: tubular, hollow-fiber, spiral or flat-sheet arrangements and they differ in material used.[8] All these membranes can be employed in what is called the filtration spectrum,[5,9] i.e. reverse osmosis (RO), nanofiltration (NF), ultrafiltration (UF), and microfiltration (MF). These membranes are suited for a variety of applications in the different formats as follows:

- Tubular membranes[8]

  Mostly used in the MF and UF spectrum because of their ability to handle process streams with high solids and high viscosity properties. Their main applications are in mining, textile and dyes, etc.

- Spiral membranes[8]

  Made from layers of flat-sheet membranes, they are energy efficient and economical. Mostly found from the NF and RO to the UF spectrum. They are used for organics removal, seawater desalination, brackish water treatment, etc.

- Hollow-fiber membranes[8]

  Widely used in the wine, food, beverage, dairy, biotechnology and beverage industries, etc. They are found in the MF and UF spectrum.

- Flat-sheet membranes[8]

  They are OSN commercial membranes that have applications in the processing industries for natural products, and in the pharmaceutical, chemical and fine chemical industries. For the purpose of this study the focus will be on OSN commercial membranes. The key properties of these membranes are[10]:

  - high fluxes
  - good mechanical, chemical and thermal stability under operating conditions,
  - narrow pore distribution or sharp molecula weight cut-off (MWCO),
  - good compatibility with operating environment, and
  - cost effective.

The molecular structures of different membranes are among the information provided by the manufacturer.[9] **Figure 2.2** shows typical materials of membranes.

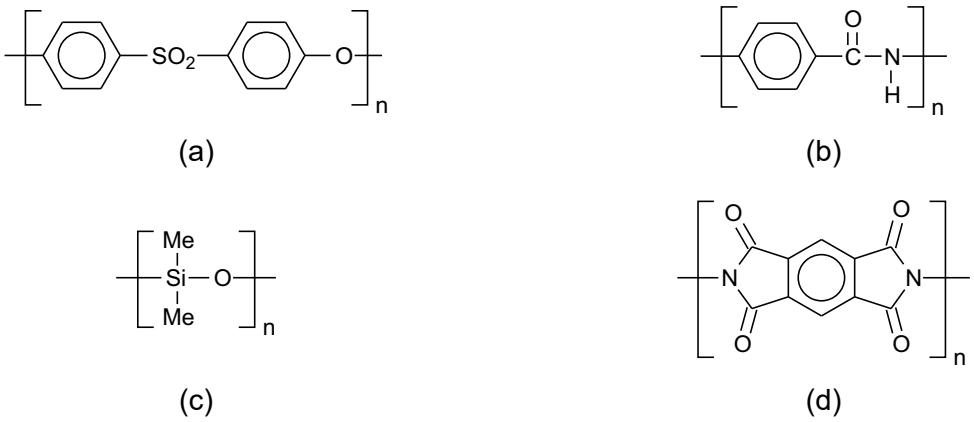

Figure 2.2: Typical structures of membranes: (a) polyethersulfone (PES), (b) polyamide (PA), (c) polydimethylsiloxane (PDMS), (d) polyimide (PI).

Membranes with the structures shown in **Figure 2.2** have been used in previous studies. One of the recent studies done on Grubbs-type catalysts was with the StarMem®-type of membranes,[35] which contain a PI molecular structure (**Table 2.1**).

Table 2.1 shows some membranes that have been used in previous studies with different molecular structures and MWCOs. MWCO is defined as the molecular weight cut off of a reference solute agreeing to a 90% rejection for a given solute or solvent.[9] It often says a lot about the quality of the membrane.[9]

Table 2.1: OSN membranes used previously with different materials and MWCO.[9]

Membrane	Manufacturer	Material	MWCO (Da)	Used since
N30F	Nadir[a]	PES	400	2000
NF-PES-010	Nadir	PES	1000	2000
MPF-44	Koch[b]	PDMS	250	2000
MPF-50	Koch	PDMS	700	2000
Desal-5-DK	Osmonics[c]	PA	150-300	2002
Desal-5-DL	Osmonics	PA	150-300	2002
HITK-1T	HITK[d]	TiO_2	220	2003
FSTI-128	VITO[e]	TiO_2	420	2003
FSTI-209	VITO	TiO_2	430	2004
StarMem® 120	MET[f]	PI	200	2005
StarMem® 122	MET	PI	220	2005
StarMem® 228	MET	PI	280	2005
DuraMem™ 150	Evonik[g]	PI	150	2010
DuraMem™ 200	Evonik	PI	200	2010
DuraMem™ 300	Evonik	PI	300	2010
PuraMem™ 280	Evonik	PI	280	2010
PuraMem™ S380	Evonik	PI	600	2010

[a] Nadir Filtration GmbH,Wiesbaden, Germany
[b] Koch membrane, Wilmington, MA, USA
[c] Osmonics GE, Vista, CA, USA
[d] HITK Hermsdorfer Institut fűr Technische Keramik, Hermsdorf, Germany
[e] VITO Vlaamse Instelling voor Technologisch Onderzoek, Mol, Belgium
[f] MET Membrane Extraction Technology, London, UK
[g] Evonik MET Ltd, Wembley, UK

2.1.3 Review of OSN membranes for homogeneous catalyst separation.[7]

Recent publications in the field of OSN, focusing on the separation of different kinds of homogeneous catalysts, are given in **Table 2.2**.

Table 2.2: Summary of the previous work done on the separation of different homogeneous catalysts via OSN.[7]

Year	Catalyst	Reaction Type	Catalyst Molecular Weight ($g.mol^{-1}$)	Membrane	Rejection (%)	Ref.
1996	Chiral polymer-enlarged	Diethylzinc addition	9600	PAH-20	99.8	11
1998	Oxazaborolidines	Reduction of ketones	13800	MPF-50	>98	12
1999	Dendritic palladium based	Allylic substitution	10200	MPF-50	99.9	13
2000	Rhodium-based	Hydroformylation	n.a.	MPF-60	n.d.	14
2001	Sharpless dihydroxylation catalyst	Dihydroxylation	>20000	unknown	n.d.	15
	Ru-BINAP	Asymmetric hydrogenation	929	MPF-60	>97	16
	Rh-EtDUPHOS	Asymmetric hydrogenation	723	MPF-60	>98	16
	BPPM catalyst	Asymmetric hydrogenation	>7460	YC05	99.1	17
	Heck-catalyst	Heck reaction	749	StarMem® 122 MPF-50 MPF-60	90 n.a. n.a.	18
2002	TOABR	Substitution reaction	546	StarMem® 122	>99	19
	TOABR	Substitution reaction	546	MPF-50 MPF-60 Desal-5 StarMem® 122 StarMem® 120 StarMem® 240 Silicone Rubber EPDM Rubber	48 86 62 >99 >99 >99 >99 >99	20
	TBABr	Substitution reaction	322	MPF-50 MPF-60 Desal-5 StarMem® 122 StarMem® 120 StarMem® 240 Silicone Rubber EPDM Rubber	61 89 55 >99 >99 80 >99 >99	20
	Jacobsen	Chiral epoxidation	622	MPF-50 StarMem® 122 StarMem® 120 StarMem® 240 Desal-5	>81.4 >95.8 99.6 95.4 >77.9	21
	Pd-BINAP	Asymmetric carbon-carbon bond	849	MPF-50 StarMem® 122 StarMem® 120 StarMem® 240 Desal-5	>93.4 1 1 >94.9 >88.6	21

Year	Catalyst	Reaction Type	Catalyst Molecular Weight ($g.mol^{-1}$)	Membrane	Rejection (%)	Ref.
2002	Wilkinson	Hydrogenation and Reduction	925	MPF-50 StarMem® 122 StarMem® 120 StarMem® 240 Desal-5	>57.8 98 99.4 78.7 93	21
	Grubbs-type	Alkene Metathesis	3230	MPF-60	n.d.	22
2003	Wilkinson	Hydrogenation and Reduction	925	SiO-membrane	>99.9	23
2004	Pd(II)-complex	Dies-Alder reaction	unknown	Silicalite membranes	>97	24
2005	Wilkinson	Hydrogenation and Reduction	925	Zeolite PDMS ZSM-5 USY MPF-50	78 98 98 81	25
2006	Co-Jacobsen	Hydrolytic kinetic resolution of epoxides	626	COK M2 COK M2 PDMS PDMS TFC-SR2 Desal GE MPF P005F NF-PES-10 Desal DL	98 83 86 78 82 ≈20 ≈15 ≈10 ≈10 ≈5	26
	Ru-BINAP	Asymmetric hydrogenation with ionic liquid	749	StarMem® 122	>94	27
	Palladium-based	Suzuki reaction	n.d.	StarMem® 122	n.d.	28
2007	Pt catalyst	Hydrosilation	n.a.	PDMS	n.d.	29
2008	Palladium catalyst	Suzuki coupling reaction	1035	StarMem® 122	90	30
	Ruthenium catalyst	Asymmetric hydrogenation	1240	Two layered ceramic membrane	97	31
2009	Ru-BINAP	Asymmetric hydrogenation	723	StarMem® 122	90	32
	Hoveyda- Grubbs type complex	Olefin-metathesis	1500	PDMS membranes	99.8	33
2010	Hoveyda-Grubbs catalyst	Olefin metathesis	280	StarMem® 228	n.d.	34
	Grubbs-type	Alkene metathesis	794-822	StarMem® 228	>99	35
	Rhodium catalyst	Hydroformylation	≈850	PI membrane	99	36
	Chromia catalyst	Dehydrogenation reaction	n.a.	DD3R Zeolite membrane	n.d.	37
	Rhodium catalyst	Hydroformylation	450	Ceramic membrane	>99.96	38
2011	Rhodium complex	Hydroformylation	n.d.	StarMem® 220	n.d.	39

Year	Catalyst	Reaction Type	Catalyst Molecular Weight ($g.mol^{-1}$)	Membrane	Rejection (%)	Ref.
2011	Nickel catalysts	Cross flow	n.d.	Ceramic Membrane	n.d.	40
	SILP Catalyst	Alkene metathesis	1277	Unknown	n.d.	41
2013	POSS-tagged Grubbs-Hoveyda-Type	Olefin metathesis	n.d. n.d. n.d.	StarMem® 228 StarMem® 280 Built-in commercial membrane	n.d. n.d. 98	42 42 43

n.a. = not available
n.d. = not determined

From **Table 2.2**, Sairam *et al.*[34] looked at olefin metathesis, as the model reaction, with the Hoveyda-Grubbs catalyst (MW = 280 $g.mol^{-1}$) and the membrane used was the StarMem® 228, and the rejection of the catalyst not determined. Van der Gryp *et al.*[35] investigated the separation and re-usability of five commercial Grubbs-type complexes with the StarMem® 228 membrane. The modeled reaction used was the self-metathesis reaction. They discovered that the OSN process with StarMem® 228 separates these Grubbs-type catalysts with a rejection greater than 99%.[35]

In 2000, Wijkens *et al.*[22] conducted an investigation on separation and the re-usability of different Grubbs-type catalysts. The ring closing metathesis reaction was the modeled metathesis reaction used. They were not successful in separating their metathesis catalytic system in an active form using OSN technology. Their conclusion was that the active area of the MPF-60 OSN membrane used for investigation deactivated the catalyst.

In 2013, Kajetanowicz *et al.*[42] synthesized weight-enlarged metathesis catalysts, that had a polyhedral oligomeric silsesquioxane (POSS) tag for a continuous metathesis reaction, and discovered that the membranes StarMem® 228 and PuraMem™280, successfully separated the catalyst from the reaction mixtures to below 3 ppm concentrations. Skowerski et al.[43] prepared a mass-tagged Grubbs-Hoveyda-type complex for olefin metathesis, the rejection was done with a built-in commercial membrane and 97.6% of the ruthenium was retained in the membrane, affording a product of high purity (<10 ppm of Ru).

In summary, this study will consider the alkene metathesis reaction as the model reaction with Grubbs-type precatalysts, using the PuraMem™ 280 and PuraMem™ S380 membranes for OSN reactions.

2.2 Alkene Metathesis

2.2.1 Introduction

In 1967, alkene metathesis was introduced by Calderon.[44] Eleuterio[45-46] wrote a patent on alkene metathesis which described the transformation of hydrocarbons. But it was only after the work of Banks and Bailey[47] that the metathesis reaction was discovered.[47] Alkene metathesis is defined as the interchange of carbon atoms between a pair of double bonds in the presence of a precatalyst,[48] as shown in **Figure 1.1**.

There are different categories of alkene metathesis reactions.[48-51] These include:

- Self-metathesis (SM)

  A SM reaction is a reaction where an alkene reacts with itself. There are two types of SM. Productive SM and non-productive or degenerate SM. Productive SM leads to the formation of new products:

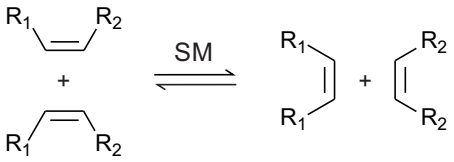

  Non-productive SM reactions do not lead to the formation of new products:

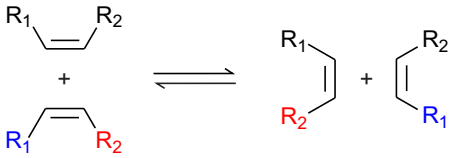

- Acyclic cross-metathesis (CM)

  CM involves different alkene substrates that are both acyclic compounds, and acyclic and cyclic compounds.

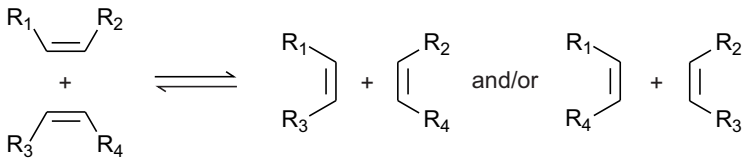

❖ Ring-closing metathesis (RCM) and ring-opening metathesis (ROM)

RCM is a unimolecular condensation reaction of a diene to form a cyclic olefin and a small condensate olefin as a byproduct. The reverse reaction is named ROM.

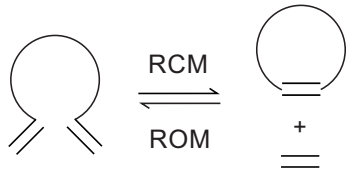

❖ Ring-opening cross-metathesis (ROCM)

ROCM is similar to the CM reaction, except that one of the acyclic alkenes is replaced with a cyclic alkene.

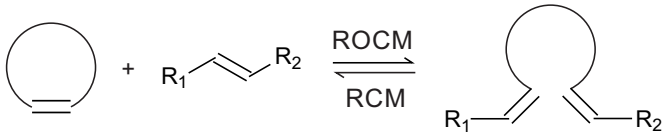

❖ Ring-opening metathesis polymerization (ROMP)

ROMP is a chain-growth polymerization reaction, which is a useful industrial process for producing unsaturated polymers from cycloalkenes. It involves a cyclic olefin and the driving force is the relief of strain in the ring.

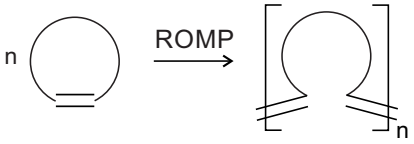

❖ Acyclic diene metathesis (ADMET)

This is a step-growth condensation reaction used to polymerize certain terminal dienes to polyenes. New bonds formed could either be in cis- or trans-configurations.

- Enyne metathesis (EYM)

  Discovered by Katz *et al.* in 1985, it is a bond reorganization of an alkene and an alkyne to give a 1,3 diene.

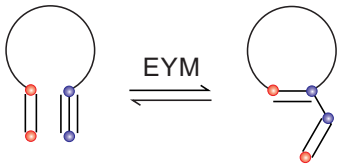

- Ring-rearrangement metathesis (RRM)

  RRM has proven to be a commanding weapon for the rapid construction of complex structures.[52] RRM refers to the combination of several metathesis transformations into a domino process in which an endocyclic double bond of a cycloolefin reacts with an exocyclic alkene.[52]

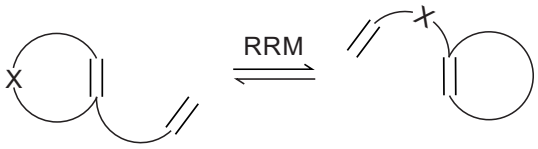

For this study the focus will be on the SM reaction of 1-octene with Grubbs-type precatalysts to give as major products two isomers, cis- and trans-7-tetradecene, and ethene.

2.2.2 Alkene metathesis industrial applications

New routes for important polymer chemicals, in petrochemical industries and research have been opened up by alkene metathesis, which is broadly applied in catalysis and synthesis reactions.[53] Large-scale olefin metathesis is key in the production of linear olefins. Its largest application being in the Shell higher olefin process (SHOP), which produces more than 10^5 tons of C_{10} and C_{20} olefins and alkenes a year.[54]

Sasol Ltd., a petrochemical company in South Africa, makes use of the Fischer-Tropsch process to produce alkenes in the range of C_5 to C_9.[55] Alkene metathesis is used to convert the low value alkenes (i.e 1-heptene) present in the Fischer-Tropsch product to high value alkenes (i.e 6-dodecene) for the production of detergent-range alcohols and other high value alkenes including C_{10} to C_{13} branched alkenes.[55] The conversion of the C_8 α-alkene to the valuable C_{14} alkene used as a detergent alcohol feedstock will also be studied.[56]

Other recent applications include, the production of pharmaceutical drugs and propylene, and the transformation of renewable plant-based raw materials into hair and skin care products.[51]

2.2.3 Catalytic systems

In general there are two main types of catalytic systems, i.e., homogeneous and heterogeneous.[57] Homogeneous catalysts offer several advantages over their heterogeneous counter-parts as shown in **Table 2.3**, which gives comparisons between heterogeneous and homogeneous catalysts.

Table 2.3: Comparison between heterogeneous and homogeneous catalysts.[55]

	Homogeneous catalysts	**Heterogeneous catalysts**
Catalyst lifetime	Short	Long
Selectivity	High	Low
Activity	High	Low
Catalyst poisoning	Low	High
Reaction conditions	Mild	Harsh
Catalyst recycling	Expensive	Cheap

During the late 1960's to the early 1980's ill-defined homogeneous and heterogeneous systems, with unknown active species that are not easily accessible, were used to initiate alkene metathesis.[58-59] In the 1990's, well-defined metal carbene homogeneous precatalyst systems based on molybdenum (Mo), tungsten (W) and ruthenium (Ru) were discovered.[60-62] With the discovery of these well-defined precatalysts by Schrock[63] and Grubbs[64] (**Figure 2.3**) the development of alkene metathesis as a weapon for organic synthesis started being of high interest.[65-66] The development of these well-defined systems is based on the premise that a metal carbene is the active species in alkene metathesis.[81]

Two types of mechanisms were suggested for metathesis with well-defined precatalysts, i.e. an associative and a dissociative mechanism. In the associative mechanism both phosphine ligands remain on the pre-catalyst while the olefin coordinates to the pre-catalyst to form the intermediate 18-electron olefin complex, followed by the actual [2+2] cycloaddition and cycloreversion steps.[80] The dissociative mechanism starts off with an initial loss of a

phosphine ligand, forming a 14-electron complex.[80] The vacant site is then occupied by the incoming olefin which undergoes metathesis to form a metallacyclobutane product, regenerating the pre-catalyst upon recoordination of the phosphine.[80]

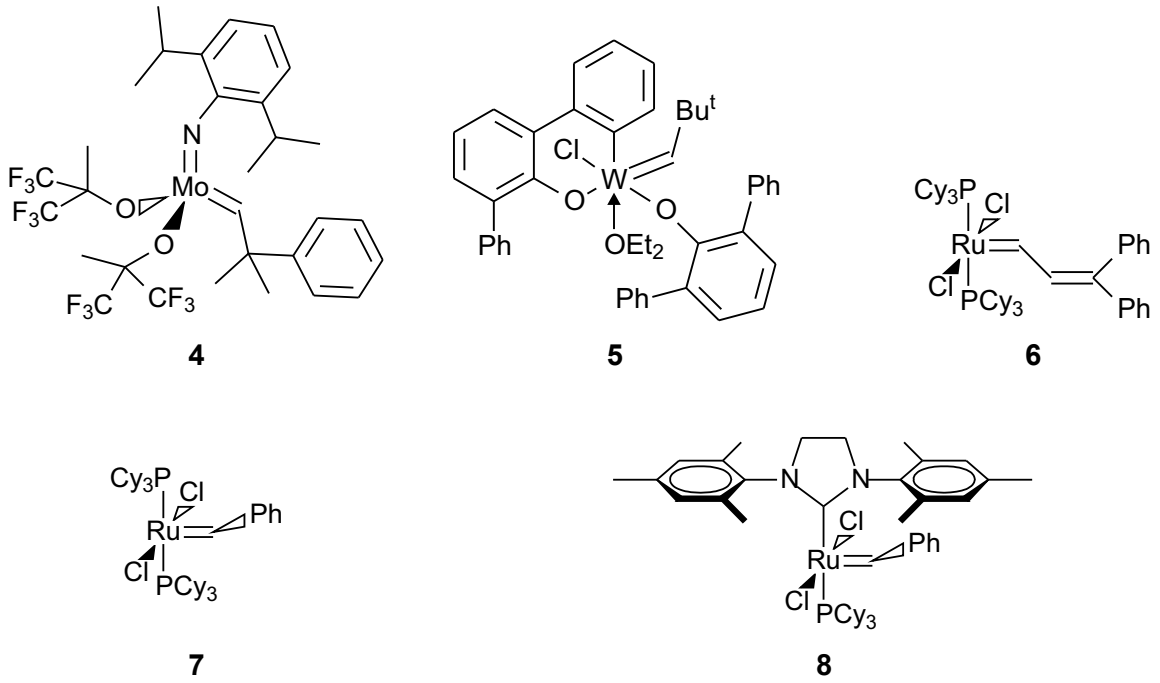

Figure 2.3: Well-defined metal alkylidene complexes.[53]

Because this study focuses on a Grubbs-type precatalyst, the dissociative mechanism[64] (**Figure 2.4**) associated with these precatalysts will be discussed. The dissociative mechanism for 1-octene metathesis with Grubbs-type precatalyst is shown in **Figure 2.4** and **Figure 2.5**.[53] The mechanism is triggered by the dissociation of the PCy_3 ligand from the benzylidene complex **A** to the active type **B**. Firstly, the precatalyst is converted from Benzylidene (A) to the methylidene (**F1**) or heptylidene (**F3 and F4**) complexes before it enters the catalytic cycle, **Figure 2.4**.[53] In **Figure 2.5**, the heptylidene is converted to methylidene, which gets converted back to heptylidene until the precatalyst has decomposed or all the C_8 has been consumed. During the conversion of methylidene to heptylidene, ethane forms, while from heptylidene to methylidene *cis*- and *trans*- 7-tetradecene are formed.[53]

Though complex **4** (has a greater tolerance for functional groups than complex **5**, their only setback was their sensitivity towards water, oxygen and other functional groups such as ketones, alcohols and aldehydes. It was through the extensive work by Grubbs[64] that ruthenium carbene complexes have come to be at the forefront of leading precatalysts due to

their stability in air and water, tolerance to various functional groups with O and N, and their handling. These homogeneous precatalysts offer several advantages over heterogeneous precatalysts such as that all sites are accessible, and it is possible to adjust the chemoselectivity, regioselectivity and enantioselectivity of the catalyst.[55,64]

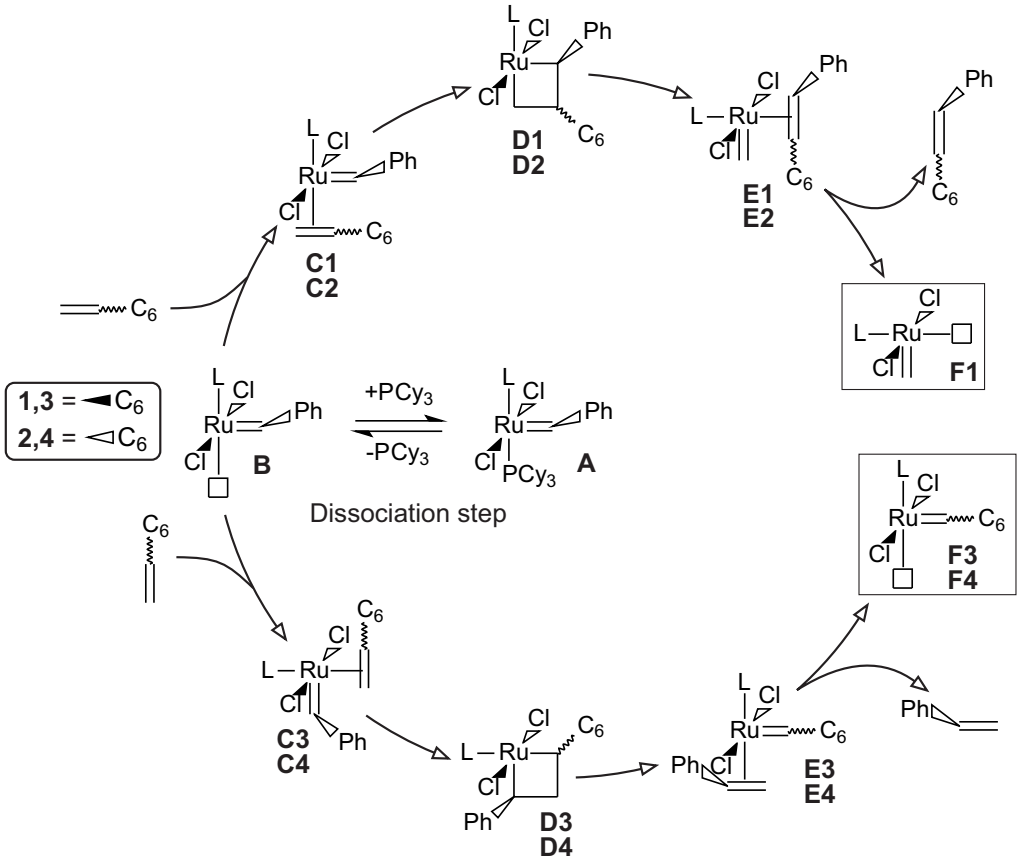

Figure 2.4: Dissociative mechanism with Grubbs-type complexes (L = Pcy_3 or H_2IMes).[53]

Research has been done in improving the reactivity and lifetime of ruthenium complexes such as complex **7** and complex **8**, with different functional groups.[53,59,67] These Grubbs precatalystcatalysts changed olefin metathesis into an all-round instrument in polymer and organic chemistry.[65,66,68]

Complex **7** and **8** operate under mild conditions and are very tolerant to air and moisture.[68-70] Although there are several advantages offered by these precatalysts, like selectivity and activity, there are still hindrances that hamper the usage of these precatalysts industrially, i.e. their relatively short catalytic lifetime. Experimental and theoretical studies have been done in trying to improve their lifetime. Though complex **7** has high selectivity during the metathesis of

alkenes, its drawback is that it is thermally unstable,[71-72] which led to the development of complex **8** by replacing the phosphine ligand with a basic N-heterocyclic carbene (NHC) ligand, which improved the thermal stability, lifetime and activity of complex **7**.[51]

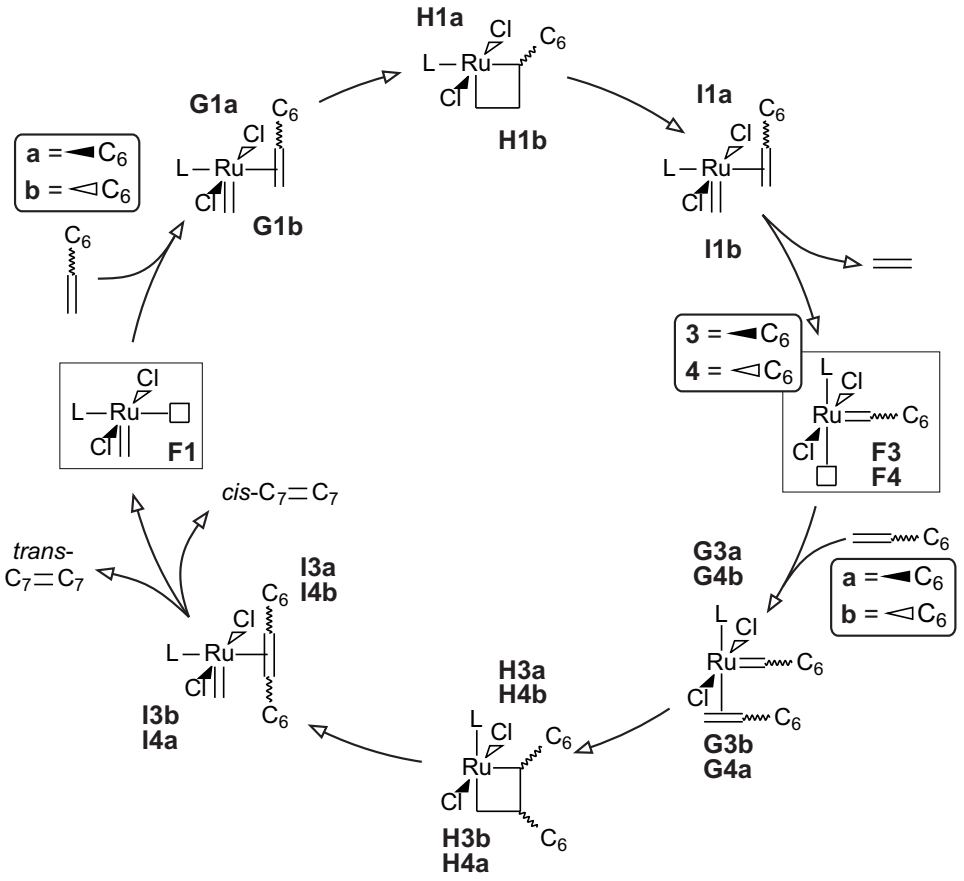

Figure 2.5: Catalytic cycle in the productive mechanism of C_8 metathesis (L = PCy_3 or H_2IMes).[53]

The lifetime of Grubbs precatalysts was shown to improve with the introduction of different ligands.[53] Past researchers, in search of a more stable and active catalytic systems for metathesis reactions, have developed different design concepts to obtain ruthenium carbene initiators for RCM/ROMP reactions (**Figure 2.6**).[53]

These designs were done to control the dissociation of L_b at room temperature. For Design 1 (**D1**), where L_b is in a position *trans* to L_a (mostly PCy_3 or NHC) too labile at room temperature. Other researchers overcame this by using chelating ligands where L_b was also attached (to the central ruthenium atom) via the carbene (D2)[53] or via the Cl position (**D3**).[53]

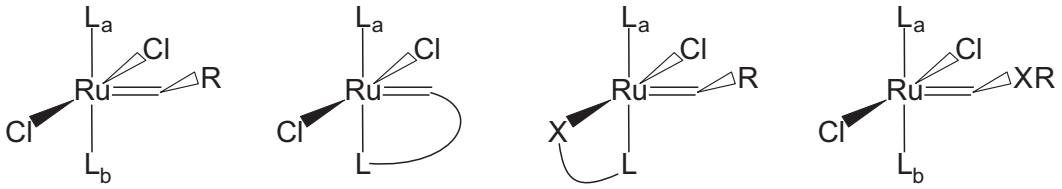

D1 **D2** **D3** **D4**

Figure 2.6: Design concepts for thermally switchable initiators.[53]

Unlike **D3**, for design 2 (**D2**) the expensive carbene ligand is destroyed during the Ru=C metathesis reaction (**Figure 2.7**). Design 4 (**D4**) catalytic systems have been mostly used for ROMP/RCM experiments at elevated temperatures (where X = O, N or S).

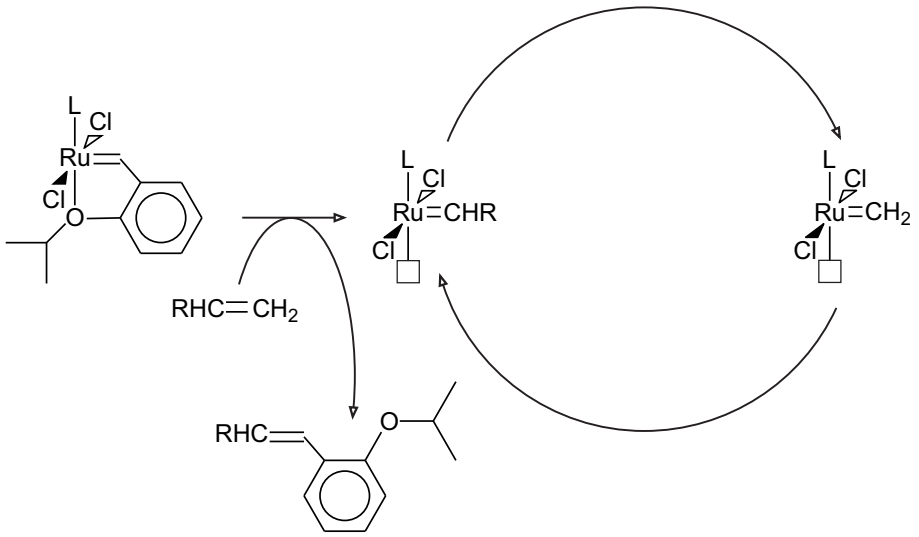

Figure 2.7: Simplified mechanism with a Hoveyda-Grubbs-type (**D2**-type) precatalyst.

The rotation of the phenyl group (**Figure 2.8**), which leads to the dissociation of the Ru-O (ether) bond, around the aromatic carbon-carbene carbon bond creates an open position. One of the unique properties of the Hoyveda-Grubbs-type complexes is the absence of the dissociative phosphine which can deactivate the Ru carbenes.

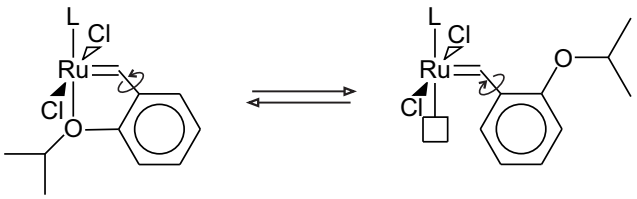

Figure 2.8: "Dissociation" step for a Hoyveda-Grubbs-type precatalyst.

It was suggested by Randl et al.[73] that activity in metathesis is dependent on the electronic properties of the Ru-carbene complex.[73] The application of bidentate ligands with a quite fixed backbone might be a way of increasing the selectivity of active complexes.[74] Hemilabile ligands have the potential to place more than two donor atoms (having different electronic properties for the formation of Z and A bond donor atoms) close to the metal atom[75] (see **Figure 2.9**), similar to chelating ligands which are ligands that can be attached to the metal atom (M) with two or more bonds.[75]

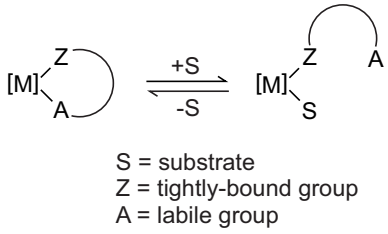

Figure 2.9: Representation of the hemilability concept.[59,67]

For Design 3 (**D3**), introduced by Grubbs[76] and Verpoort,[77] a bidentate O,N-chelated Schiff-base ligand was introduced into **7** to give control of the *cis/trans* selectivity in alkene metathesis and maintaining high activity. The catalytic activity increases with an increase in reaction temperature.[53] A Schiff-base is a weakly basic ligand with a general formula of $R_1R_2C{=}NR_3$ were R_3 is an alkyl or an aryl group.[59] The purpose of this aryl or alkyl group is to make a Schiff-base ligand a stable imine.[59] The idea worked so well during the Ru=C metathesis reaction because the ligand is not destroyed (**Figure 2.10**) which increases the activity of the precatalyst.[53]

Jordaan et al.[53] applied concept **D3** by using a hemilabile pyridinyl-alcoholato ligand.[53] Herrmann[78] and Hafner[79] also used the same design with hemilabile pyridinyl-alcoholato, alkylphosphine, and pyridinyl alcoholate ligands in the alkene metathesis reaction.[78-79] These studies were undertaken to improve the activity, selectivity and lifetime of Grubbs-type precatalysts.[53] Jordaan[53] discovered that the R groups of the N^O hemilabile ligand had a significant influence on the activity, stability, selectivity and longer lifetime in the 1-octene metathesis reaction with precatalyst **9** (**Figure 2.11**) as compared to complex **8**.

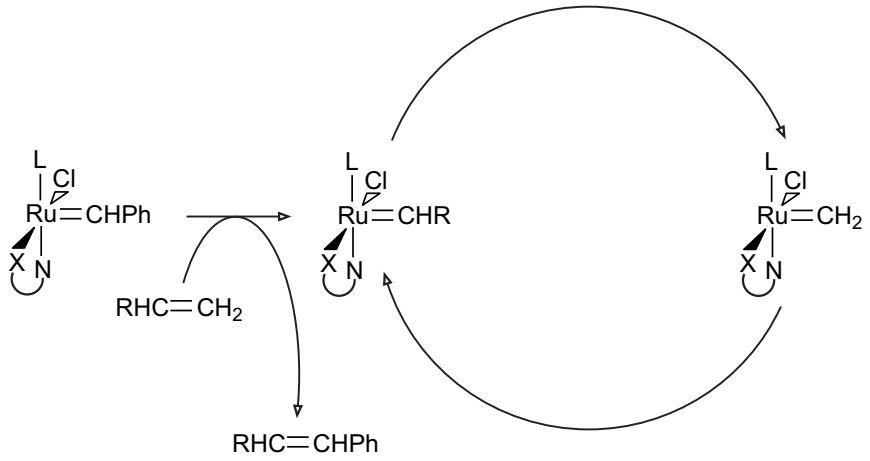

Figure 2.10: Simplified mechanism with **D3**-type precatalysts.

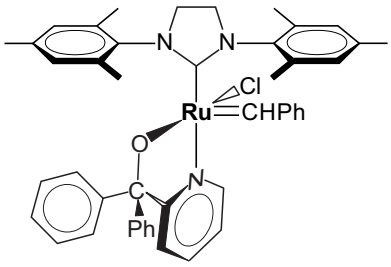

Figure 2.11: The PUK-Grubbs-2 precatalyst (**9**).[53]

Jordaan[53] identified several bidentate ligands like O,O-; O,N-; O,S-, as hemilabile ligands for incorporation into complex **7** and **8**. Her study combined experimental and theoretical studies to gain detailed information on the mechanism of the metathesis reactions and to help predict structural and reactivity trends of the catalytic systems. The O,N- alcoholato ligands with different steric bulks were successfully incorporated into complex **7** and **8**. These ligands

improved the thermal stability, activity, selectivity and lifetime of complex **7** and **8** towards the metathesis reaction of 1-octene.

Huijsmans[59] investigated varying substituents on the α-position of the O,N- ligands by theoretical and experimental methods. The study was undertaken to further improve the properties of these precatalysts in terms of stability, activity, selectivity and lifetime towards the metathesis reaction of 1-octene. Her synthesized complexes were found to be active, and as predicted by the molecular modelling, the activity of those complexes was found to be lower than that of **9**. Her synthesized complexes proved to have a much longer lifetime and higher TONs.

Loock[67] used **9** in her study of different 1-alkenes (1-hexene, 1-heptene, 1-nonene and 1-decene) with the reaction conditions optimized to determine whether the precatalyst is of value to the metathesis reaction. Her results of the 1-alkene metathesis reaction showed that precatalyst **9** increased the lifetime to 35 days. The reactions with **9** showed improved results in terms of primary metathesis products (PMPs) and TON because of the NHC and O,N-ligands which stabilized the precatalyst.

Van der Gryp[7] studied the recyclability of four commercially available Grubbs-type catalysts (Hoveyda-Grubbs 1, Hoveyda-Grubbs 2, complex **7** and **8**) and the self-synthesized **9** with the commercially available StarMem® membranes for the metathesis reaction of 1-octene by varying operating parameters such as reaction temperature, catalyst load and reaction enviroment. A dead-end setup was used for the study with the StarMem® 228, which successfully separated all these five Grubbs-type precatalysts from their reaction mixtures with catalyst rejections greater than 99%. He did a coupled reaction-separation investigation to demonstrate the re-usability of **9**.

Van der Gryp[7] again showed that commercially available **7**, **8**, Hoveyda-Grubbs 1 and Hoveyda-Grubbs 2 showed no activity after the first separation cycle, due to their short lifetimes of less than 10 h compared to that of **9**. It was also found that it was possible to separate **9** in an active form for consecutive reuse, which improved the overall TON from 1400 for a single pass reaction to 5500 for the overall consecutive reaction-separation steps.[7]

The above-mentioned leads to our study with the aim to find other possible nanofiltration membranes that can separate these kinds of precatalysts for the metathesis of 1-octene with complex **1**, **2** and **3** and their lifetime studies. This study will also attempt to recycle these precatalyst employing the OSN technique after the metathesis reaction of 1-octene.

2.3 References

1. Silva, P., Hans, S., Livingston, A. G., *J. Membr. Sci.,* 2005. **262**. 49

2. Pink, C. J., Wong, H., Ferreira, F. C., Livingston, A. G., *Org. P. Res. Develop*., 2008, **12**, 589
3. Bargeman, G., Vollenbroek, J. M., Straatma, J., Schroen, C. G. P. H., Boom, R. M., *J. Membr. Sci*., 2005, **247**, 11
4. Porter, M.C., Handbook of Industrial Membrane Technology, 1st ed.: Crest Publishing House, 2005
5. Mulder, M., Basic Principles of Membrane Technology, 2nd ed., Dordrecht: Kluwer Academic., 1996
6. Bergbreiter, D. E., *Catal Today*, 1998, **42**, 389
7. Van der Gryp, P., Separation of Grubbs-Based catalysts with nanofiltration, PhD-thesis, (North-West University), 2008
8. Kock Membrane Systems. 2014 Membrane Products [Online]. http://www.kochmembrane.com/Membrane-Products.aspx, 10 Jul 2014
9. Geens, J., Mechanism and Modelling of Nanofiltration in organic media, PhD-thesis, (Catholic University of Leuven), 2006
10. Razdan, U., Joshi, S. V., Shah, V. J., *Curr. Sci. India*., 2003, **85**, 761
11. Kragl, U. and Dreisbach, C. *Angew. Chem*., *Int. Ed. Engl*., 1996, **35**, 642
12. Giffels, G., Beliczey, J., Felder, M., Kragl, U., *Tetrahedron: Asym*., 1998, **9**, 691
13. Brinkmann, N., Giebel, D., Lohmer, G., Reetz, M.T., Kragl, U., *J. Catal*., 1999, **183**, 163
14. De Groot, D., Emmerink, P.G., Coucke, C., Reek, J.N.H., Kamer, P.C.J., Van Leeuwen, P.W.N.M., *Inorg. Chem. Commun*., 2000, **3**, 711
15. Woltinger. J., Henninges. H., Krimmer. H-P., Bommarius. A. S., Drauz. K., *Tetrahedron: Asym.*, 2001, **12**, 2095
16. De Smet, K., Aerts, S., Ceulemans, E., Vankelecom, I.F.J., Jacobs, P.A., *Chem. Commun*., 2001, 597
17. Dwars, T., Haberland, J., Grassert, I., Oeheme, G., Kragl, U., *J. Mol. Catal. A: Chem*., 2001, **168**, 81
18. Nair, D., Scarpello, J.T., White, L.S., Freitas dos Santos, L.M., Vankelecom, I.F.J., Livingston, A.G., *Tetrahedron Lett*., 2001, **42**, 8219
19. Nair, D., Luthra, S.S., Scarpello, J.T., White, L.S., Freitas dos Santos, L.M., Vankelecom, I.F.J., Livingston, A.G., *Desalination*., 2002, 1**47**, 301
20. Luthra, S.S., Yang, X., Freitas dos Santos, L.M., White, L.S., Livingston, A.G., *J. Membr. Sci*., 2002, **201**, 65
21. Scarpello, J.T., Nair, D., Freitas dos Santos, L.M., Livingston, A.G., *J. Membr. Sci*., 2002, **203**, 71
22. Wijkens, P., Jastrezebski, J.T.B.H., van der Schaaf, P.A., Kolly, R., Hafner, A., van Koten, G., *Org. Lett.,* 2000, **2**, 1621
23. Goetheer, E.L.V., Verkerk, A.W., van den Broecke, L.P.J., de Wolf, E., Deelman, B.J., van Koten, G., Keurentjies, J.T.F., *J. Catal*. 2003, **219**, 126
24. Gallego. I., Mallada. R., Urriolabeitia. E. P., Navaro. E. P., Menendez. M., Santanamaria. J., *Inorg. Chim. Acta*, 2004, **357**, 4577
25. Gevers, L.E.M., Vankelecom, I.F.J., Jacobs, P.A., *Chem. Commun*., 2005, 2500
26. Aerts, S., Weyten, H., Beukenhoudt, A., Gevers, L.E.M., Vankelecom, I.F.J., Jacobs, P.A., *Chem. Commun*., 2004, 710

27. Hau-to, W., See-Toh, Y.H., Ferreira, F.C., Crook, R., Livingston, A.G., *Chem. Commun*., 2006, 2063

28. Hau-to, W., Pink, C.J., Ferreira, F.C., Livingston, A.G., *Green Chem*., 2006, **8**, 373

29. Seung-Hak, C., Jeong-Hoon, K., Lee, S.B., *J. Membr. Sci*., 2007, **299**, 54

30. Pink, J.C., Hau-to, W., Ferreira, F.C., Livingston, A.G., *Org. Process. Res. Development*, 2008, **12**, 589

31. Gaikwad, A.V., Boffa, V., ten Elshof, J.E., Rothenberg, G., *Angew. Chem. Int. Ed*. 2008, **47**, 5407

32. Nair, D., Hau-Toh, W., Han, S., Vankelecom, I.F.J., White, L.S., Livingston, A.G., Boam, A.T., *Org. Process. Res. Develop.*, 2009, **13**, 863

33. Schoeps, D., Buhr, K., Dijkstra, M., Ebert, K., Plenio, H., *Chem. Eur. J*. 2009, **15**, 2950

34. Sairam, M., Loh, X.X., Bhole, Y., Sereewatthanawut, I., Li, K., Bismarck, A., Steinke, J.H.G., Livingston, A.G., J*. Membr. Sci*., 2010, **349**, 123.

35. Van der Gryp, P., Barnard, A., Cronje, J.P., De Vlieger, D., Marx, S., Vosloo, H.C.M., *J. Membr. Sci*., 2010, **353**, 70

36. Priske, M., Wiese. K.-D., Drews. A., Kraume, M., Baumgarten. G., *J. Membr. Sci*. 2010, **360**, 77

37. Van der Bergh, J., Cucuyener, C., Cascon, J., Kapteijn, F., *Chem. Eng. J*., 2011, **166**,368

38. Janssen, M., Wilting, J., Müller, C., Vogt, D., *Angew. Chem. Int. Ed*. 2010, **49**, 7738

39. Fang, J., Jana, R., Tunge, J.A., Subramaniam, *B., Appl. Catal*. A., 2011, **393**, 294

40. Zhong, Z., Li, W., Xing, W., Xing, W., Xu, N., *Sep. Purif. Technol*, 2011, **76**, 223

41. Doque, R., Öchsner, E., Clavier, H., Caijo, F., Nolan, S. P., Mauduit, M., Cole-Hamilton, D. J., *Green Chem*., 2011, **13**, 1187

42. Kajetanowicz, A., Czaban, J., Krishnan, G., Malińska, M., Waźniak, K., Siddique, H., Peeva, L. G., Livingston, A. G., Grela, K., *ChemSusChem*, 2013, **6**, 182

43. Skowerski, K., Wierzbicka, C., Grela, K., *Curr. Org. Chem*., 2013, **17**, 2740

44. Calderon, N., Chen, H. Y., Scott, K. W., *Tetrahedron Lett*, 1967, **8**, 3327

45. Eleuterio, H. S., *J. Mol. Catal*., 1991, **65**, 55

46. Eleuterio, H. S., Polymerization of cyclic olefins., Patent: US 3 074918, 5 Sep 2012

47. Banks, R. L., Bailey, G. C., *Ind. Eng. Chem., Prod. Res. Dev*., 1964, **3**, 170

48. Ivin, K. J., Mol J.C., Olefin Metathesis and Metathesis Polymerization, 1997, San Diego: Academic Press

49. Deshmukh. P. H., Blechert. S., Alkene Metathesis: the search for better catalysts., Royal Society of Chemistry, 2007, pp. 2479

50. Mol, J.C., Applied Homogeneous Catalysis with Organometallic Compounds., Cornils, B and Hermann, W. A., Eds., Metathesis, vol.2, VCH (Weinheim), 1996, p. 318

51. Grubbs, R.H., *Tetrahedron Lett*, 2004, **60**, 7117

52. Holub, N., Blechert, S., *Chem. Asian J*., 2007, 1064

53. Jordaan, M., Experimental and Theoretical Investigation of New Grubbs-type Catalysts for the Metathesis of Alkenes, PhD-thesis, (North-West University), 2007

54. Brugmaghim, J. L., Girolami, G. S., *Organometallics*, 1999, **18**, 192

55. Van der Gryp, P., Separation of Grubbs-Based catalysts with nanofiltration, PhD-thesis, (North-West University), 2008

56. Mol, J. C., *J. Mol. Catal. A: Chem*., 2004, **213**, 39

57. Cotton, F. A., Wilkinson, G., Murillo, C.A., Bochmann, M., *Advanced Inorganic Chemistry*, 1999, John Wiley & Sons, Inc

58. Kirk, M.M., Ruthenium based homogeneous olefin metathesis, MSc-dissertation, (University of the Free State), 2005

59. Loock, M. M., The alkene metathesis reactivity of the PUK-Grubbs 2-precatalyst, MSc-dissertation, (North-West University), 2009

60. Grubbs, R. H., Chang, S., *Tetrahedron lett.*, 1998, **54**, 4413

61. Grubbs, R. H., *J. Mol. Struct-Pure Appl.Chem. A*., 1994, **11**, 1829

62. Pine, S. H., Zahler, R., Evans, D. A., Grubbs, R. H., *J. Am. Chem. Soc*., 1980, **102**, 3270

63. Schrock, R. R., *Acc. Chem. Res*., 1990, **23**, 158

64. Grubbs, R. H., Miller, S. T., Fu, G. C., *Acc. Chem. Res*., 1995, **28**, 446

65. Cavallo, L., *J. Am. Chem. Soc*., 2002, **124**, 8965

66. Chase, P. A., Lutz, M., Spek, A. L., van Klink, G. P. M., van Koten, G., *J. Mol. Catal.*, 2006, **254**, 2

67. Huijsmans, C.A.A., Modelling and synthesis of Grubbs-type complexes with hemilabile ligands, MSc-dissertation, (North-West University), 2009

68. Scholl, M., Ding, S., Lee, C. W., Grubbs, R. H., *Org. Lett*., 1999, **1**, 953

69. Nguyen, S. T., Trnka, T. M., Handbook of metathesis, Grubbs, R. H., Ed., The discovery and development of well-defined Ruthenium-Based Olefin Metathesis catalysts. Vol.1, Wiley, 2003, p. 61

70. Pariya, C., Jayaprakash, K. N., Sarkar, A., *Coord. Chem. Rev*., 1998, **168**, 1

71. Huang, J., Stevens, E. D., Nolan, S. P., Petersen, J. L., *J. Am. Chem. Soc*.,1999, **121**, 2674

72. Huang, J., Schanz, H. J., Stevens, E. D., Nolan, S. P., *Organometallics*, 1999, **18**, 2370

73. Randl, S., *Synth. Lett*., 2001, **3**, 430

74. Le Gall, I., Laurent, P., Soulier, E., Salaûn, J. Y., Des Abbayes, H., *J. Organomet. Chem*., 1998, **567**, 13

75. De Clerq, B and Verpoort, F., *Tetrahedron Lett*., 2002, **43**, 9101

76. Chang, S., Jones II, L., Wang, C., Henling, L. M., Grubbs, R. H., *Organometallics*, 1998, **17**, 3460

77. De Clercq, B., Verpoort, F., *J. Mol. Catal. A:Chem*., 2002, **180**, 67

78. Denk, K., Friedgen, J., Herrmann, W. A., *Adv. Synth Catal*., 2002, **344**, 666

79. Van der Schaaf, P. A., Muhlbach, A., Hafner, A., Kolly, R., 1999. Heterocyclic ligand containing ruthenium and osmium catalysts. Patent: WO 99/29701, 6 Mar 2013

80. Adlhart, C. and Chen, P., *J. Am. Chem. Soc*., 2004, **126**, 3496

81. Herisson, J.L and Chauvin, Y., *Makromol. Chem*., 1997, **141**,161

Chapter 3
Experimental

3.1 Materials

3.1.1 Chemicals

Diethyl ether (96%, Labchem, b.p. 36.6 °C), THF (99%, Saarchem, b.p. 66 °C) and toluene (95%, Merck, b.p. 110-111 °C) were distilled under N_2 from sodium with benzophenone as indicator. Pentane (96%, Labchem, b.p. 35-36 °C) was distilled under N_2 from CaH_2.

Tetrahydrofuran and toluene were stored over 4Å mol sieves. Diethyl ether and Pentane were used straight from distillation.

1-Octene (98%, Sigma-Aldrich) was purified by filtering the solution through an alumina column, after the alumina column had been dried overnight at 700 °C. The solution was stored over 3Å mol sieves. 1-Tetradecene (95%) and 7-tetradecene (97%) were both purchased from Sigma-Aldrich.

n-Butyl lithium (2.5 M in hexanes), 2-bromopyridine (99%), isobutyro-phenone, 2-methyl benzophenone, Grubbs second generation (**8**) precatalyst were purchased from Sigma-Aldrich and used as is. tert-Butyl hydroperoxide (5.5 M in decane) and nonane (99%) were purchased from Fluka, and the first mentioned was stored over 4Å mol sieves.

All gases used during this study were purchased from Afrox.

3.1.2 Membranes

The membranes selected for this study were PuraMem™ 280 and PuraMem™ S380 purchased from Evonik MET Ltd, UK. These membranes were supplied with a polyethylene glycol preservative that is easily washed off with a solvent such as toulene, ethanol, acetone, THF or DMF (200 mL) at a filtration pressure of 20-30 bar to ensure complete removal of the preserving agent (lube oil). The MWCO of these membranes given by the manufacturer are listed in **Table 3.1**.

Table 3.1: Summary of the manufacturer specification sheet for PuraMem™ series of membranes.

	PuraMem™ 280	**PuraMem™ S380**
MWCO ($g.mol^{-1}$)	280	600
Permeability ($L.m^{-2}.h^{-1}$)	80	160
Membrane type	polyimide	polyimide
All PuraMem™ membranes are stable in the following solvents:	Toluene, Xylene	
	Butanol, Ethanol, Isopropanol	
	Hexane, Heptane	
	Methyl ethyl ketone, Methyl iso-butyl ketone	
	Methyl tert-butyl ether	

3.2 Analytical techniques and calculation methods

3.2.1 Analytical techniques

❖ **Gas chromatography (GC-FID)**

The analyses were conducted on an Agilent 6890 GC with a flame ionization detector (FID). The GCs are equipped with an HP-5 (95 % methylsiloxane and 5 % phenyl methyl siloxane), capillary column (30 m x 320 µm x 0.25 µm) and an HP-1 (100 % methyl siloxane), capillary column (30 m x 320 µm x 0.25 µm).

The GC settings were as follows:

Injection volume:	0.2 µL
Inlet Temperature:	200 °C
Split ratio:	50.4:1
N_2 carrier gas flow:	1.4 $mL.min^{-1}$
Air flow rate:	40 $mL.min^{-1}$
H_2 flow rate:	450 $mL.min^{-1}$
Detector temperature:	300 °C
Oven programming:	60 to 110 °C at 25 $°C.min^{-1}$
	110 °C for 16 min
	110 to 300 °C at 25 $°C.min^{-1}$
	300 °C for 5 min

❖ **Fourier Transform Infrared spectrometry (FTIR)**

A Nicolet FTIR 550 spectrophotometer was used for the analysis of the ligands. Samples were prepared by mixing a minimal amount of sample was mixed with dry KBr together and compressing the mixture into a sample disc.

❖ **Mass spectrometry (MS)**

A Bruker microTOF-Q II was used for Electron Spray Ionization (ESI) and Atmospheric Pressure Chemical Ionization (APCI) experiments. Dry sample in glass capillary, positive ion mode detection and dry heater in normal MS mode.

❖ **Nuclear magnetic resonance spectrometry (NMR)**

^{1}H-, ^{31}P-, ^{13}C-NMR spectra were obtained by using a Bruker UltraShield 600 MHz Avance III spectrometer. The samples were prepared by dissolving the crystals (2 mg for ^{1}H-NMR and ^{31}P-NMR, 20 mg for ^{13}C-NMR) in deuterated chloroform ($CDCl_3$) and filtered into an NMR-tube under inert argon for the precatalysts.

❖ **Gas chromatograph with a mass selective detector (GC/MSD)**

GC/MSD was used for alcohol derivatives verification. A 6890N GC with an HP-5 capillary column and an Agilent 5973 mass selective detector (MSD) was used. The samples were dissolved in diethyl ether and analysed.

❖ **Inductively coupled plasma (ICP-OES)**

The concentration of ruthenium content in the retentate and permeate samples was determined with an ICP-OES spectrometer, in parts per million (ppm). Reaction mixtures were dissolved in aqua regia (molar ratio of 1:3 nitric acid and hydrochloric acid).

3.2.2 Calculation methods

❖ **GC Response factor**

The response factor (RF) was determined by preparing 4 GC vials which contained:

0.25 mL nonane + 1.00 / 0.75 / 0.5 / 0.25 mL 1-octene ($C_{8)}$.

Each sample was injected into the GC and the RF was calculated by plotting

$$(\frac{A_{nonane}}{A_{1\text{-octene}}})v/s(\frac{V_{nonane}}{V_{1\text{-octene}}})$$

to give a slope, i.e. RF, of 0.9683 (**Figure 3.1**).

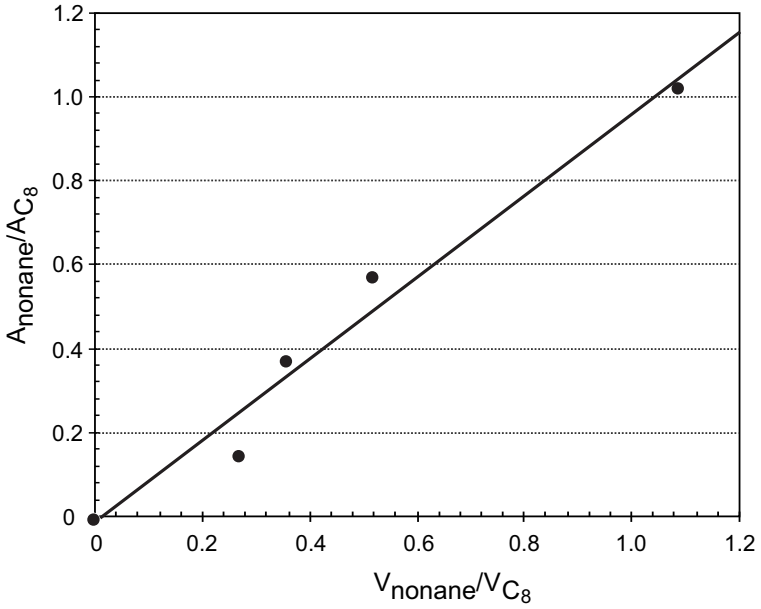

Figure 3.1: A calibration curve for the determination of the GC response factor for 1-octene.

❖ **Calculations of mole percentages, turnover numbers and selectivities**

For determining the volumes of C_8, PMPs, SMPs or IPs:

$$V_X = V_{is} \times (A_x \times A_{is}) \times \left(\frac{1}{RF}\right) \qquad 3.1$$

where V_x = Volume of 1-Octene, PMPs, SMPs, or IPs

V_{is} = Volume of internal standard nonane at t = 0

A_x = Area of C_8, PMP, SMP, IP

A_{is} = Area of internal standard C_9

RF = Response factor

$$V_{is} = \left(\frac{V_{nonane}}{V_{1\text{-}octene}}\right) \times V_{sample} \qquad 3.2$$

where V_{nonane} = Volume of nonane at t = 0 (1 mL)

$V_{1\text{-octene}}$ = Volume of 1-octene at t = 0 (20 mL)

V_{sample} = Volume of sample taken from the flask (0.3 mL)

$$= \left(\frac{1}{20}\right) \times 0.3 = 0.015$$

For determining the moles of C_8, IPs, PMPs or SMPs:

$$n_x = \frac{V_x \times \rho_x}{MW_x} \qquad 3.3$$

where n_x = Moles of C_8, IPs, PMPs or SMPs
V_x = Volume of C_8, IPs, PMPs or SMPs
ρ_x = Density of C_8, IPs, PMPs or SMPs
MW_x = Molecular weight of C_8, IPs, PMPs or SMPs

For determining the mole percentage of C_8, IPs, PMPs or SMPs:

$$\%n_x = \left(\frac{n_x}{n_{tot}}\right) \times 100 \qquad 3.4$$

where $\%n_x$ = mole percentage of C_8, IPs, PMPs or SMPs
n_x = moles of C_8, IPs, PMPs or SMPs
n_{tot} = sum of moles of C_8, IPs, PMPs or SMPs

For determining the selectivity:

$$S = \left\{\frac{\%PMPs}{\%(PMPs + SMPs)}\right\} \times 100 \qquad 3.5$$

For determining the turnover number:

$$TON = \left\{\frac{\%PMPs \times (1\text{-octene/Ru})}{100\%}\right\} \qquad 3.6$$

where 1-octene/Ru = 1-octene:Ru molar ratio at t = 0

3.3 OSN experimental procedures and set-up

Nanofiltration experiments were carried out in a stainless steel dead-end pressure cell by Van der Gryp *et al.*[7] (**Figure 3.2** and **Figure 3.3**).[7] In literature, the OSN experimental procedure has been thoroughly described by Van der Gryp *et al.*[7] The pressure cell is cylindrical and has an end-plate at the bottom and top part. The bottom part of the body is fitted with a stirrer, and the bottom plate has a porous stainless disk and a permeate outlet, while the top part has a cell pressure gauge, safety release valve, pressure release valve and an inlet valve which is connected to a nitrogen gas cylinder. The typical set-up used is shown (**Figure 3.4**).

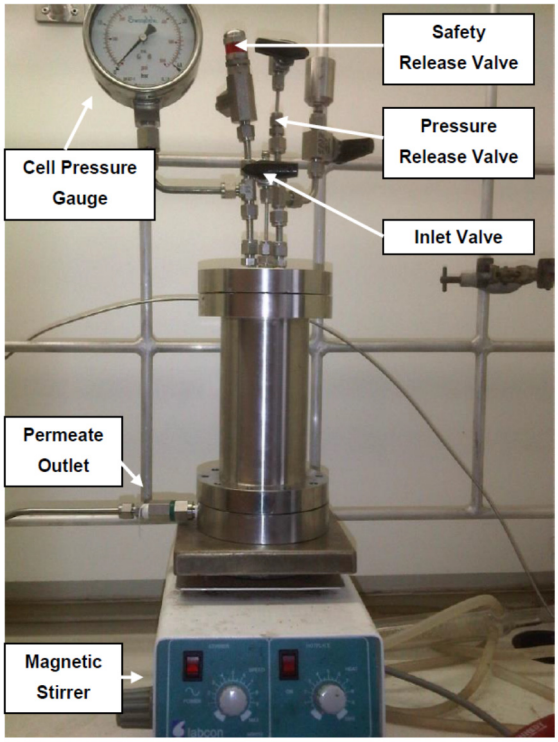

Figure 3.2: Photo of the OSN experimental set-up used.[7]

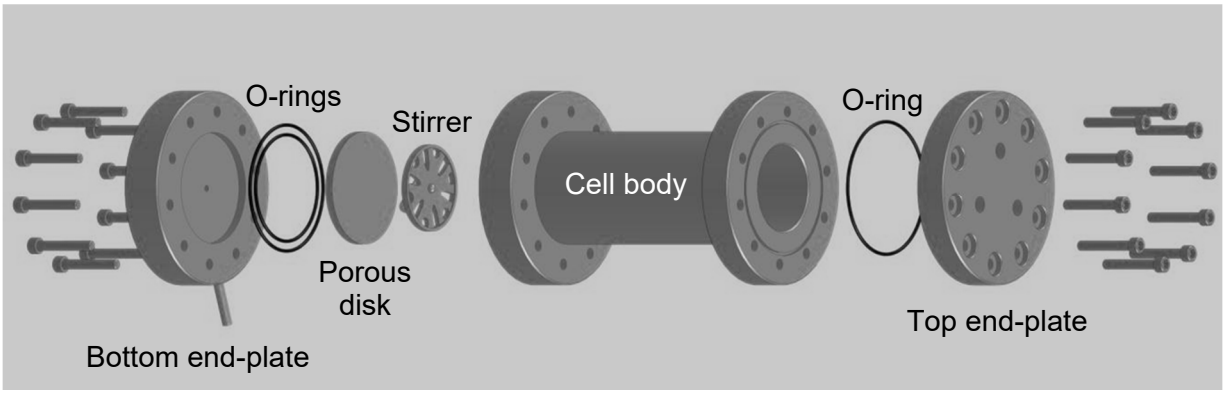

Figure 3.3: Solid-Works diagram showing different parts of the OSN cell.[7]

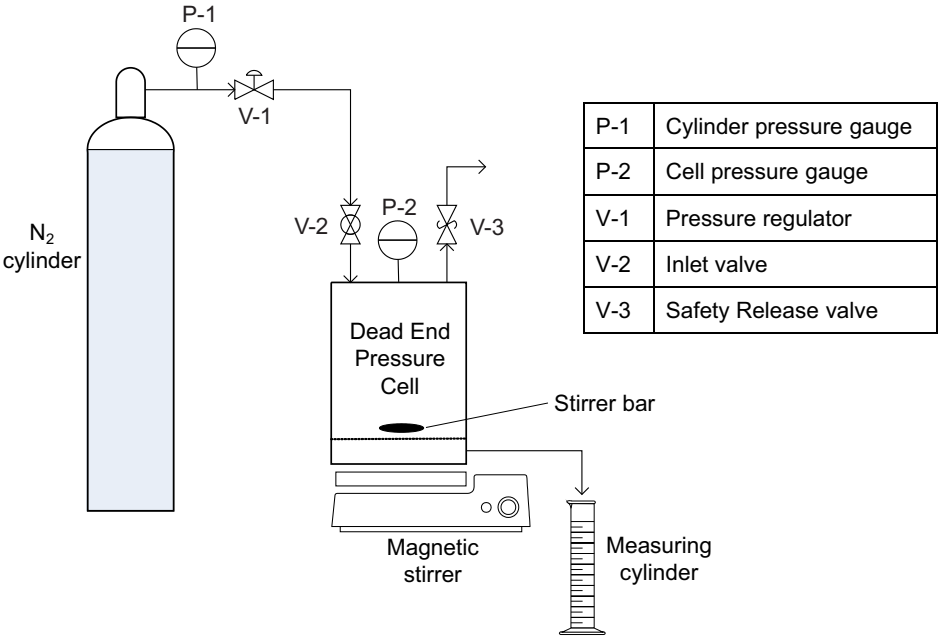

Figure 3.4: A schematic representation of the OSN experimental set-up.

From an A4 sheet, the membrane is cut into a desired circular disk and fitted between the O-rings that seal the bottom end-plate with the active layer of the membrane facing the liquid on top of the porous disk.

For steady state characterization, the cell was loaded with 100 mL of the desired 1-octene or 1-tetradecene or combination of both (1-octene/1-tetradecene) and set to the desired pressure. If the steady state flux condition had not been reached after 50 mL had permeated, the cell was depressurized via the inlet valve and the 1-octene or 1-tetradecene or combination of both mixtures introduced again into the cell. The cell was set to the desired pressure again, and the procedure repeated until steady-state conditions were achieved.
The permeation performance of the solvent/solvent-mixtures was monitored with a millisecond stopwatch at intervals of 10 mL. The characterization procedure was stopped when the membrane had reached its steady state.

The performance of the membrane was assessed using two parameters: (i) solvent flux, and (ii) solute rejection.[6-8] The solvent flux, using equation 2.1, was determined by measuring the volume permeated per unit area per unit time. The rejection percentage (R), defined by equation 2.2, of species for a given membrane is a measure of its separation performance.

3.4 Preparation of complexes

3.4.1 Preparation of pyridinyl alcohols

For the synthesis of the pyridinyl alcohols (**Figure 3.5**) the Herman *et al*.[1] synthetic route was chosen due to its simplicity. The alcohols were synthesized under inert conditions. A 200 mL three-neck round-bottomed flask was filled with 50 mL diethyl ether and cooled to -78 °C while stirring. To this flask nBuLi (50 mmol, 2.5 M in hexane) was added slowly to the flask followed by the dropwise addition of 2-bromopyridine (47.5 mmol, in 12.5 mL diethyl ether) at -78 °C while the mixture was stirred for 30 min to give a dark reddish solution.[1-4]

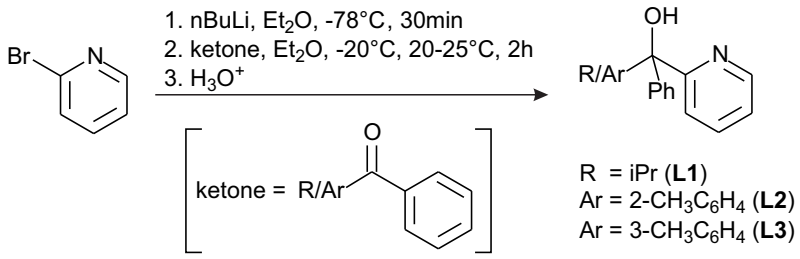

Figure 3.5: Synthesis of ligands **L1** – **L3**.

The reaction temperature was increased to -20 °C for the slow addition of meta- or para-methylbenzophenone (52.5 mmol in 20 mL diethyl ether) to the reaction mixture and the temperature increased to room temperature, the mixture was stirred for 2 h. After the reaction was complete, the reaction mixture was hdrolysed and the organic phase was separated from the aqueous phase and extracted with 2 M HCl (5 x 10 mL). 2 M NaOH was added to neutralize the aqueous phase and thereafter extracted with diethyl ether. For the organic phase, $MgSO_4$ was added to dry the organic phase and the solvent evaporated to give a crystalline-solid product.

Characterization results:

2-Methyl-1-phenyl-1-pyridin-2-yl-propan-1-ol (**L1**)

GC-MS: 261 m/z.

FTIR (cm^{-1}): ν(OH) = 3342; ν(C-H, aromatic) = 3075, 3018, 756; ν(C=C & N=C, aromatic) = 1591, 1571; ν(C-O, aliphatic) = 1168, 1126.

^{1}H NMR (600 MHz, $CDCl_3$): δ_H **=** 8.59 (d, J = 4.9 Hz, 1H, H-6 of C_6H_4N), 7.62 (td, J^1 = 7.7 Hz, J^2 = 1.8 Hz, 1H, H-4 of C_6H_4N), 7.45-7.19 (m, 11H, H-5 of C_5H_4N & 10H of 2Ph), 7.12 (d, J = 7.9 Hz, 1H, H-3 of C_6H_4N), 6.30 (s, 1H, OH).

^{13}C NMR (150 MHz, $CDCl_3$): δ_C **=** 163.2 (qC, C-2 C_6H_4N), 147.7 (CH, C-6 C_6H_4N), 146.1 (2qC, C-1 Ph), 136.4 (CH, C-4 C_6H_4N), 128.1 (4CH, C-3 & C-5 Ph), 127.3 (4CH, C-2 & C-6 Ph), 122.9 (2CH, C-4 Ph & C-3 C_6H_4N), 122.3 (CH, C-5 C_6H_4N), 80.8 (C-OH).

1-(2'-Pyridinyl)-1-(2'-methylphenyl),1-phenyl-methanol (**L2**)

GC-MS: 275 m/z.

FTIR (cm^{-1}): ν (O-H) = 3430; ν (C-H, aromatic) = 3047, 3013, 779; ν (C-H aliphatic) = 2931, 2874; ν (C=C & N=C, aromatic) = 1588, 1669; ν (CH_3, bending) = 1347; ν (C-O, aliphatic) = 1166, 1025.

^{1}H NMR (600 MHz, $CDCl_3$): δ_H **=** 8.60 (d, 1H, *J* = 4.95 Hz, H-6 of C_6H_4N), 7.61 (dt, 1H, J^1 = 7.44, J^2 = 1.46 Hz, H-4 of C_6H_4N), 7.35 (d, 2H, *J* = 7.31 Hz, H-3 of C_6H_4N & H-4 of substituted Ph), 7.30 (t, 2H, *J* = 7.19 Hz, 4-H of unsubstituted Ph & H-5 of C_6H_4N), 7.27-7.21 (m, 2H, H-3 & H-5 of unsubstituted Ph), 7.17 (d, 2H, *J* = 4.26 Hz, H-2 & H-6 of unsubstituted Ph), 7.02 (d, 1H, *J* = 7.92 Hz, H-6 of substituted Ph), 6.50 (d, 1H, *J* = 7.80 Hz, H-3 of substituted Ph), 6.32 (s, 1H, OH), 2.10 (s, 3H, CH_3).

^{13}C NMR (150 MHz, $CDCl_3$): δ_C **=** 163.24 (qC, C-2 C_6H_4N), 147.76 (CH, C-6 C_6H_4N), 146.02 (qC, C-1 substituted Ph), 143.76 (qC, C-1 unsubstituted Ph), 139.02 (qC, C-2 substituted Ph), 136.36 (CH, C-4 C_6H_4N), 132.51 (CH, C-3 of substituted Ph), 128.85 (CH, C-6 of substituted Ph), 128.02 (2CH, C-3 & C-5 of unsubstituted Ph), 127.68 (CH, C-4 of unsubstituted Ph), 127.49 (2CH, C-2 & C-6 of unsubstituted Ph), 127.08 (CH, 5-H of substituted Ph), 124.68 (CH, 4-H of substituted Ph), 123.18 (CH, C-3 C_6H_4N), 122.24 (CH, C-5 C_6H_4N), 81.58 (qC, COH), 21.73 (CH_3).

1-(2'-Pyridinyl)-1-(3'-methylphenyl),1-phenyl-methanol (**L3**)

GC-MS: 275 m/z.

FTIR (cm^{-1}): ν (O-H) = 3407; ν (C-H, aromatic) = 3072, 3020, 782; ν (C-H aliphatic) = 2916, 2855; ν (C=C & N=C, aromatic) = 1589, 1570; ν (CH_3, bending) = 1352; ν (C-O, aliphatic) = 1142, 1041.

^{1}H NMR (600 MHz, $CDCl_3$): δ_H **=** 8.54 (d, 1H, *J* = 4.96 Hz, H-6 of C_6H_4N), 7.58 (dt, 1H, J^1 = 7.51 Hz, J^2 = 1.60 Hz, H-4 of C_6H_4N), 7.29-7.24 (m, 4H, H-5, & H-3 of C_6H_4N and H-2 & H-6 of unsubstituted Ph), 7.24-7.16 (m, 2H, H-3 & H-5 of unsubstituted Ph), 7.13 (t, 2H, H-4 of unsubstituted Ph and H-5 of substituted Ph), 7.08 (d, 1H, *J* = 7.88 Hz, H-6 of substituted Ph), 7.04 (d, 1H, J = 7.41 Hz, H-2 of substituted Ph), 6.97 (d, 1H, *J* = 7.92 Hz, H-4 of substituted Ph), 6.24 (s, 1H, OH), 2.25 (s, 3H, CH_3).

^{13}C NMR (150 MHz, $CDCl_3$): δ_C = 163.23 (qC, C-2 C_6H_4N), 147.67 (CH, C-6 C_6H_4N), 136.5 (CH, C-4 C_6H_4N), 122.7 (CH, C-3 C_6H_4N), 122.5 (CH, C-5 C_6H_4N), 145.6 (qC, C-1 substituted Ph), 146.16 (qC, C-1 of unsubstituted Ph),145.98 (qC, C-1 of substituted Ph), 137.58 (qC, C-3 of substituted Ph), 136.35 (CH, C-4 C_6H_4N), 128.69 (CH, C-2 substituted Ph), 128.11 (2CH, C-3 substituted Ph), 128.06(CH, C-4 Ph), 127.87 (2CH, C-2 & C-6 of unsubstituted Ph), 127.68 (CH, C-4 of substituted Ph), 127.24 (CH, C-4 of unsubstituted Ph), 125.27 (CH, C-6 of substituted Ph), 122.89 (CH, C-3 of C_6H_4N), 122.29 (CH, C-5 of C_6H_4N), 80.77 (qC, COH), 21.55 (CH_3).

3.4.2 Preparation of lithium salts

To a Schlenk tube containing the alcohol pyridinyl methanol (2 mmol), THF (20 mL) was added under argon, **Figure 3.6**. After the alcohol had dissolved, nBuLi (2 mmol, 2.5 M in hexane) was added dropwise, while the reaction mixture was stirred for 2 h. After stirring the solvent was removed under reduced pressure and the remaining white solid precipitate was washed with pentane (5 mL x 2). A gastight syringe was used to remove the pentane and left to dry under reduced pressure. The white powder was used without further characterization because of its sensitivity to air.

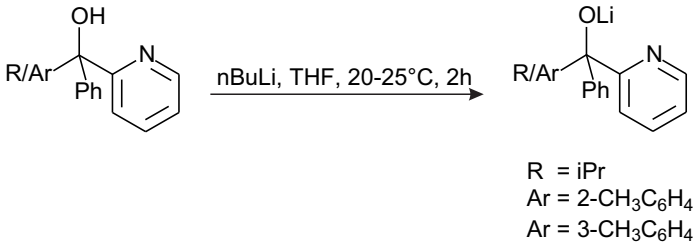

Figure 3.6: Lithiation of ligands **L1** – **L3**.

3.4.3 Synthesis of precatalysts

For thesynthesis of the precatalysts (**1**, **2** or **3**), **8** (0.6 mmol, in 5-10 mL THF) and the lithium salt of the pyridinyl alcohol (0.6 mmol, in 5 mL THF) were added to the Schlenk tube under inert conditions. The reaction, **Figure 3.7**, was stirred for 48 h at room temperature. The reaction progress was monitored with TLC until there was only a green spot which showed that the Grubbs precatalyst had been consumed.

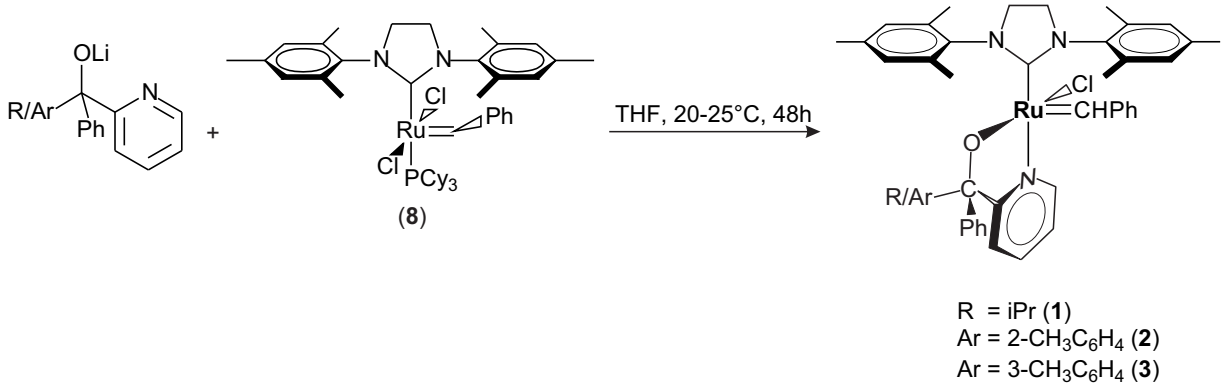

Figure 3.7: Synthesis of complexes **1** - **3**.

The solvent was removed under reduced pressure in an inert enviroment to leave behind a dark green residue. Toluene (7 mL) was added and all the contents of the Schlenk tube transferred to a clean Schlenk tube using a gastight syringe fitted with a filter. The solvent was removed under rduced pressure, THF (1 mL) and pentane (5-10 mL) were added to the remaining black residue and the mixture left until a precipitate formed. The liquid was removed with a gastight syringe and the product was washed with pentane (5 mL) using an ultrasonic bath for 5 min once and 3 – 4 times without ultrasonication. The solvent was removed using a gastight syringe and the product was dried under reduced pressure in an inert atmosphere.

Characterization results:

Benzylidene-chloro[1,3-bis-(2,4,6-trimethylphenyl)-2-imidazolidinylidene]-[1-(2'-pyridinyl)-1- isopropyl-1-phenyl-methanolato]ruthenium (**1**)

GC-MS: 793.23 m/z.

FTIR (cm^{-1}): ν(C-H, aromatic) = 3055, 3019, 760; ν(CH_3) = 2921, 2849, 1379; ν(C=N, & C=C, aromatic) = 1592, 1568; ν(C-N) = 1262; ν(C-O, aliphatic) = 1165, 1024.

^{1}H NMR (600MHz, $CDCl_3$): δ_H = 17.10 (s, 1H, carbeen), 9.61 (d, 1H, *J* = 5.48 Hz, H-6 of C_5H_4N), 7.62 (t, 1H, *J* = 7.58 Hz, H-4 of C_5H_4N), 7.31-7.19 (m, 11H, H-3 of C_5H_4N & all H's of 2Ph), 7.17-7.06 (m, 6H, all H's of carbeen Ph & H-5 of C_5H_4N), 6.64 (s, 4H, H-3 of mesityl), 3.99 (m, 4H, H of $N(CH_2)_2N$), 2.61/2.27/2.19 (3s, 18H, $6CH_3$ of mesityl); ^{31}P NMR (242 MHz, $CDCl_3$) no signal.

^{13}C NMR (150 MHz, $CDCl_3$): δ_C = 291.70, 214.44, 171.21, 151.55, 149.88, 149.75, 143.58, 139.21, 137.32, 136.62, 133.94, 129.63, 128.84, 128.39, 127.89, 126.97, 126.84, 126.58, 126.29, 126.11, 122.39, 120.94, 93.94, 51.33, 20.95, 19.07, 18.89.

Benzylidene-chloro[1,3-bis-(2,4,6-trimethylphenyl)-2-imidazolidinylidene]-[1-(2'-pyridinyl)-1-4'-methylphenyl-1-phenyl-methanolato]ruthenium (**2**)

GC-MS: 807.25 m/z.

FTIR (cm^{-1}): ν(C-H, aromatic) = 3056, 3016, 771; ν(C-H, aliphatic) = 2923, 2851; ν(C=N & C=C, aromatic) = 1599, 1566; ν(CH_3, bending) = 1410; ν(C-N, aliphatic) = 1264; ν(C-O, aliphatic) = 1160, 1020.

^{1}H NMR (600MHz, $CDCl_3$): δ_H = 17.32 (s, 1H, carbene H), 17.12 (s, 1H, carbene H), 9.76 (d, 1H, *J* = 5.59 Hz, H-6 of C_5H_4N), 9.52 (d, 1H, *J* = 5.43 Hz, H-6 of C_5H_4N), 7.75 (d, 1H, *J* = 7.10 Hz, H-4 of C_5H_4N), 7.41 (t, 1H, H-4 of CHPh), 7.36-7.27 (dd, 2H, J^1 = 24.53 Hz, J^2 = 7.58 Hz, H-3 & H-5 of CHPh), 7.27-7.12 (m, 11H, H-3 & H-5 of C_5H_4N, all H's of unsubstituted Ph, H-4 & H-6 of substituted Ph), 7.09 (t, 1H, H-5 of substituted Ph), 7.09 (t, 1H, 3-H of substituted Ph), 6.99/6.98 (2s, 4H, H-3 of mesityl Ph), 3.97 (m, 4H, $N(CH_2)_2N$), 2.66/2.25/2.21/2.13 (4s, 18H, $6CH_3$ of mesityl), 2.19 (s, 3H, CH_3 of substituted Ph).

^{13}C NMR (150 MHz, $CDCl_3$): δ_C = 293.39, 290.40, 215.15, 213.96, 172.75, 171.39, 152.20, 150.76, 150.06, 149.62, 148.91, 146.72, 141.69, 139.28, 137.34, 137.09,

136.95, 136.81, 134.20, 134.07, 131.28, 131.23, 129.54, 128.62, 127.61, 127.22, 126.84, 126.78, 126.67, 126.41, 126.23, 126.18, 126.08, 125.93, 124.94, 124.23, 124.14, 123.17, 121.65, 120.88, 120.71, 94.56, 94.23, 51.56, 22.79, 20.91, 18.97, 18.84.

Benzylidene-chloro[1,3-bis-(2,4,6-trimethylphenyl)-2-imidazolidinylidene]-[1-(2'-pyridinyl)-1-3'-methylphenyl-1-phenyl-methanolato]ruthenium (**3**)

GC-MS: 807.25 m/z.

FTIR (cm^{-1}): ν(C-H, aromatic) = 3054, 3019, 758; ν(C-H, aliphatic) = 2920, 2849; ν(C=N & C=C, aromatic) = 1599, 1569; ν(CH_3, bending) = 1411; ν(C-N, aliphatic) = 1261; ν(C-O, aliphatic) = 1163, 1029.

^{1}H NMR (600MHz, $CDCl_3$): δ_H = 17.10 (s, 1H, carbene H), 9.63 (d, 1H, *J* = 5.02 Hz, 6-H of C_5H_4N), 7.27 (t, 1H, *J* = 6.15, 4-H of carbene Ph), 7.19-7.10 (m, 3H, 3-,4-, & 5-H of C_5H_4N), 7.09-6.90 (m, 9H, H of unsubstituted 2Ph), 6.80-6.59 (2m, 8H, H of substituted and mesityl Phs), 4.00 (m, 4H, $N(CH_2)_2N$), 2.61/2.28/ 2.20 (3s, 18H, mesityl $6CH_3$), 2.21 (s, 3H, CH_3 of substituted Ph).

^{13}C NMR (150 MHz, $CDCl_3$): δ_C = 292.09, 291.64, 214.72, 214.48, 171.33, 151.51, 149.84, 149.80, 143.84, 139.23, 137.42, 137.35, 137.31, 136.65, 133.93, 129.64, 129.58, 128.94, 128.84, 128.51, 128.44, 127.15, 126.96, 126.91, 126.81, 126.60, 126.48, 126.34, 126.25, 126.20, 126.04, 125.94, 122.43,120.93, 120.89., 93.25, 51.33, 21.65, 20.97, 19.12, 18.92.

3.5 Metathesis experiments

3.5.1 Apparatus and Method

The metathesis reaction was performed in a 100 mL three-neck round-bottomed flask fitted with a condenser, argon/nitrogen inlet line, septum and thermometer (**Figure 3.8**). The flask was immersed into an oil bath to control the reaction temperature and the oil bath was set to the desired temperature before the metathesis reaction.

The three-necked flask with a mixture of 1-octene (20 mL, 126.5 mmol) and nonane (1 mL, 5.57 mmol), used as an internal standard, was heated to 80 °C under argon/nitrogen. The precatalyst (13 to 20 mg) was added and the reaction mixture was continuously stirred with a magnetic stirrer until no further primary metathesis products formed.

GC analyses were carried out using a 1 mL GC vial which contained:

- 0.3 mL of sample withdrawn by syringe during the reaction at different time intervals.
- 2 drops of tert-butyl hydrogen peroxide for quenching the reaction sample.
- 0.3 mL toluene to increase/make up the volume of the sample.

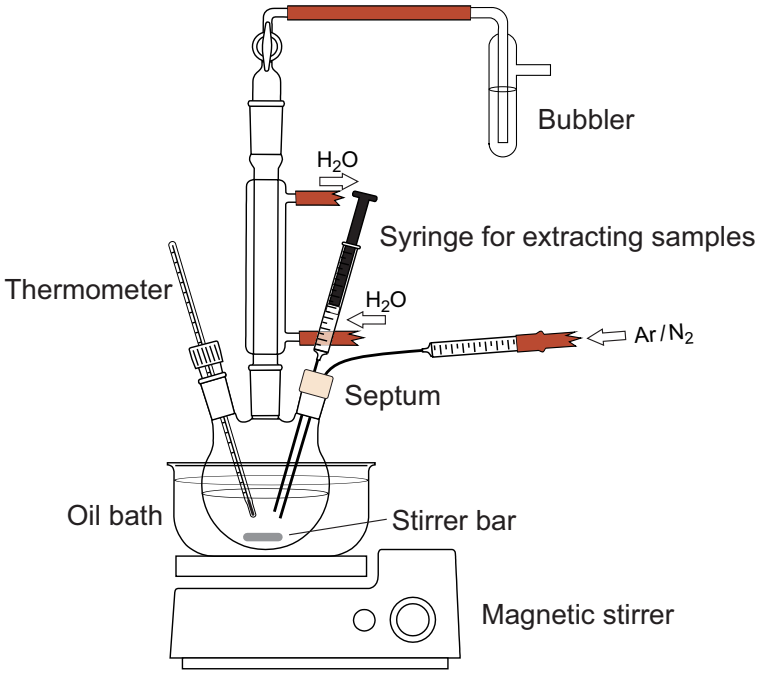

Figure 3.8: A schematic diagram for performing metathesis reaction.

3.6 Ruthenium extraction methodology and ICP-OES analysis[11]

An ICP-OES Spectrometer was used to analyse the concentration of the retentate and permeate feeds. The samples needed to be pretreated from an organic environment to an aqueous environment suitable for the ICP-OES because the ICP-OES cannot analyse organic chemicals.[11] Manual control checks were performed and a calibration curve for Ru (264.8) was obtained from the ICP results.

The reaction mixture (5 mL) was transferred to a 50 mL beaker with a stirrer and placed on a magnetic stirrer and stirred for 2 h. After the stirring, 17 mL water was added, followed by 30% aqueous hydrogen peroxide (17 mL) and the mixture was stirred for 1 hour. A blue/black precipitate/oil formed.

The mixture was transferred to a separating funnel and the layers were separated. The aqueous layer was extracted with dichloromethane (2 x 30 mL). The organic solution was then dried with $MgSO_4$ and filtered through a small plug of silica gel. The filtrate and dichloromethane washings were evaporated. Note: The liquid was not all evaporated as it becomes difficult to dissolve the catalyst once it adheres to the walls of the flask.[11] The filtrate and dichloromethane washings were combined with an aqua regia volume ratio of 1:3

concentrated nitric acid and concentrated hydrochloric acid in a 100 mL volumetric flask containing 94 mL of distilled water.

3.7 References

1. Hermann, W.A., Haider, J.J., Fridgen, J., Lobmaier, G.M., Spiegler, M., *J. Organomet. Chem*., 2000, **603**, 69
2. Kuhn, F.E., Santos, A.M., Lopes, A.D., Goncalves, I.S., Rodriguez-Borges, J.E., Pillinger, M., Romao, C.C., *J. Organomet. Chem*., 2001, **621**, 207
3. Goto, S., Velder, J., El Sheikh, S., Sakamoto, Y., Mitani, M., Elmas, S., Adler, A., Becker, A., Neudörfl, J., Lex, J., and Schmalz, H.G., *Synlett*., 2008, **9**, 1361
4. Huijsmans, C. A. A., Modelling and Synthesis of Grubbs-type complexes with hemilabile ligands, MSc-dissertation, (North-West University), 2009
5. Jordaan, M., Experimental and Theoretical investigation of Grubbs pre-type catalysts for the metathesis of alkenes., PhD Thesis, (North-West University), 2007
6. Sairam, M., Loh, X.X., Bhole, Y., Sereewatthanawut, I., Li, K., Bismarck, A., Steinke, J.H.G., Livingston, A.G., J*. Membr. Sci*., 2010, **349**, 123
7. Van der Gryp, P., Barnard, A., Cronje, JP., De Vlieger, D., Marx, S., Vosloo, H.C.M., *J. Membr. Sci*., 2010, **353**, 70
8. See Toh, Y. H., Loh, X. X., Bismarck, A., Li, K., Livingston, A. G., *J. Membr. Sci*., 2007, **291**, 120
9. Nair, D., Hau-Toh, W., Han, S., Vankelecom, I.F.J., White, L.S., Livingston, A.G., Boam, A.T., *Org. Process. Res. Dev*., 2009, **13**, 863
10. Rundel, J. T., Paul, B. K., Remcho, V. T., *J. Chromatogr*., 2007, **1162**, 167
11. Knight, D.W., Morgan, I.R., Proctor, A.J., *Tetrahedron Lett*., 2010, **51**, 638

Chapter 4
Results and Discussions

4.1 Membrane characterization and selection

4.1.1 Introduction

Characterization of membrane parameters are described as either being morphology related or performance related.[1] Morphological parameters describe the structure of the membrane (physical and chemical parameters).[1] Performance related parameters describe membrane flux, rejection and stability.[1]

It is therefore important that one must be careful when choosing a membrane for a particular application. The selection of appropriate membranes for separating Grubbs-type precatalysts was based on:

i) Tolerance for different organic solvents. Certain organic solvents can cause changes in the structure of polyimide membranes.[2,3] The membranes had to be soaked for at least 24 h to observe whether there was any active layer dissolution. Both the membranes were found to be stable in organic solvents such as toluene, DMF, THF, 1-octene, 1-tetradecene and acetone as recommended by the manufacturer and clearly stated in literature.[3]

ii) An average MWCO of less than 600 g.mol^{-1} of the membrane because the precatalysts used in this study have molecular weights of between 700 to 800 g.mol^{-1}. As reported in literature Van der Gryp *et al.*[3] and White *et al.*[4] proved, without doubt, that PI membranes can successfully separate light hydrocarbons from lube oil with reasonable rejections and fluxes.

The PuraMem^{TM} series of membranes were therefore found to be suitable for the OSN experiments in this study.

4.1.2 Membrane evaluation

4.1.2.1 Proof of Steady state

To achieve a good representation of the PuraMem^{TM} separation performance during the OSN process, steady-state conditions had to be achieved. The time needed for every membrane to reach a steady-state was determined and shown in **Figure 4.1** to **4.4** for both 1-octene and 1-tetradecene. PuraMem^{TM} 280, **Figure 4.1**, gave good fluxes at 10 – 50 bar.

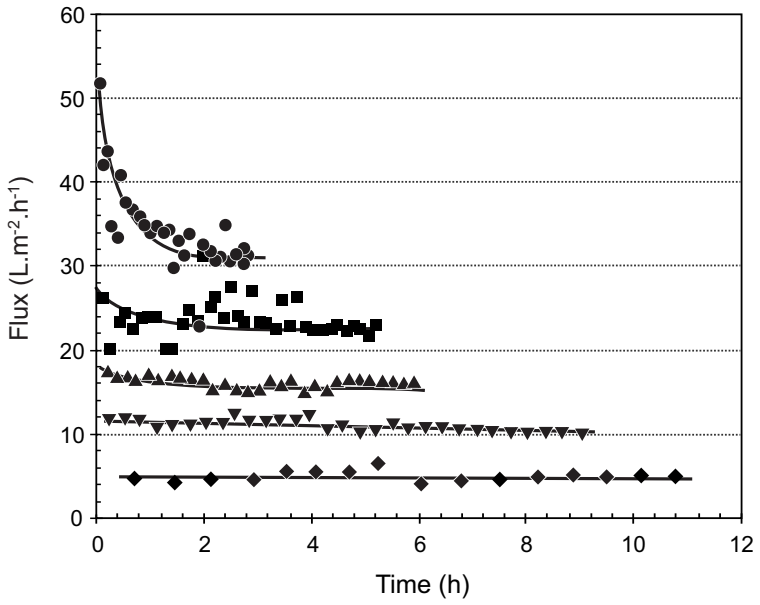

Figure 4.1: Pure 1-octene flux vs time at different pressures with PuraMem™280 [● 50 bar; ■ 40 bar; ▲ 30 bar; ▼ 20 bar; ◆ 10 bar]

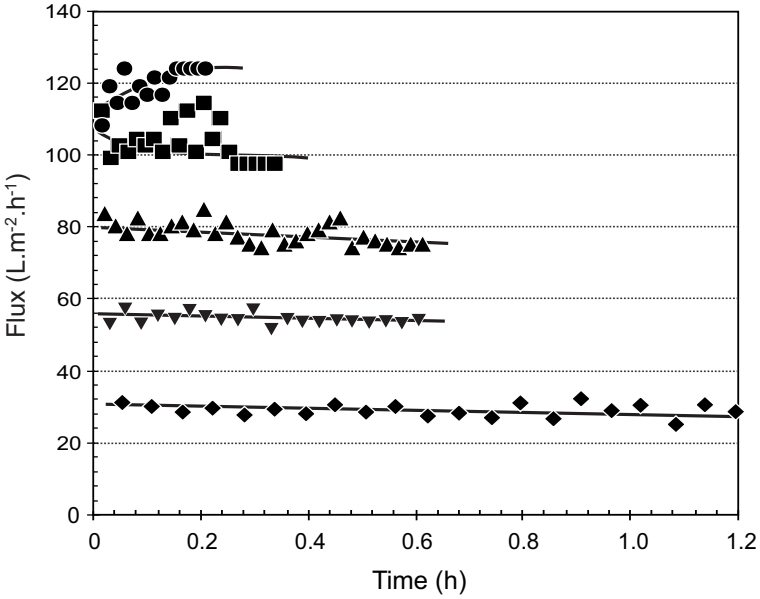

Figure 4.2: Pure 1-octene flux vs time at different pressures with PuraMem™ S380 [● 50 bar; ■ 40 bar; ▲ 30 bar; ▼ 20 bar; ◆ 10 bar].

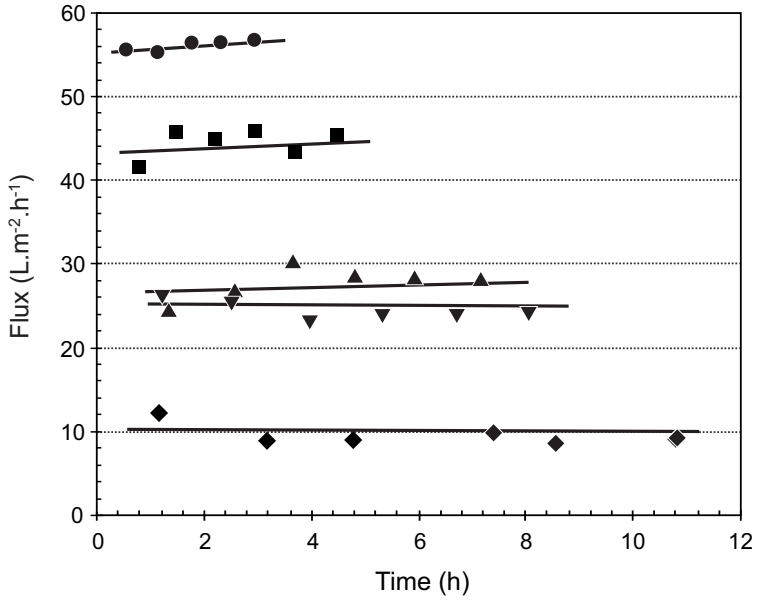

Figure 4.3: Pure 1-tetradecene flux vs time at different pressures with PuraMem™ 280 [● 50 bar; ■ 40 bar; ▲ 30 bar; ▼ 20 bar; ◆ 10 bar].

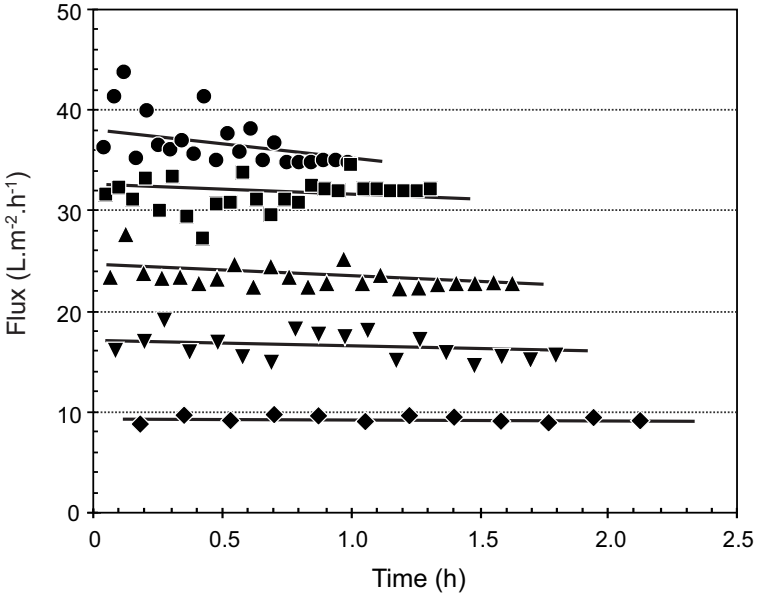

Figure 4.4: Pure 1-tetradecene flux vs time at different pressures with PuraMem™ S380 [● 50 bar; ■ 40 bar; ▲ 30 bar; ▼ 20 bar; ◆ 10 bar].

PuraMem™ S380 gave better fluxes (**Figure 4.2**) than PuraMem™ 280 (**Figure 4.1**) for pure 1-octene because of its higher MWCO. PuraMem™S380 gave higher fluxes of 1-octene ranging from 124 to 29 $L.m^{-2}.h^{-1}$.

For the PuraMem™ 280 (**Figure 4.3**), there was some permeation though the fluxes were very low. It was evident enough that there was permeation of the 1-tetradecene. PuraMem™ S380 (**Figure 4.4**), again gave higher fluxes because of its bigger MWCO, which allows the 1-tetradecene to permeate more easily, achieving a high flux of 35 $L.m^{-2}.h^{-1}$ at 50 bar and a low flux of 9 $L.m^{-2}.h^{-1}$ at 10 bar of 1-tetradecene with the PuraMem™ S380.

4.1.2.2 Binary mixtures permeation

For the selection of an appropriate membrane for the separation of different Grubbs-type precatalysts from the binary mixture of 1-octene (reagent) and 7-tetradecene (metathesis product), the permeation flux between the different membranes is of great importance. Here the permeation performance of PuraMem™ 280 and PuraMem™ S380 were characterized for the binary mixtures of 1-octene and 1-tetradecene (used instead of 7-tetradecene, the metathesis product, which is expensive).

Figure 4.5 and **Figure 4.6** illustrate perfectly that as the percentage of 1-octene decreased the total permeation flux decreased exponentially for the two chosen membranes. As compared to PuraMem™ 280, PuraMem™ S380 offered a higher permeation rate of the binary mixtures of 1-octene and 1-tetradecene.

PuraMem™ 280 (**Figure 4.5**) gave a low permeation performance less than 5 $L.m^{-2}.h^{-1}$ at 50:50, 40:60, 20:80, and 100% 1-tetradecene, which implies that it was very hard for the 1-tetradecene to permeate the membrane.

PuraMem™ S380 (**Figure 4.6**) gave a higher permeation of greater than 9 $L.m^{-2}.h^{-1}$. It was expected of the PuraMem™ S380 to give higher permeation rates due to the large gap difference of the MWCO (600 $g.mol^{-1}$) compared to the molecular weights of 1-octene (112.24 $g.mol^{-1}$) and 1-tetradecene (196.37 $g.mol^{-1}$).

In summary, as can be seen from **Figure 4.1** to **Figure 4.6** the screened membranes all start with high flux and decreased over time.[5] Flux always decreases due to concentration polarization, which is the accumulation of solutes on top of the membrane surface which increases their concentration, even when stirred.[5] Murthy and Chaudhari[6] found the same trend between pressure and flux: as pressure decreases so does the flux. Ebert *et al.*[7]

observed the same exponential trend for solvent mixtures of ethanol and n-pentane. Van der Gryp *et al.*[3] observed that the feed concentration of 1-octene increased exponentially at 30 Bar and attributed it to the combined effects of viscosity and structural size. **Tables 4.1** and **4.2** provide summary of the findings.

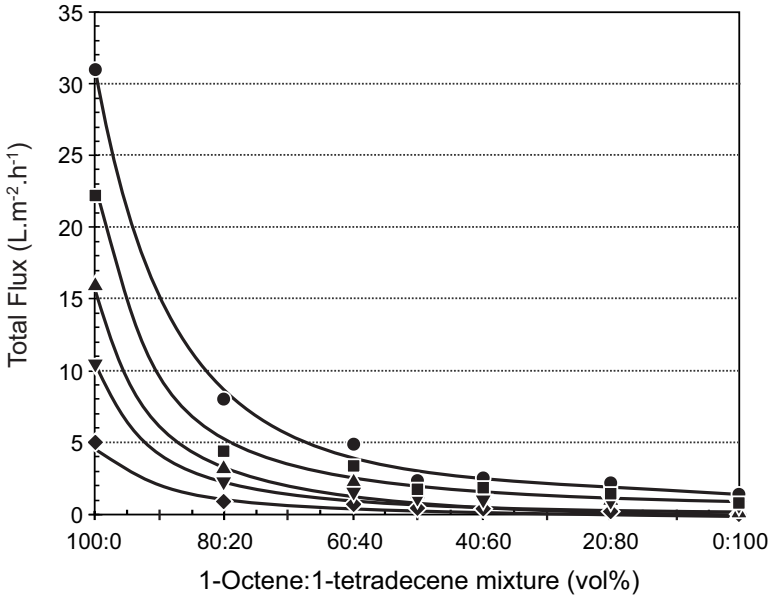

Figure 4.5: Plot of pure C_8, C_{14} and binary mixture compositions vs Total Flux of binary mixture (1-octene & 1-tetradecene) for PuraMem™ 280 [● 50 bar; ■ 40 bar; ▲ 30 bar; ▼ 20 bar; ◆ 10 bar].

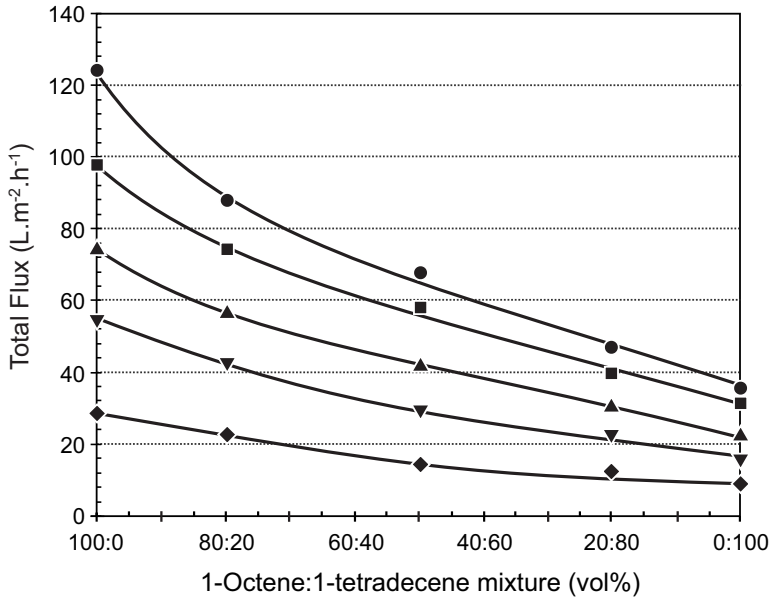

Figure 4.6: Plot of pure C_8, C_{14} and Binary mixture compositions vs Total Flux of binary mixture (1-octene & 1-tetradecene) for PuraMem™ S380 [● 50 bar; ■ 40 bar; ▲ 30 bar; ▼ 20 bar; ◆ 10 bar].

Typical flux values reported in literature,[3] for 1-octene at different pressures (10, 20, 30, 40 bar) with the StarMem® 228 membrane (MWCO = 280 g.mol^{-1}), which has the same MWCO as PuraMem™ 280 (280 g.mol^{-1}), are 3.1, 6.01, 9.19, and 12.31 L.m^{-2}.h^{-1}, respectively,[3] while that of 1-tetradecene are 0.68, 1.40, 2.01, 2.62 L.m^{-2}.h^{-1}. Thus PuraMem™ 280 performed much better than the StarMem® 228 membrane.

Table 4.1: Flux results of pure 1-octene with PuraMem™ membranes at different pressures.

	PuraMem™ Membranes		**Pressure (bar)**
MWCO =	280	600	
1-octene flux (L.m^{-2}.h^{-1}) =	31	124	50
	22	98	40
	16	75	30
	11	55	20
	5	29	10

Table 4.2: Flux results of pure 1-tetradecene with PuraMem™ membranes at different pressures.

	PuraMem™ Membranes		**Pressure (bar)**
MWCO =	280	600	
1-tetradecene flux (L.m^{-2}.h^{-1}) =	1.12	35	50
	0.91	32	40
	0.57	23	30
	0.48	16	20
	0.32	9	10

The separation performance of the binary mixture in this study is explained in **Figure 4.7** and **Figure 4.8** for PuraMem™ 280 and PuraMem™ S380. In **Figure 4.7**, 1-octene permeation increases exponentially with increasing 1-octene feed composition[3], while 1-tetradecene permeation decreases exponentially with increasing 1-tetradecene feed composition. From this we can conclude that 1-octene separates from 1-tetradecene i.e, if there is more 1-octene conversion there will be more 1-tetradecene permeating through the PuraMem™ 280 or if

there is less conversion of 1-octene, there will be less 1-tetradecene in the permeate and more 1-octene.

The same can be said for PuraMem™ S380 as for PuraMem™280 (**Figure 4.8**). At 80% 1-tetradecene, permeation is higher at 50 Bar and 10 Bar for both PuraMem™ 280 and PuraMem™ S380 and 1-octene permeation is slightly lower.

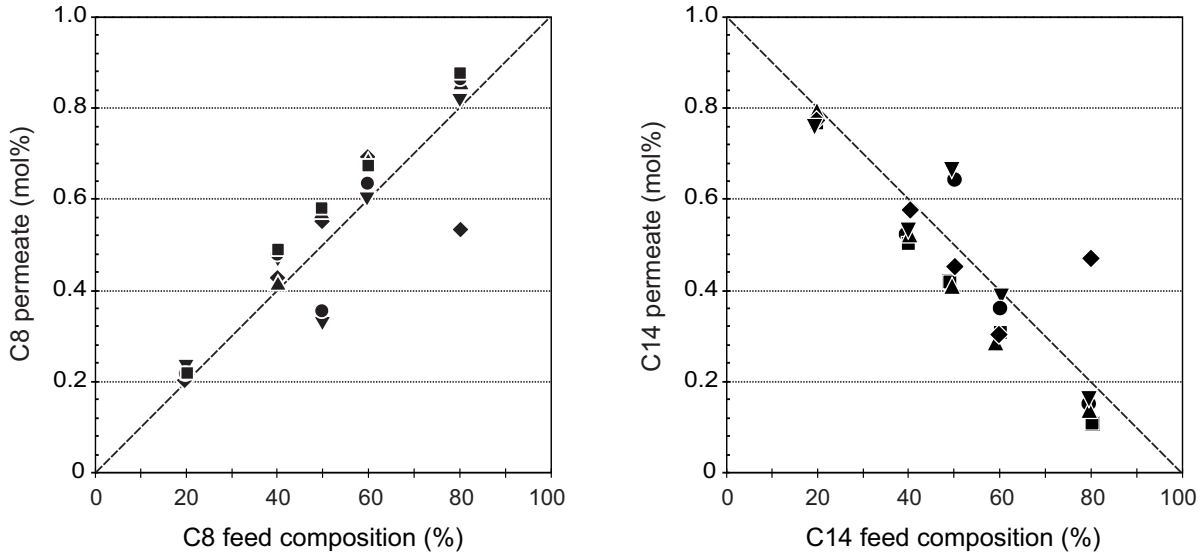

Figure 4.7 A plot of feed composition vs permeate composition of binary mixtures (1-octene and 1-tetradecene) for PuraMem™ 280
[● 50 bar; ■ 40 bar; ▲ 30 bar; ▼ 20 bar; ◆ 10 bar].

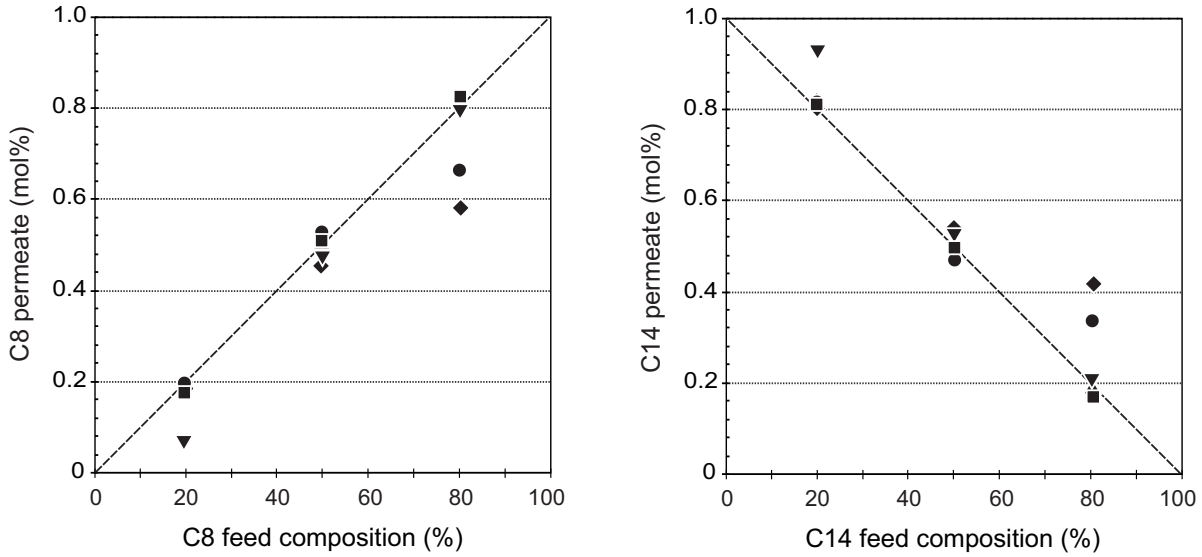

Figure 4.8 A plot of feed composition vs permeate composition of binary mixtures (1-octene & 1-tetradecene) for PuraMem™S380.

4.2 Metathesis

4.2.1 Introduction

Throughout the metathesis reaction, 1-octene decreases as a mixture of products are formed due to self-metathesis and cross-metathesis reactions, and alkene isomerization. The three formed groups of alkenes are PMP, SMP, and IP. The PMPs are ethylene and 7-tetradecene. The SMPs are nonene, decene, dodecene, tridecene, undecene, pentadecene and hexadecene. The IPs are 2-octene, 3-octene, 4-octene.

The metathesis reactions of two Grubbs-type precatalysts, complex **1** (**Figure 4.9**), complex **2** (**Figure 4.10**), and complex **3** (**Figure 4.11**) were conducted and discussed. The efficiency of these precatalysts was described in terms of selectivity and TON, which is the number of 1-alkene molecules that are converted to metathesis products by one molecule of a precatalyst. A summary of the metathesis reaction results of 1-octene at 80 °C and a molar ratio of 1:7000 (Ru/1-octene molar ratio) for the catalyst rejection with PuraMem^{TM}280 and PuraMem^{TM}S380 is given in **Table 4.3** and **Table 4.4**.

4.2.2 Metathesis with complexes 1 - 3

This section will discuss the activity and selectivity of all three precatalysts, the conversion of 1-octene and formation of PMP, IP and SMP as shown by **Figure 4.9** - **4.11**. The TON of these precatalysts will also be determined to show the efficiency of each precatalyst (**Table 4.4**). The complex were tested in a 1-octene metathesis reaction at 80 °C, with a molar ratio of 1:7000 (Ru/1-octene molar ratio).

All the complexes showed to have very high activity with fast conversion of more than 50% of 1-octene after 7h. Complex **1** (**Figure 4.9**) shows formation of 75% PMP and 0.072% formation of SMP, while 0.028% formation of IP at 80 °C. Both the reactions did equilibrate to 2100 min with the results being repeatable. High TON are reported for both tests, 4944 and 5268 respectively with selectivity >99% reported. Complex **2** (**Figure 4.10**) gave relatively large conversion of 1-octene equilibrating to 2100 min with the formation of 87% PMP. This high 1-octene conversion resulted in higher TON of 6989 and 5983, greater than that of complex **1**. Complex **3** (**Figure 4.11**) reported 91% formation of PMP for both tests with TON of 6304 and 6401 with selectivity >99%.

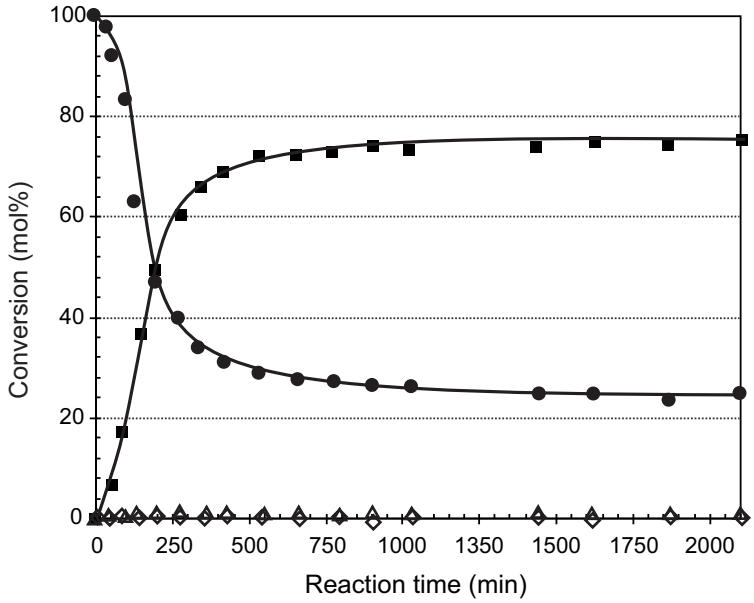

Figure 4.9: The conversion of 1-octene and the formation of PMPs, IPs and SMPs with complex **1** at 80°C and a Ru:1-octene molar ratio of 1:7000 (Ru/1-octene molar ratio). [● 1-octene; ■ PMPs; △ IPs; ◇ SMPs]

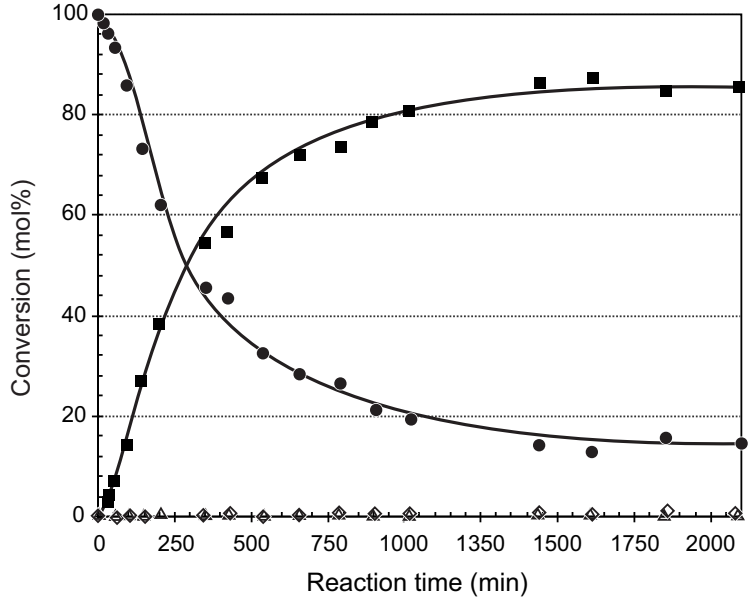

Figure 4.10: The conversion of 1-octene and the formation of PMPs, IPs and SMPs with complex **2** at 80°C and a Ru:1-octene molar ratio of 1:7000 (Ru/1-octene molar ratio). [● 1-octene; ■ PMPs; △ IPs; ◇ SMPs]

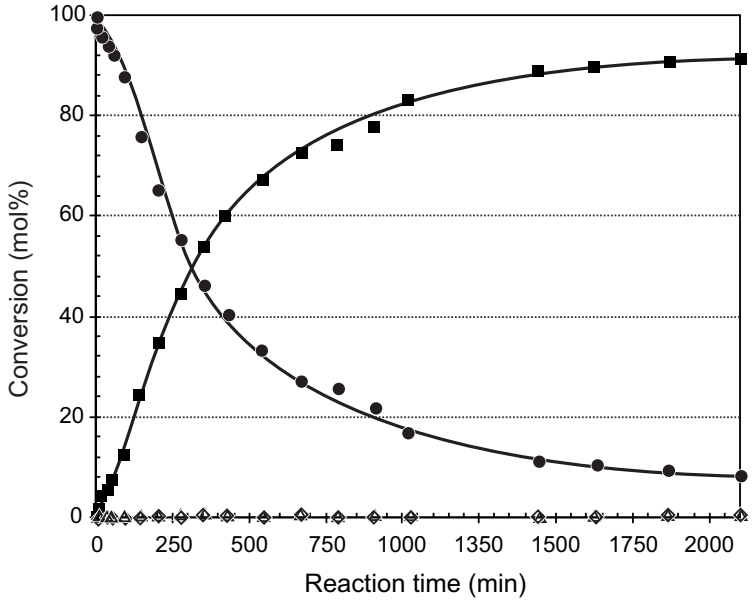

Figure 4.11: The conversion of 1-octene and the formation of PMPs, IPs and SMPs with complex **3** at 80°C and a Ru:1-octene molar ratio of 1:7000 (Ru/1-octene molar ratio). [● 1-octene; ■ PMPs; △ IPs; ◇ SMPs]

Table 4.3 presents the data summary of the 1-octene metathesis reactions using complex **1**-**3**. A high PMP formation is observed when using complex **2** and **3** as shown by **Table 4.3**. In conclusion, all the results showed to be repeatable, although all the complexes showed to be faster at 540 min, only complex **2** and **3** showed to convert more 1-octene molecules into PMPs with greater TON. Complex **2** and **3** showed higher PMPs formation, selectivity and TON as compared to **9** from literature[3] at 80 °C and Ru/1-octene molar ratio of 1:7000 (Ru/1-octene molar ratio).

Table 4.3: Summary of metathesis reaction results of 1-octene at 80 °C and a Ru/1-octene molar ratio of 1:7000 (Ru/1-octene molar ratio) at 2100 min compared to that of **9**.[3]

Precat.	1-octene (n%)	PMPs (n%)	IPs (n%)	SMPs (n%)	S (%)	TON	TOF ($x10^2$ s^{-1})
1	24.7	75.3	0.03	0.1	99.90	5268	4.18
2	14.4	85.5	0.04	0.1	99.88	5983	4.75
3	8.3	91.5	0.18	0.1	99.85	6401	5.08
9	14.7	73.4	0.70	11.2	85.99	5138	0.20

4.3 Lifetime of complexes 1-3

For lifetime studies **Figure 4.12** – **4.17** shows the formation of PMP and the time it takes for the complexes to consume 1-octene. To investigate the lifetime of complex **1** – **3**, the 1-octene (20 mL) was added when most of the PMP had formed. The activity and TON of the complexes gets lower after the introduction of fresh 1-octene into the reaction. Same applies to the formation of PMP and selectivity, they are lower than the earlier reached maximum. Also the catalyst loading gets lower every time a sample is taken from the reaction mixture.

Complex **1**, **Figure 4.12**, showed very poor activity after the second addition of 1-octene, with 5.33% formation of PMP. However complex **2** – **3** showed activity after second addition of 1-octene. Complex **2**, **Figure 4.13**, gave 56% PMP formation though lower than the first addition while third addition of 1-octene only yielded 1.6% PMP formation because the pre-catalyst had already decomposed at that stage. Complex **1** proved to be active for only 1,2 day (1740 min), while complex **2** showed to be active for 4,8 days (6940 min).

Complex **3**, **Figure 4.14**, showed higher formation of 66% PMP at the second addition of 1-octene, and 14% PMP formation at the third addition. Though for the second test the formation of PMP (26%) at second addition of 1-octene was a bit lower than the first test, the pre-catalyst remained active for more than two days (3320min).

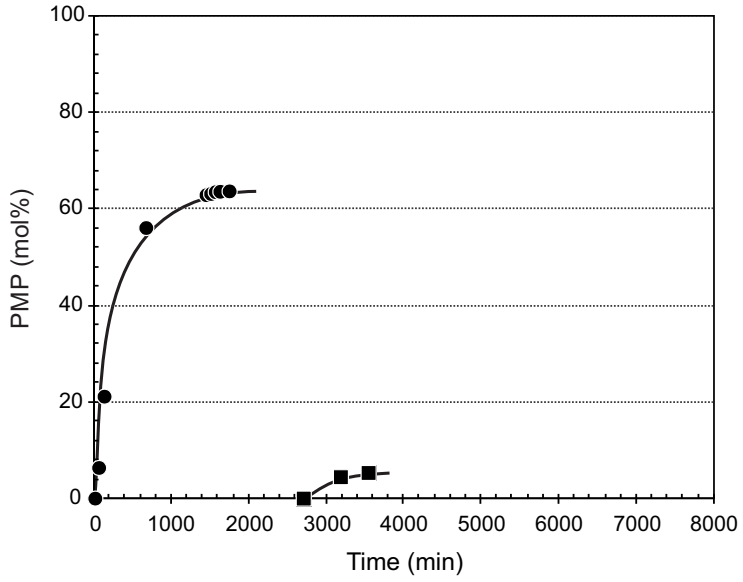

Figure 4.12: PMP formation upon succesive additions of 1-octene during metathesis in the presence of **1** at 80 °C and a Ru:1-octene molar ratio of 1:7000 [● Addition 1; ■ Addition 2].

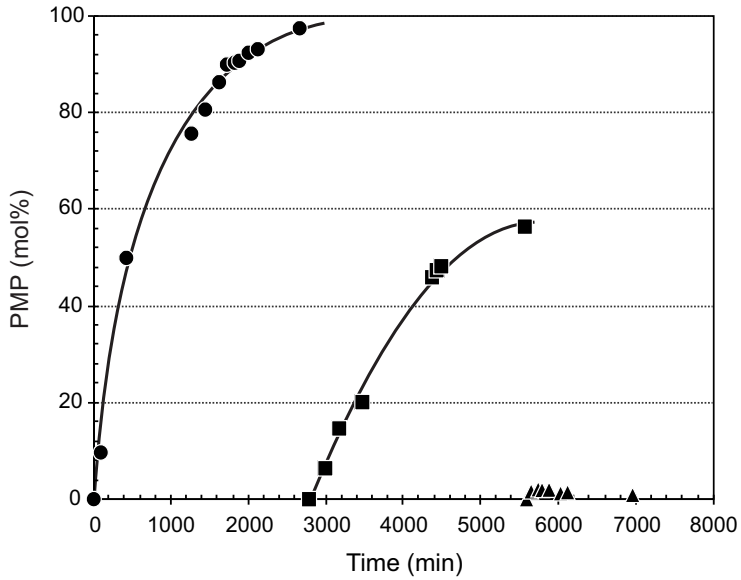

Figure 4.13: PMP formation upon succesive additions of 1-octene during metathesis in the presence of **2** at 80 °C and a Ru:1-octene molar ratio of 1:7000 [● Addition 1; ■ Addition 2; ▲ Addtion 3].

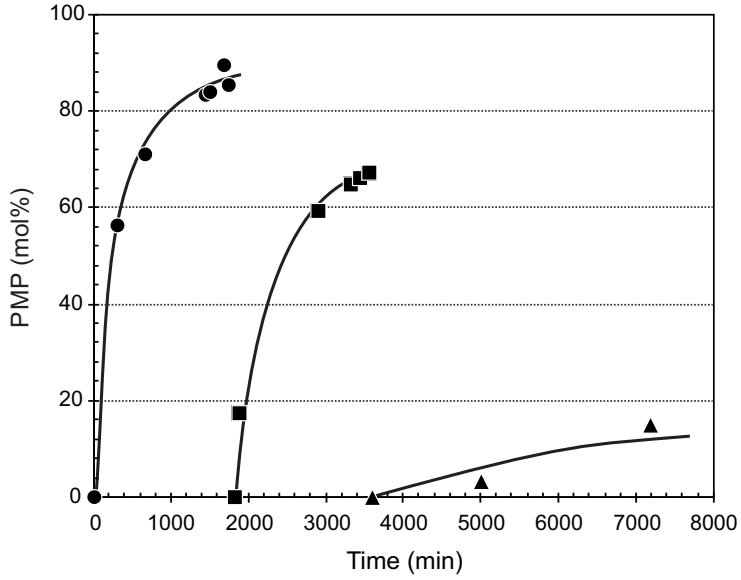

Figure 4.14: PMP formation upon succesive additions of 1-octene during metathesis in the presence of **3** at 80 °C and a Ru:1-octene molar ratio of 1:7000 [● Addition 1; ■ Addition 2; ▲ Addtion 3].

4.4 Organic Solvent Nanofiltration (OSN) Rejection Results and Discussion.

4.4.1 Introduction

The main part of this sub-section is to show that it is possible to conduct a post-reaction mixture OSN, and trap the catalyst in the retentate and isolate the products in the permeate. In this part, the successful separation of Grubbs-type **2** precatalysts in the presence of a reaction mixture of 1-octene is studied and illustrated with PuraMem™ 280 and PuraMem™ S380, which allow the catalyst to be re-used based on its lifetime.

4.4.2 Catalyst rejection experimental results

Metathesis reactions at 80 °C, **Figure 4.15** - **4.20**, were conducted for separation with PuraMem™ 280 and PuraMem™ S380. The metathesis reactions with complex **1 - 3** were conducted in a three necked flask (as discussed in Chapter 3), and transferred to the pressure cell for separation with PuraMem™ series of membranes.

4.4.2.1 OSN recyclability with PuraMem™ 280

Complex **1**, **Figure 4.15**, showed no activity after the second cycle which is attributed to the decomposition of the catalyst in solution and its short catalytic lifetime with catalyst rejection >97%, **Table 4.4**. The first cycle reached its steady state achieving a maximum of 63 % PMP.

Complex **2**, **Figure 4.16**, reports an extreme decline in PMP formation of 15 – 19 % in the second cycle from 80 % in the first cycle while the third cycle showed no activity presumably because the catalyst had already decomposed. Catalyst rejection was >99% for complex **2**.

Complex **3**, **Figure 4.17**, showed higher activity during the second cycle of the reaction than the other precatalysts with a 40 % formation of PMP after 87 % during the first cycle, with a catalyst rejection >97%. The third cycle only produced 2 – 6 % PMP formation. The reaction time was for four days (6330min).

The inactivity of complex **2**, **Figure 4.16**, in the second cycle can be attributed to the complex decomposition in the solution in the reactor for separation, as it took longer to separate the reaction mixtures. Complex **3**, **Figure 4.17**, showed the similar trend for both tests and almost similar catalyst rejection as complex **1**.

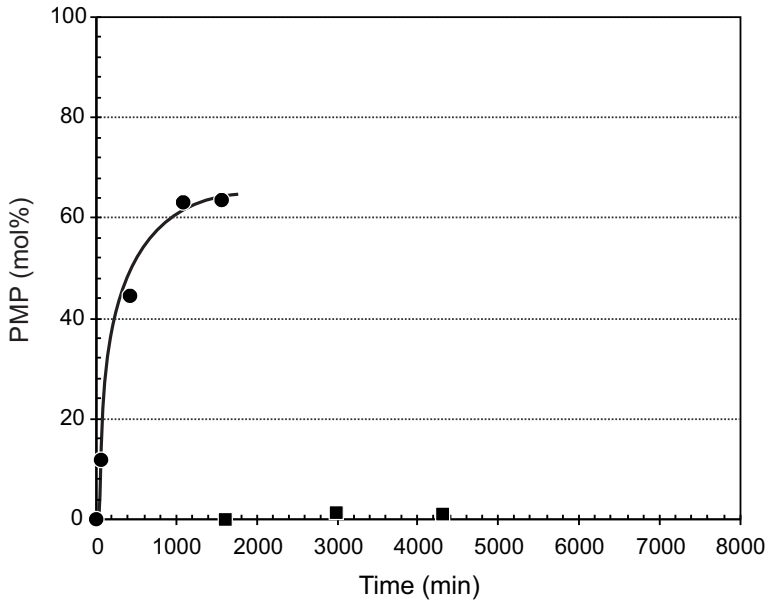

Figure 4.15: PMP formation of successive metathesis reactions at 80 °C and a Ru:1-octene molar ratio of 1:7000 after OSN recycling of **1** with PuraMem™ 280 [● Reaction 1; ■ Reaction 2].

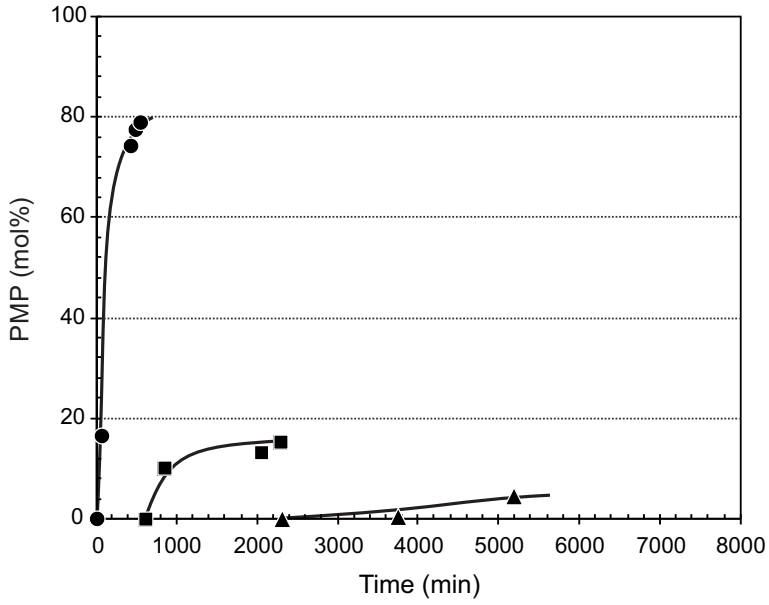

Figure 4.16: PMP formation of successive metathesis reactions at 80 °C and a Ru:1-octene molar ratio of 1:7000 after OSN recycling of **2** with PuraMem™ 280 [● Reaction 1; ■ Reaction 2; ▲ Reaction 3].

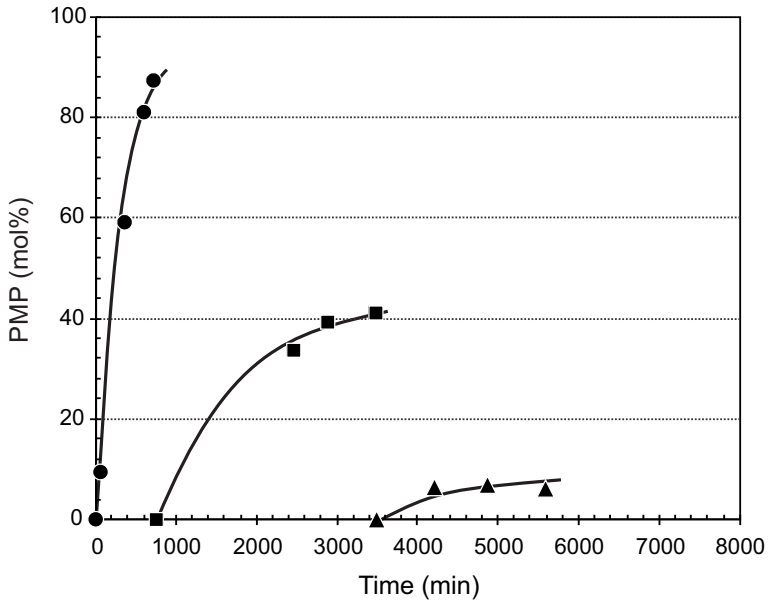

Figure 4.17: PMP formation of successive metathesis reactions at 80 °C and a Ru:1-octene molar ratio of 1:7000 after OSN recycling of **3** with PuraMem™ 280 [● Reaction 1; ■ Reaction 2; ▲ Reaction 3].

Table 4.4: Rejection results for PuraMem™ 280 with complexes **1**, **2** and **3**.

Precatalyst	Pressure (bar)	Rejection (%)
1	50	97.94
2	50	99.99
3	50	97.57

4.4.2.2 OSN recyclability with PuraMem™ S380

For all the tests done with PuraMem™ S380, poor rejections (**Table 4.5**) were obtained with the least being that of complex **2** (**Figure 4.19**) reporting just above 6% rejection. Poor rejection was obtained again for complex **1** (**Figure 4.18**) and **3** (**Figure 4.20**) gave 22.45% and 77.85% respectively. This poor rejections are as a result of the PuraMem™ S380 having a larger MWCO of 600 which is closer to the molecular weight of the precatalysts.

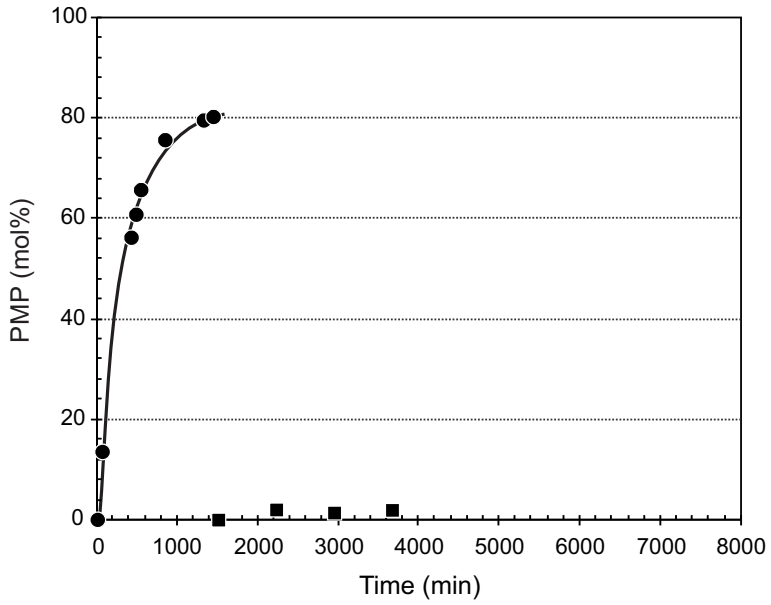

Figure 4.18: PMP formation of successive metathesis reactions at 80 °C and a Ru:1-octene molar ratio of 1:7000 after OSN recycling of **1** with PuraMem™ S380 [● Reaction 1; ■ Reaction 2].

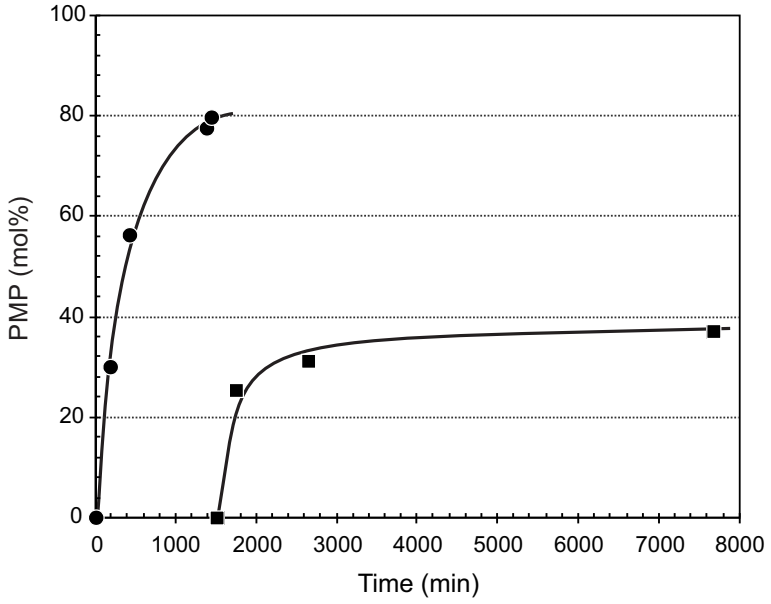

Figure 4.19: PMP formation of successive metathesis reactions at 80 °C and a Ru:1-octene molar ratio of 1:7000 after OSN recycling of **2** with PuraMem™ S380 [● Reaction 1; ■ Reaction 2].

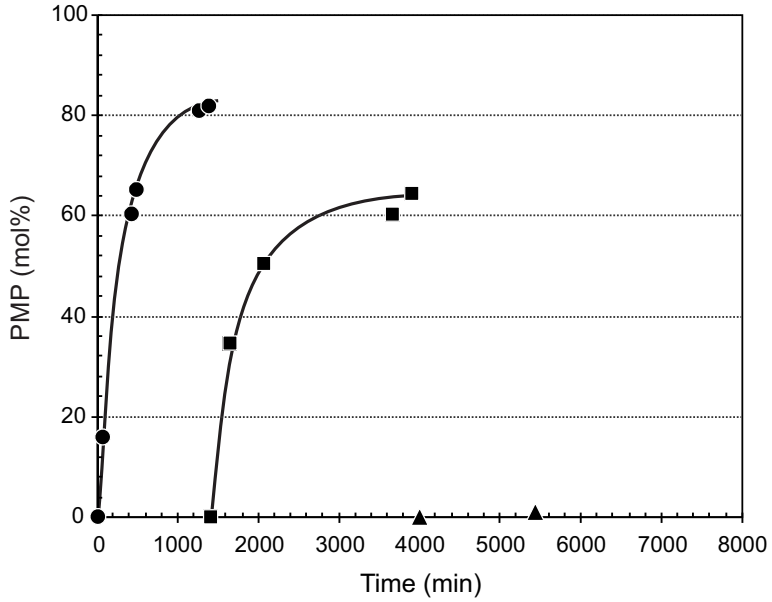

Figure 4.20: PMP formation of successive metathesis reactions at 80 °C and a Ru:1-octene molar ratio of 1:7000 after OSN recycling of **3** with PuraMem™ S380 [● Reaction 1; ■ Reaction 2; ▲ Reaction 3].

Table 4.5: Rejection results for PuraMem™ S380 with complexes **1**, **2** and **3**.

Precatalyst	Pressure (bar)	Rejection (%)
1	50	22.45
2	50	6.11
3	50	77.85

Higher PMPs formation for complex **3** is a result of faster permeation of the reaction mixtures through the membrane as compared to that of PuraMem™ 280, and a bit of the catalyst that permeate with the permeation time being less than an hour.

4.5 Concluding remarks

It was shown in this chapter that it is possible to conduct a metathesis reaction of 1-octene with with all the three complexes with greater TONs. For lifetime studies, complexes **2** perfomed very well as compared to complex **1** and **3** with respect to PMP formation in the second 1-octene addition cycle. It was also possible to successfully separate all the

complexes from their reaction mixtures with PuraMem™ 280 except for PuraMem™ S380 which gave very poor rejections of all the complexes. PuraMem™ 280 rejections compared very well to that found in literature >97%.[3] PuraMem™ 280 is a better preferred membrane for this type of catalyst in terms of membrane separation in the 1-octene metathesis.

4.6 References

1. Cuperus, F.P, Smolders, C.A., *Adv. Colloid Interf. Sci*., 1991, **34**, 135
2. Yang, X.J., Livingston, A.G., Freitas Dos Santos, L., *J. Membr. Sci*, 2001, **190**, 45
3. Van der Gryp, P., Barnard, A., Cronje, J.P., De Vlieger, D., Marx, S., Vosloo, H.C.M., *J. Membr. Sci*., 2010, **353**, 70
4. White, L.S., Nitsch, A.R., *J. Membr. Sci*, 2000, **179**, 267
5. Mulder, M., Basic Principles of Membrane Technology, 2nd ed., Dordrecht: Kluwer Academic., 1996
6. Murthy, Z.V.P., Chaudhari, L.B., *Desalination*, 2009, **247**, 610
7. Ebert, K., Koll, J., Dijstra, M.F.J., Eggers, M.J., *J. Membr. Sci*., 2006, **285**, 75

Chapter 5
Conclusions and Recommendations

5.1 Conclusions

5.1.1 Introduction

The aim of this study was to add to what is already in literature regarding the efficiency of the recovery of the metal precatalysts by selected nanofiltration membranes. Grubbs precatalysts **1**, **2**, and **3** were used for the metathesis reaction of 1-octene. Experimental work was done on these catalysts for the metathesis reaction and the OSN reactions were conducted to remove the catalyst from their post-reaction mixtures with PuraMem™ 280 and PuraMem™ S380 from Evonik MET.[3]

5.1.2 Metathesis reactions

Complexes **1**, **2**, and **3** were used to conduct metathesis reactions under the following conditions at 80 °C and with a ruthenium: 1-octene molar ratio of 1:7000. All the pre-catalysts showed to be active in the metathesis reaction of 1-octene after testing. Complex **3** was the very active catalyst with TON of 6400 followed by complex **2** with TON of 6000 and complex **1** with TON of 5000. Complex **3** converted more than 90% of 1-octene to PMPs, complex **2** more than 85% and complex **1** more than 70%.

5.1.3 Lifetime reactions

Complex **2** showed the formation of the most PMPs (56%) upon the second addition of 1-octene followed by complex **3** with 46 % PMPs and complex **1** with almost no PMPs.

5.1.4 Organic Solvent Nanofiltration (OSN)

The OSN technique was successfully applied with PuraMem™ 280 and PuraMem™ S380 for the re-usability of complex **2** and **3**. Complex **1** did not show any catalytic activity after the first separation due to its short lifetime compared to **2** and **3**. These membranes were found to be suitable for the study based on their performance in terms of tolerance to organic solvents like toluene, DMF, THF, 1-octene, 1-tetradecene and acetone, and also in terms of their permeation performance with fluxes ranging from 9 - 35 $L.m^{-2}.h^{-1}$.

PuraMem™ 280 outperformed PuraMem™ S380 in terms of separating complexes **1**, **2**, **3**. PuraMem™ 280 gave way better rejections >97% showing its ability to separate almost all the

precatalyst from its products. Therefore, it is recommended from this study to use PuraMem™ 280 when dealing with such precatalyst.

5.2 Recommendations

- To use other methods to successfully synthesize other Grubbs-type precatalysts and test them for the OSN experiments.
- To improve the activity of complex **1** for lifetime studies.
- To describe the transport mechanism through PuraMem™ membranes.
- Investigate to what extent these membranes can be implemented industrially.

5.3 References

1. Huijsmans, C. A. A., Modelling and Synthesis of Grubbs-type complexes with hemilabile ligands, MSc-dissertation, (North-West University), 2009
2. Jordaan, M., Experimental and Theoretical investigation of Grubbs-type catalysts for the metathesis of alkenes., PhD Thesis, (North-West University), 2007
3. Evonik Membrane Extraction Technology (MET) Ltd, Unit 8 Wharfside, Rosemont Road, London HAO 4PE, United Kingdom, [Web] (www.duramem.evonik.com), 2011

Appendix – FTIR spectra

Spectrum 1

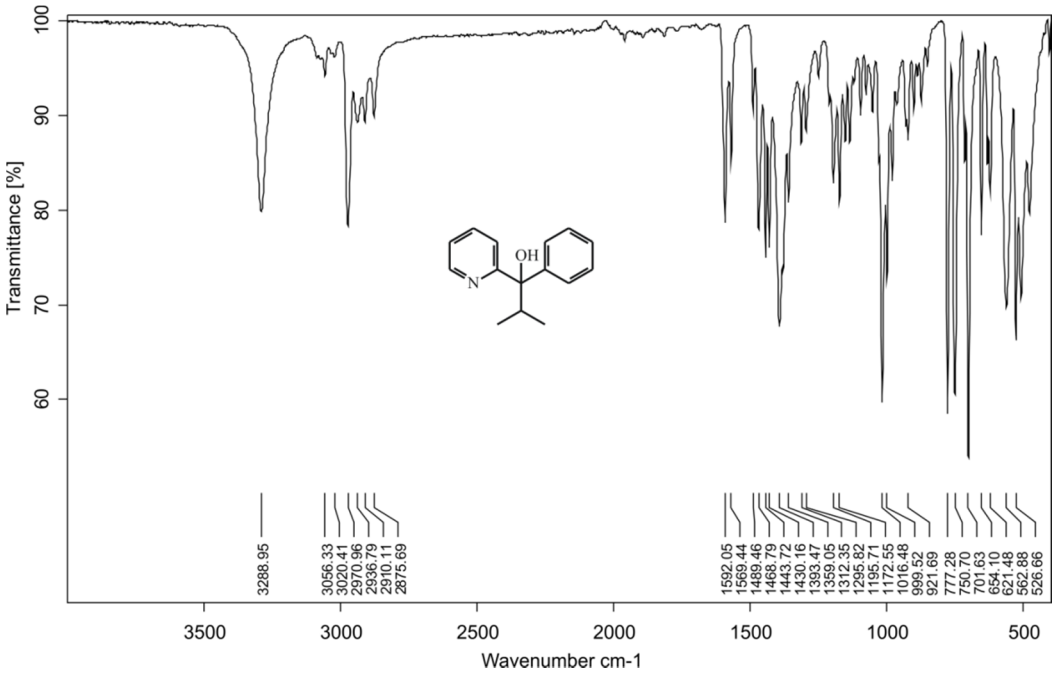

Spectrum 2

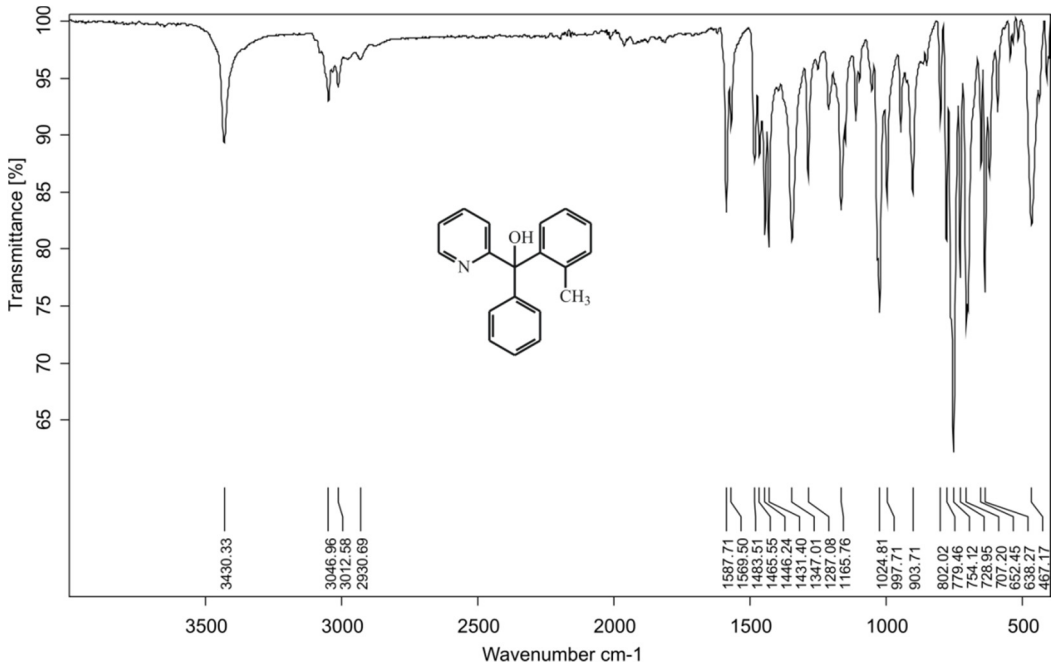

Spectrum 3

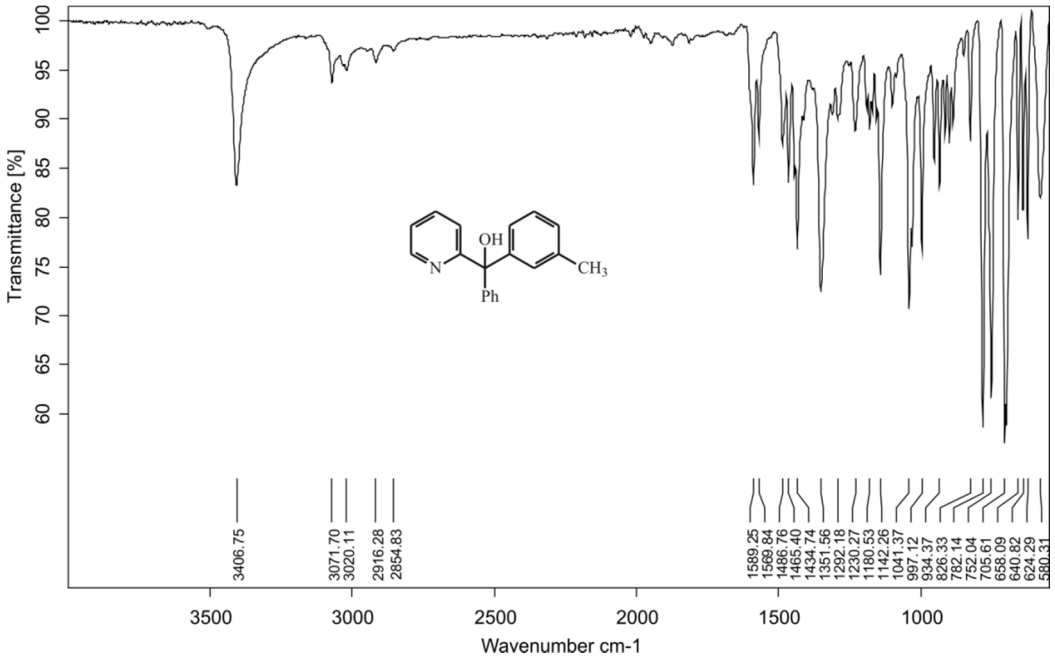
Transmittance [%]
100
95
90
85
80
75
70
65
60
OH
N
CH3
Ph
3406.75
3071.70
3020.11
2916.28
2854.83
1589.25
1569.84
1486.76
1465.40
1434.74
1351.56
1292.18
1230.27
1180.53
1142.26
1041.37
997.12
934.37
826.33
782.14
752.04
705.61
658.09
640.82
624.29
580.31
3500
3000
2500
2000
1500
1000
Wavenumber cm-1

Appendix – Mass spectra

Spectrum 4

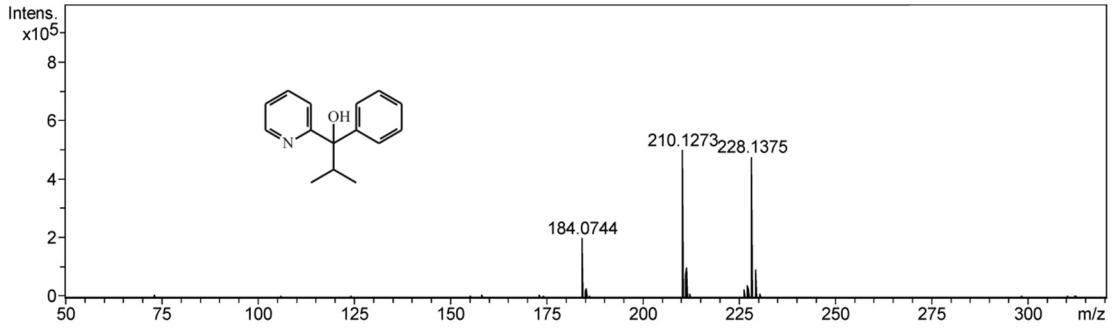

Spectrum 5

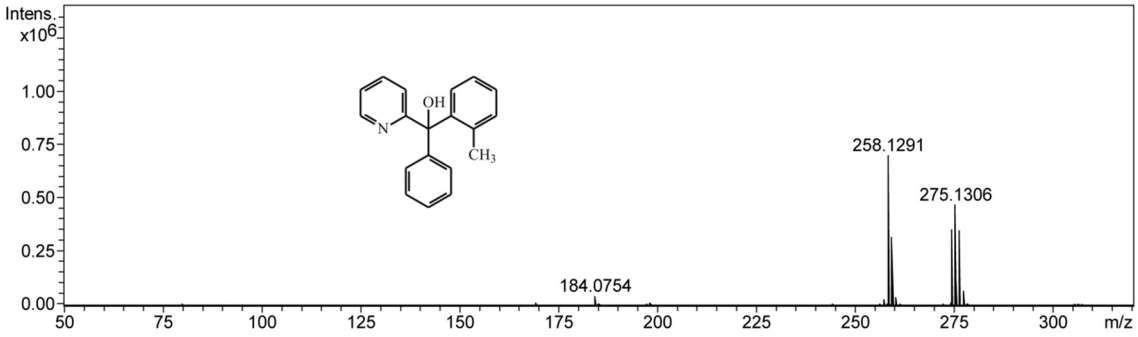

Spectrum 6

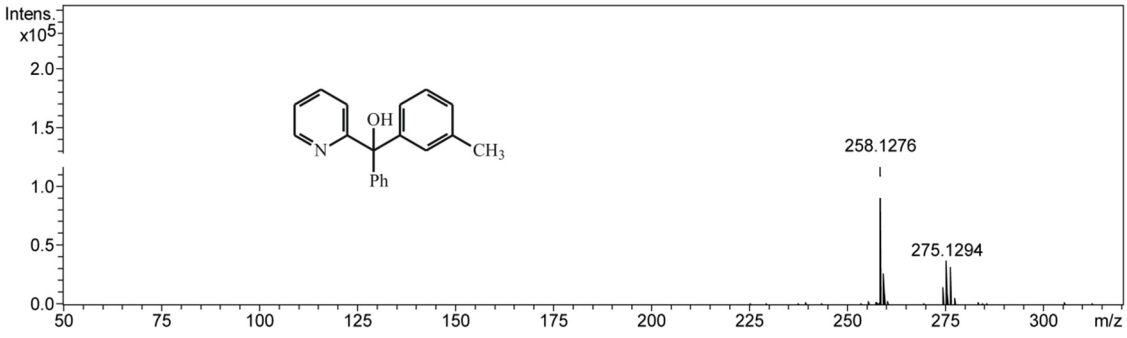

Appendix - ^{1}H-NMR spectra

Spectrum 7

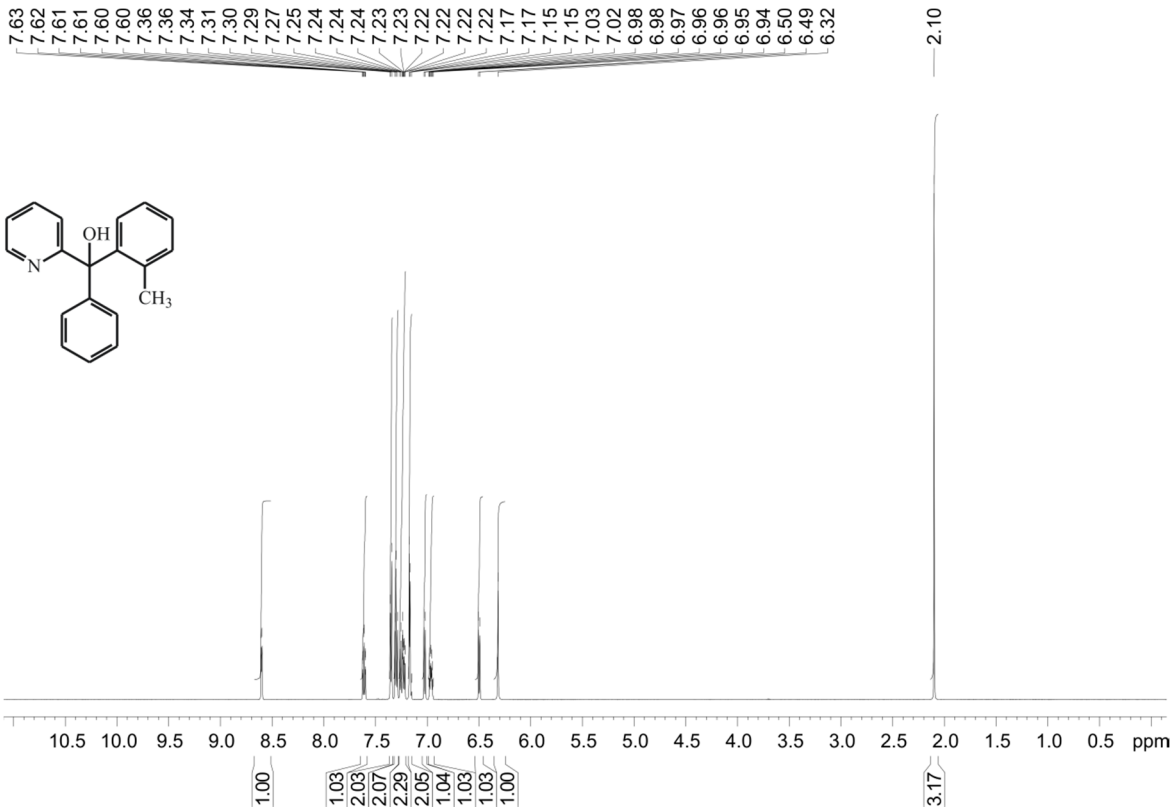

Spectrum 8

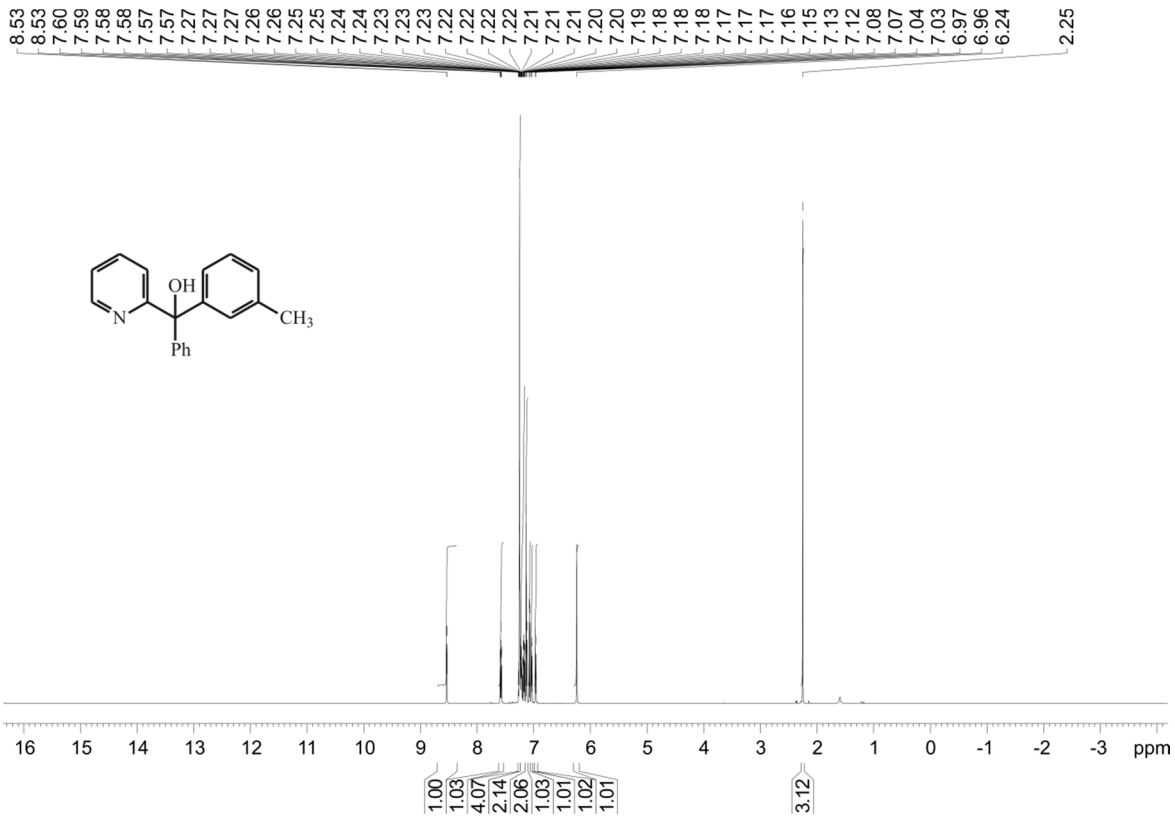

Spectrum 9 Complex **1**

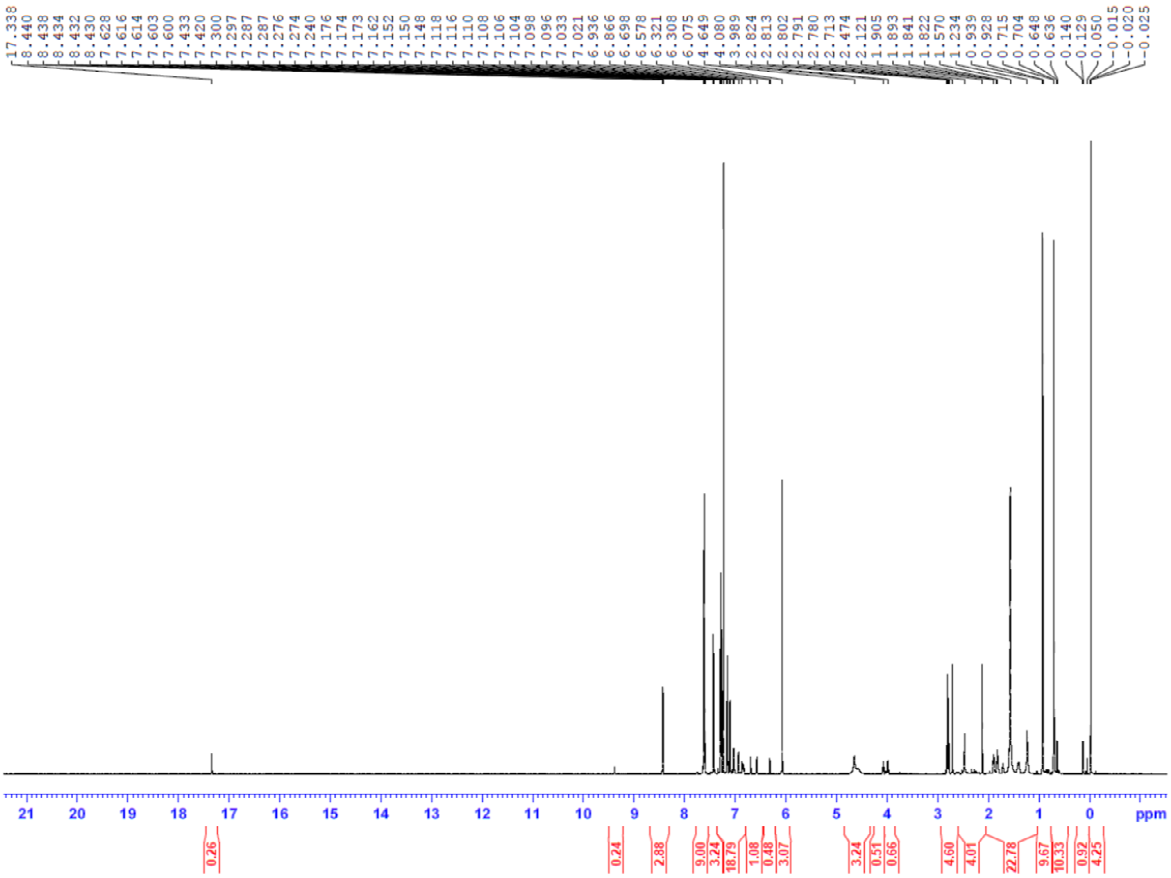

Spectrum 10 Complex **2**

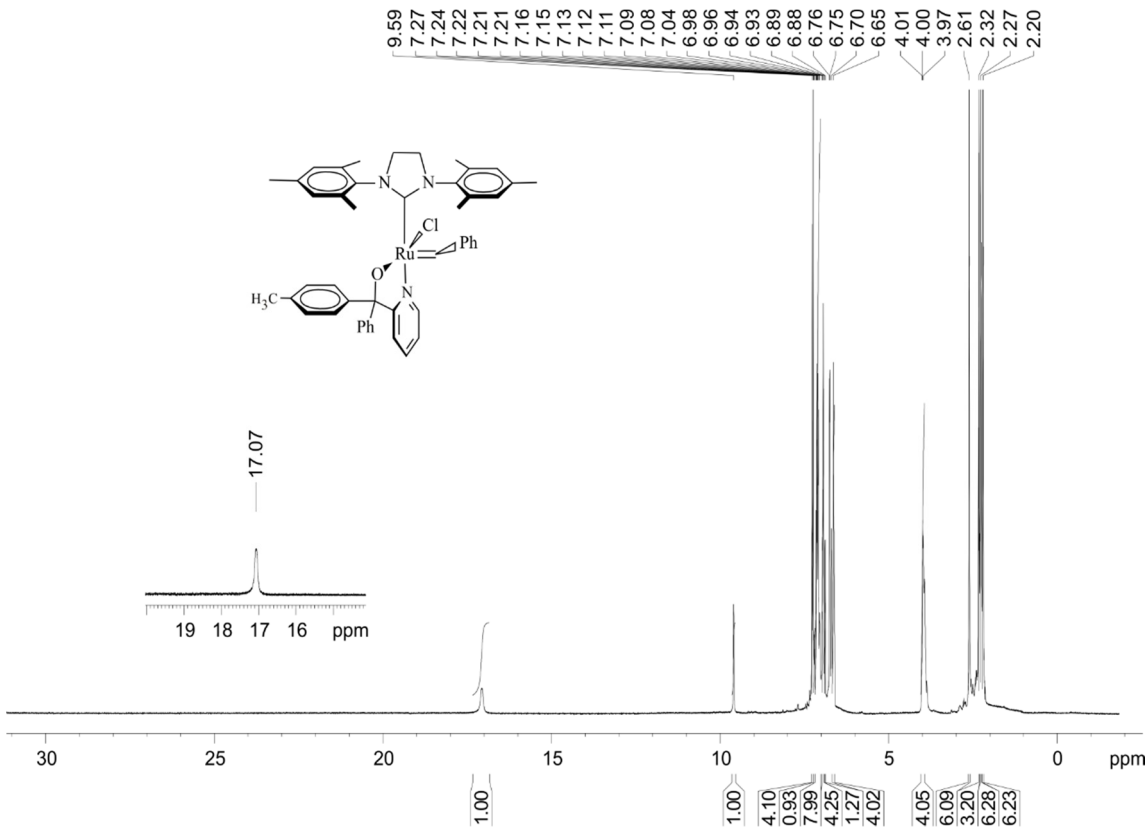

Spectrum 11 Complex **3**

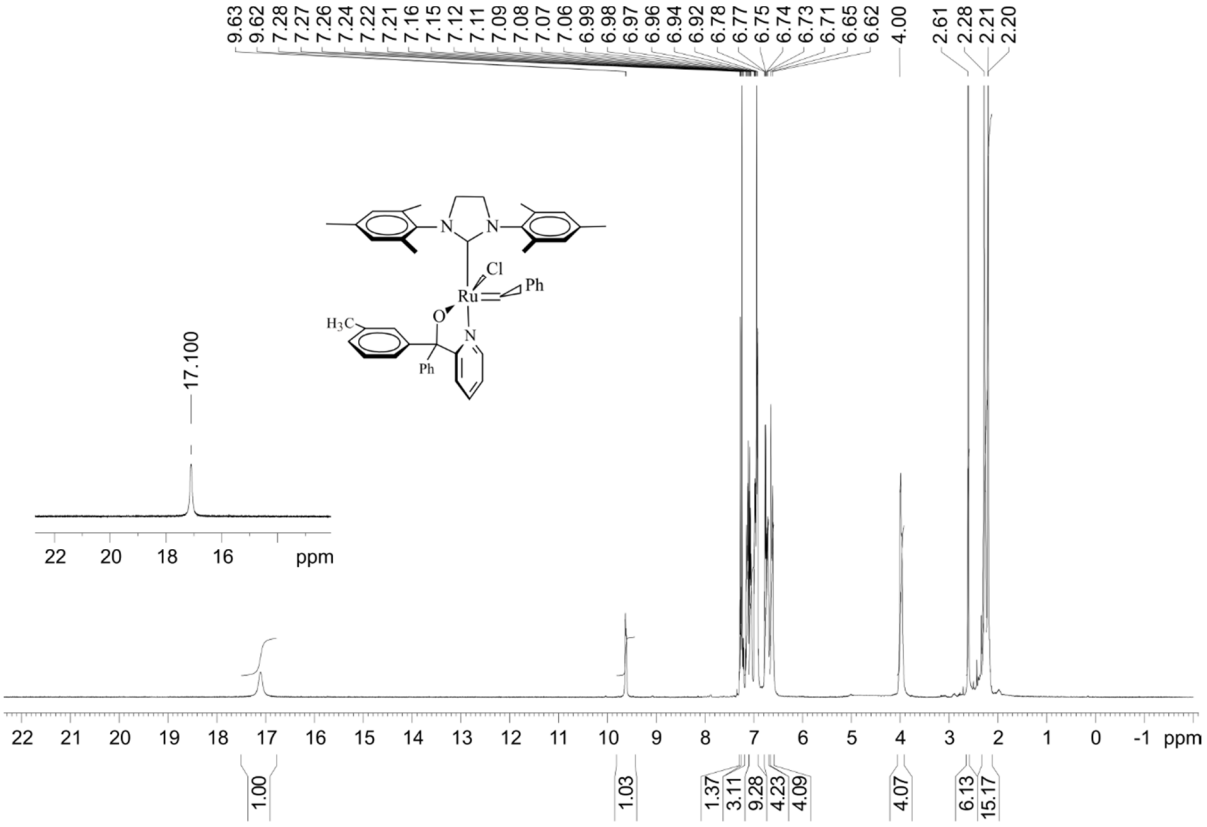

Appendix - ^{13}C-NMR spectra

Spectrum 12

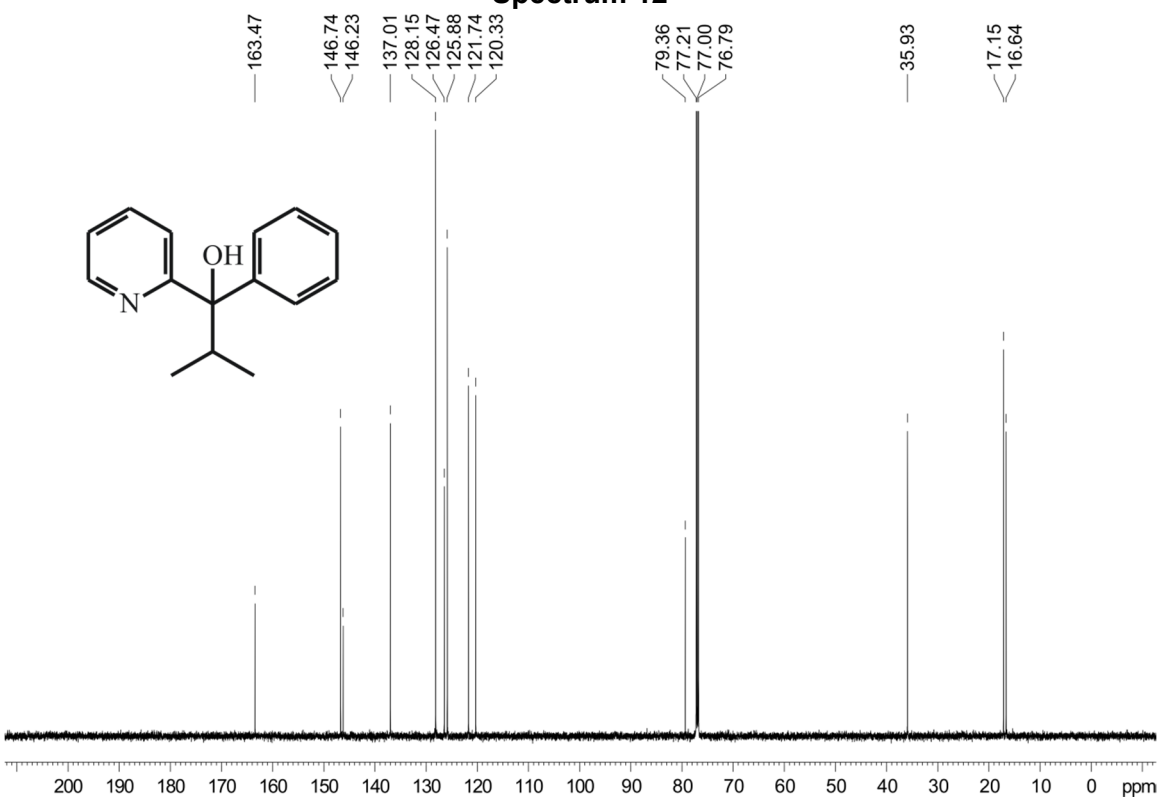

Spectrum 13

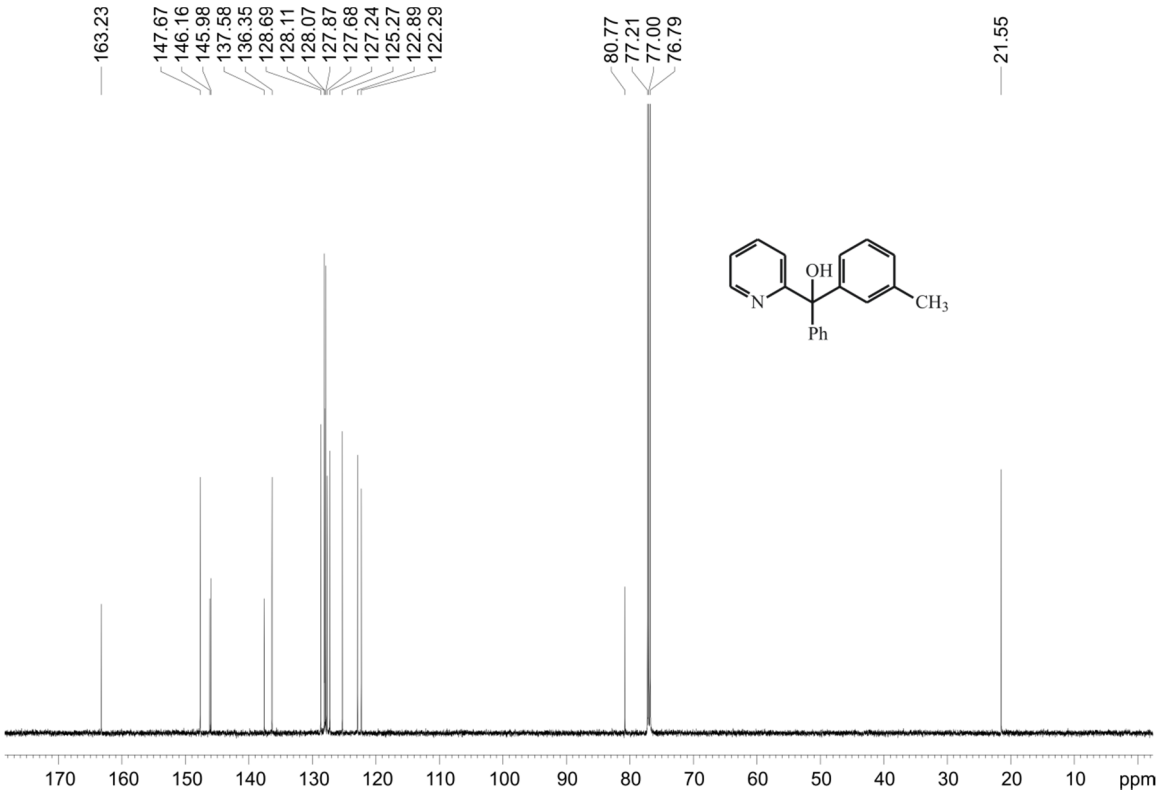

Spectrum 14 Complex **1**

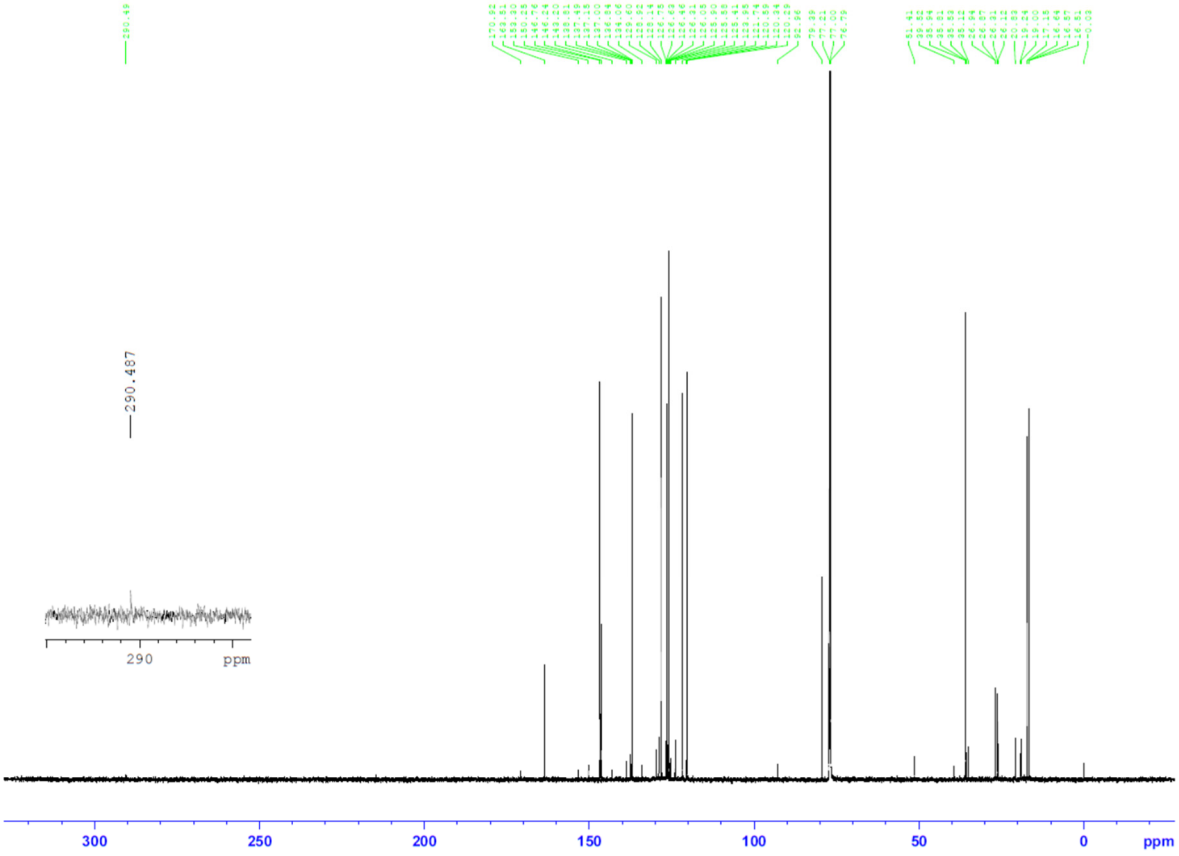

Spectrum 15 Complex **2**

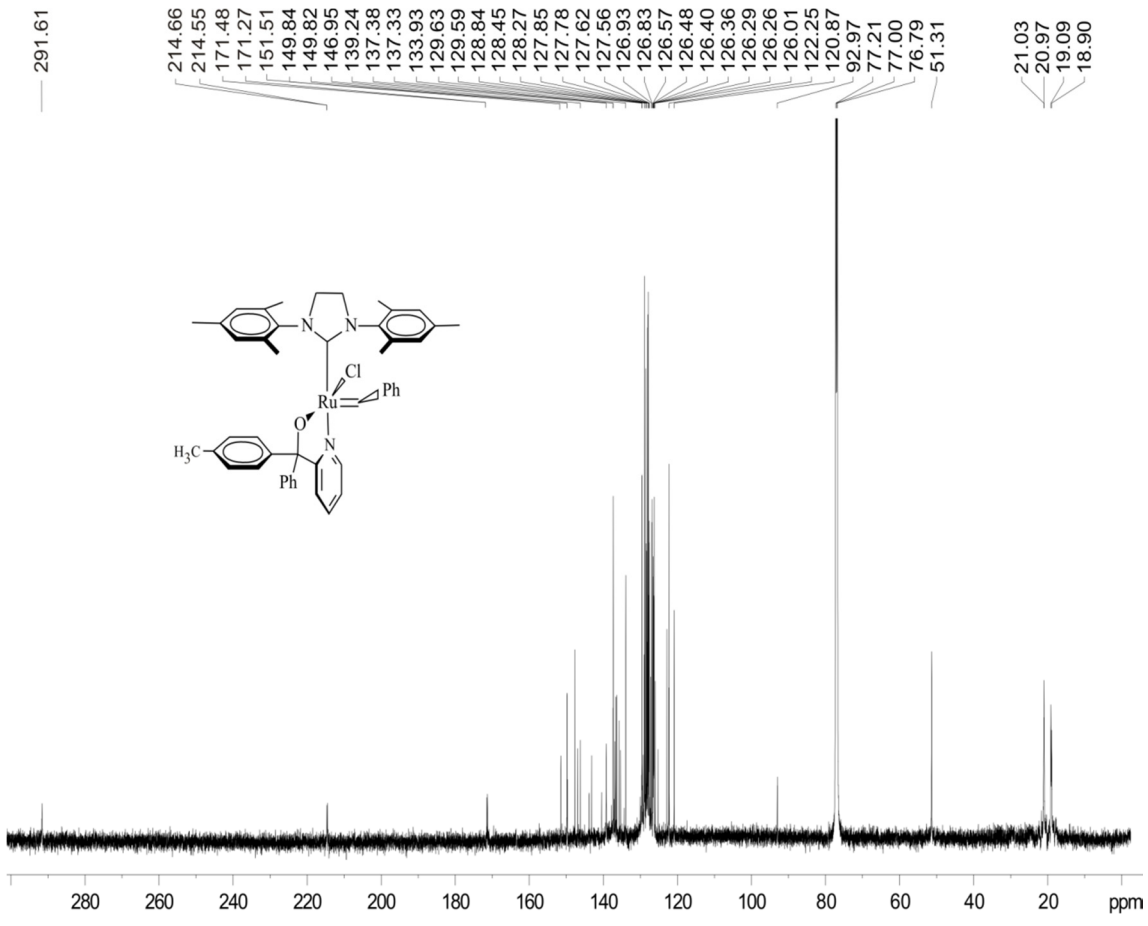

Spectrum 16 Complex **3**

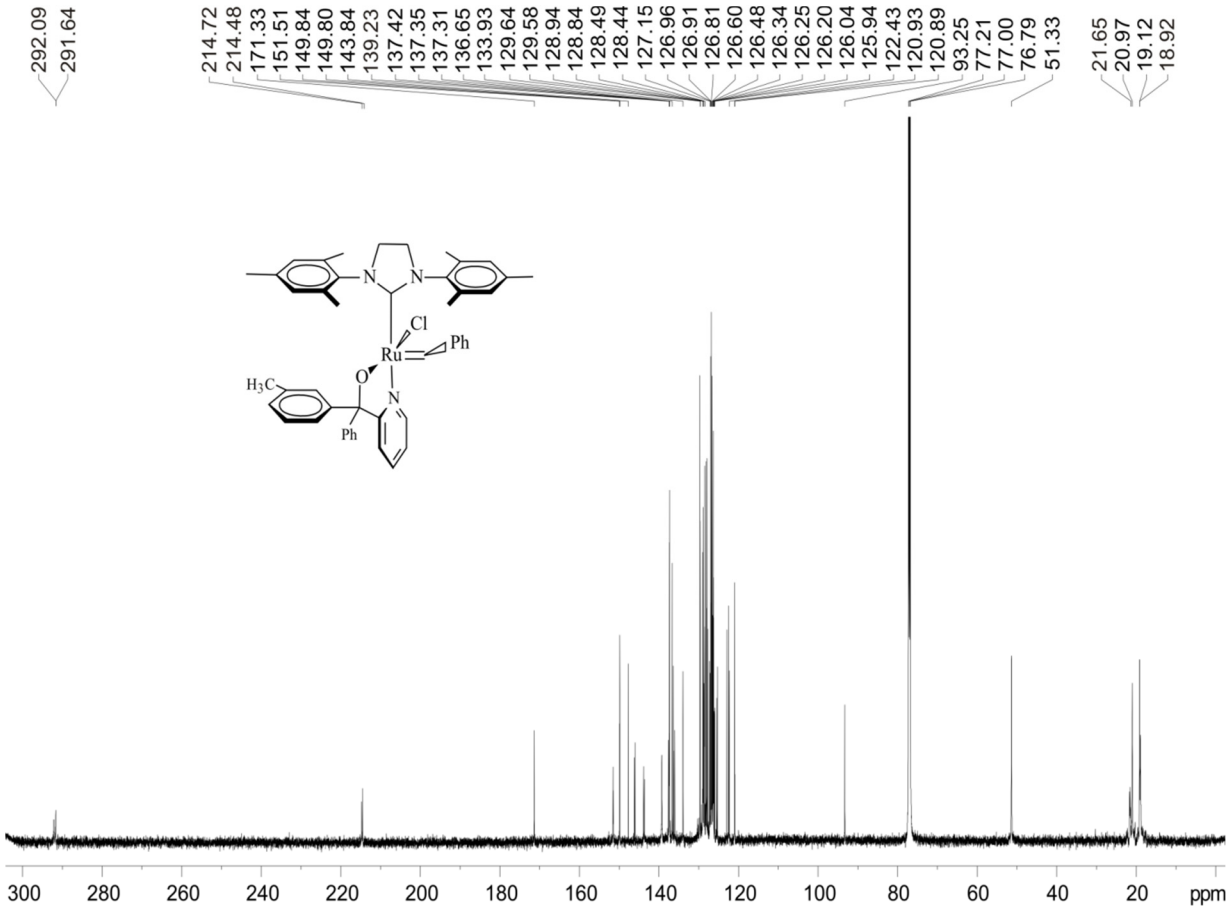

Appendix - ^{31}P-NMR spectra

Spectrum 17 Complex **1**

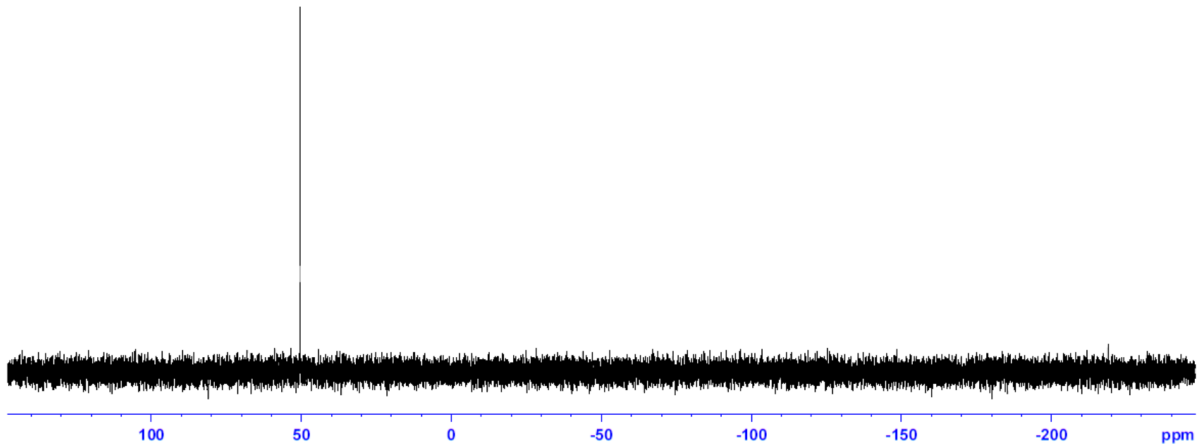

Spectrum 18 Complex **2**

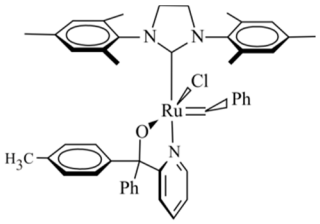

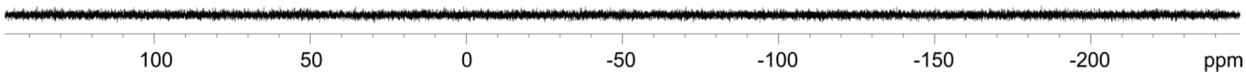

Spectrum 19 Complex **3**